EFFECT OF NIOBIUM, MOLYBDENUM AND VANADIUM

ON STATIC RECOVERY AND RECRYSTALLI-

ZATION IN MICROALLOYED STEELS

by

HERALDO LEITE DE ANDRADE

A Thesis Submitted to the
Faculty of Graduate Studies and Research
in Partial Fulfillment of the Requirements for the
Degree of Master of Engineering

Department of Mining and Metallurgical Engineering
McGill University
Montreal, Canada

© June 1982

EFFECT OF SOLUTES ON STATIC RECRYSTALLIZATION OF MICROALLOYED

AUSTENITE

ABSTRACT

Constant strain rate, interrupted compression tests were carried out at temperatures of 1000 and 900°C on a series of four steels. The base steel had a composition of 0.06% C and 1.43% Mn and the others contained one of the following set of additions: (i) 0.115% V; (ii) 0.29% Mo; and (iii) 0.035% Nb. In, the latter steel, the Mn level was raised to 1.90%. The load-free time was decreased from 5000 s to 50 ms and the degree of static softening during this period was calculated from the reloading yield stress, which was measured by two different techniques: (i) back extrapolation; (ii) the conventional offset method. Fractional softening vs. holding time curves were prepared from these data and the influence of Mo, Nb and V addition on the softening behavior was determined.

The results show that the presence of Nb, Mo and V <u>in solution</u> retards static recovery and recrystallization in a significant way. On an equal atom fraction basis, Nb has a considerably greater retarding effect than either Mo or V, which has the least effect. In the Nb steel at 900°C, the strain induced precipitation of Nb(C,N) after a holding time of around 10 s led to a further delay of about an order of

magnitude in the onset of static recrystallization. No precipitate retardation was observed in the V steel. The use of graphite instead of glass lubrication decreased the retardation of static softening in the Nb steel. This result is attributed to the presence of undissolved precipitates of NbC after the austenitization heat treatment, which reduced the amount of Nb in solution before deformation. Values of the Solute Retardation Parameter were determined for Nb, Mo and V under static conditions. Although the comparison with the corresponding dynamic quantities showed the same rank order of effectiveness, considerably higher SRP's were obtained under static conditions. The total amounts of softening due to static recovery calculated by the offset method are twice those determined by back extrapolation. The latter technique is considered to be more useful for predicting the influence of recovery on mill loads in industrial practice.

RÉSUMÉ

Des tests de compression avec interruption et à vitesse de déformation vraie constante ont été effectués à 900 et 1000°C sur une série de quatre aciers. À la composition de base 0.06% C et 1.43% Mn ont été ajoutés successivement: (i) 0.115% V; (ii) 0.29% Mo et (iii) 0.035% Nb. Dans ce dernier cas, la concentration en manganèse a été augmentée à 1.90%. Le temps d'interruption variait de 5000 s à 50 ms et le taux d'adoucissement statique pendant cette période a été calculé d'après la limite élastique après interruption, mesurée de deux manières différentes: (i) par extrapolation inverse (ii) par la méthode 'offset' classique. La variation du taux d'adoucissement en fonction du temps de maintien a pu être ainsi déterminée et l'influence de l'addition de Mo, Nb ou de V déduite.

Les résultats montrent que la présence de Nb, Mo et V en <u>solution</u> retarde la restauration statique et la récristallisation de manière significative. Pour une même fraction atomique, le niobium a un effet retardateur beaucoup plus important que le molybdène lui même plus efficace que le vanadium. Dans l'acier au niobium à 900°C, la précipitation de Nb(C,N) induite par la déformation, après un temps de maintien de l'ordre de

10 s, conduit à une augmentation d'un ordre de grandeur le
temps du début de recristallisation statique. Aucun retard
dû à une éventuelle précipitation n'a été observé dans l'acier
au vanadium. L'utilisation du graphite au lieu de verre comme
lubrifiant diminue le retard de l'adoucissement statique dans
l'acier au niobium. Ceci est attribué à la présence de pré-
cipités non dissous de Nb(C,N) après le traitement d'austénitisa-
tion, ce qui réduit le pourcentage de niobium en solution avant
la déformation. La valeur du Paramètre de Retard en Solution
Solide a été calculée pour le Nb, Mo et le V dans le cas
statique. Bien que la comparaison avec les quantités corres-
pondantes dans le cas dynamique ait montré le même ordre
d'efficacité, les valeurs du PRSS obtenues dans le cas statique
sont beaucoup plus grandes. Le taux d'adoucissement dû à la
restauration statique calculé par la méthode 'offset' est deux
fois plus important que celui déterminé par extrapolation.
Cette seconde technique est considérée comme beaucoup plus
utile pour prédire l'influence de la restauration sur les
charges de laminages dans les procédés industriels.

RESUMO

Testes de compressão com interrupção e a uma velocidade de deformação constante foram realizados à 1000 e 900°C em uma série de quatro aços. Ao aço de base, com uma composição química de 0.06% C e 1.43% Mn, foram feitas as seguintes adições: (i) 0.115% V; (ii) 0.29% Mo; e (iii) 0.035% Nb. Neste último aço, o teor de Mn foi aumentado para 1.90%. O intervalo de interrupção variou de 5000 s a 50 ms e o grau de amolecimento estático durante este período foi calculado a partir do limite de escoamento no recarregamento, o qual foi medido por meio de duas diferentes técnicas: (i) o método de extrapolação inversa, e (ii) o convencional método 'offset'. Curvas de percentagem de amolecimento vs. tempo de interrupção foram plotadas a partir destes dados e a influência de adições de Mo, Nb e V na taxa de amolecimento foi determinada.

Os resultados mostram que a presença de Nb, Mo e V, em solução retarda, de uma maneira significante, os processos de recuperação e recristalização estática. Para uma mesma fração atômica, o efeito de retardamento devido ao Nb é consideravelmente maior que o do Mo ou V, o qual apresenta um efeito mínimo. No aço com Nb a 900°C, a precipitação induzida por deformação de Nb(C,N), após um tempo de interrupção de 10 s, conduziu a um posterior atraso de cerca de uma ordem de

magnitude no processo de recristalização estática. Nenhum
retardamento devido a precipitados foi observado no aço com V.
O uso de uma lubrificação com grafite ao invés de vidro
diminuiu o retardamento dos processos de amolecimento no aço
com Nb. Este resultado é atribuído à presença de precipitados
de NbC que não foram dissolvidos durante o tratamento térmico de
austenitização. Estes precipitados decresceram a quantidade de
Nb em solução antes do material ser deformado. Valores do
Parâmetro de Retardamento devido a Solutos (PRS) foram deter-
minados para Nb, Mo e V em condições estáticas. Embora a com-
paração com as correspondentes quantidades obtidas em condições
dinâmicas tenha mostrado a mesma ordem de efetividade, valores
consideravelmente maiores do PRS foram obtidos em condições
estáticas. As quantidades totais de amolecimento devido à
recuperação estática calculadas pelo método 'offset' são o
dobro das determinadas por extrapolação inversa. Esta última
técnica é considerada como a mais indicada para prever a
influência da recuperação nas cargas de laminação durante os
processos industriais.

ACKNOWLEDGEMENTS

AGRADECIMENTOS

O autor é grato ao seu orientador, Dr. J.J. Jonas por suas estimulantes discussões e sugestões e constante encorajamento durante todo o período desta pesquisa. Sua gradidão se extende a todos os seus colegas de pós-graduação e aos professores visitantes por seu interesse e apoio e por criarem um agradavel ambiente de trabalho.

Especiais agradecimentos são devidos ao Dr. Nicholas Christodoulou por sua inestimável assistência na preparação do progroma de computador para os testes e também na operação de máquina de compressão MTS. O autor é particularmente grato à Dr. M.G. Akben pela ajuda e apoio recebidos durante a realização deste trabaho. Ele também expressa seu reconhecimento a Martin Knoepfel pela sua assistência na preparação dos corpos de prova.

O autor gostaria de expressar sinceros agradecimentos ao CANMET pelo fornecimento do material para as experiências.

Ele deve agradecimentos à Canadian International Development Agency pela concessão da bolsa de estudos de Pós-graduação e ao STI/MIC e à Usinas Siderúrgicas de Minas Gerais S.A. - USIMINAS, Brasil, por assegurarem o período de ausência durante o qual este estudo foi efetuado.

To my mother and my wife,

the two treasures of my life.

A minha esposa e a minha mãe,

os dois tesouros de minha vida.

TABLE OF CONTENTS

LIST OF FIGURES

Figure

Figure

Figure

Page

LIST OF TABLES

CHAPTER 1

INTRODUCTION

The controlled rolling of microalloyed steels has been
successfully applied to the mass production of HSLA steels for
the past decade and a half. During these years, the increas-
ing demand for steels with high yield strengths, superior frac-
ture toughness and improved weldability has been the main
factor responsible for the development and improvement of this
rolling technique. Recently, the need for saving energy and
decreasing production costs, coupled with still more demanding
property requirements, are making imperative the optimization
of the design of controlled rolling schedules. Also playing a
role in the need for higher efficiency is the selection of the
steel chemistry on the basis of rational principles. This can
only be achieved if a clear understanding of the role played
by the microalloying elements is available. For example, the
influence of additions of Nb, Mo, Ti and V on the retardation
of both static recovery and static recrystallization in de-
formed austenite must be well understood. Two mechanisms have
been proposed to date regarding the modification of these
softening processes by the microalloying elements: the pinning

effect of strain induced precipitates; and the drag effect attributable to the presence of solute atoms. Which of these has the more important role has been subject to great debate and a general consensus has not yet been reached regarding their specific contributions. Some researchers have favoured an explanation based solely on solute effects; others have concluded that the key mechanism is the process of strain induced precipitation; still others support the idea of a combination of both effects.

It was the main purpose of the present investigation to shed more light on this debate, and in order to accomplish this aim, the effects of Mo, Nb and V addition on the retardation of static recovery and recrystallization were determined in a series of microalloyed steels. Each of these steels contained one of the above elements as a single addition. The retarding influence of each element was investigated by measuring the amount of softening taking place after an interval of deformation at an elevated temperature. The solute effects of Nb and V were distinguished from their effects as precipitates by the determination of the influence of these elements on the static softening rates after intervals of deformation as short as 0.05 s and, therefore, prior to precipitation. A secondary objective of this research was to compare the static retardations determined here with the dynamic ones obtained

in previous investigations and to try to establish a calibration or conversion factor linking the onsets of static and dynamic recrystallization. Finally, an inadvertent modification of the previous technique led to the presence during testing, of undissolved precipitates. This accidental result permitted the analysis of the influence of undissolved precipitates on the static recovery and recrystallization of hot worked austenite.

CHAPTER 2

CONTROLLED ROLLING OF MICROALLOYED STEELS

2.1 - THE CONTROLLED ROLLING PROCESS

2.1.1 Historical Considerations

Before the development of the High Strength Low Alloy (HSLA) steels, hot rolled C-Mn steels were used for most structural applications. The requirements for higher strength were achieved by increasing the C and Mn contents up to 0.35 and 1.50%, respectively. However, the impact properties and weldability of these steels were relatively poor (1,2). A solution to this problem was obtained by lowering the carbon content; compensation for the loss of strength was made by increasing the levels of elements such as silicon and phosphorus, or by adding chromium, nickel or copper (2).

By the early 1950's, it was well established that a fine ferrite grain size leads to an increase in yield strength coupled with a decrease in the transition temperature (3-5). The normalized, grain refined steels were introduced and the first grain refining agent used was aluminum (in conjunction with nitrogen) (6). Later, small additions of other grain refining elements, such as niobium, vanadium, titanium and

molybdenum, were found to have the additional benefit of contributing to precipitation hardening and therefore to higher yield strengths in this way (7,8).

At this time, HSLA steel products were manufactured through hot mill processing and heat treatment schedules closely related to the concepts developed in the production of plain C-Mn steels. This procedure led to a coarse, as-rolled austenite grain size and the optimum properties of the alloyed grades were not generally reached (2). The solution to this problem was the use of controlled rolling at a low finish-rolling temperature.

The term 'controlled rolling' was already used in 1958 and it was first applied to rolling schedules in which the finishing temperature was substantially lower than that employed in conventional practice (9). Such a low temperature rolling technique led to a refinement of the ferrite grain structure and to a corresponding improvement in the mechanical properties (10). This procedure also eliminated the need for further heat treatment. Despite the improvements that could be achieved through well designed rolling schedules, the process did not begin to be widely accepted until about the mid 1960's. This was probably influenced by the inconsistencies that occurred in some cases due to variations in the processing parameters and/or as a result

of an incomplete knowledge of the mechanisms involved (11).

Increasing demands by the oil and gas industry for steels with high yield strengths, superior fracture toughness and improved weldability were the principal factors responsible for the development and, finally, the universal acceptance of the controlled rolling process. The properties of these steels, used for line pipes, could not be entirely satisfied by either the conventional hot rolled or the normalizing processes, but could be comfortably met with control rolled low carbon steels containing microalloying elements such as niobium and vanadium. The term controlled rolling has now assumed a wider significance and describes the rolling technique where a low finishing temperature is employed in conjunction with a rolling schedule and particularly a cooling rate, all of which are closely controlled (12).

Recently, rising demands for saving energy and lowering production costs are leading to the application of controlled rolling techniques in the manufacture of plates up to about 40 mm thick for ships, pressure vessels and seamless pipes, of coils of hot strip, as well as of section mill products. Furthermore, the increasing requirements for large diameter and thicker wall line pipe have accelerated the development of the technology for producing steels with still higher toughnesses and strengths.

2.1.2 - <u>Aims and Principles</u>

The major purpose of controlled rolling is to promote ferrite grain refinement as a result of two mechanisms:

(i) refinement of the austenite grain size by hot rolling at intermediate temperatures (about 1000°C);

(ii) production of very fine grained ferrite through the γ-to-α transformation of deformed austenite grains.

The controlled rolling process can be divided into 3 stages of rolling (13-15):

- deformation in the recrystallized austenite region (temperature range above about 1000°C);

- deformation in the unrecrystallized austenite region (temperature range from about 950°C to the γ-to-α transformation temperature - Ar_3); and

- deformation in the ($\alpha+\gamma$) two phase region (below Ar_3).

In the first stage, the initial, very coarse austenite grains are refined by repeated deformation and recrystallization. The number of recrystallization cycles depends on the temperature, reduction per pass and the initial austenite grain size (16). Recrystallization can take place during rolling (dynamic recrystallization) and/or during the interpass time (static recrystallization). The processing conditions which favor the first process are high temperature, large reductions and low strain rate.

The recrystallized austenite grain size depends on factors such as deformation temperature, amount of reduction and initial austenite grain size. It decreases with decrease in rolling temperature and in initial austenite grain size. Increase in the amount of reduction also decreases the recrystallized grain size. However, during this first stage of rolling, austenite grains can only be refined to a limiting size of about 20 μm, which is larger than that obtained by the conventional normalizing treatment (17).

By rolling in the unrecrystallized austenite region, austenite grains are elongated and numerous deformation bands are produced. As the austenite-to-ferrite transformation takes place preferentially at austenite grain boundaries and deformation bands, deformation in this region produces very fine ferrite grains because of the significant increase in the density of ferrite nucleation sites. Recrystallization is prevented in part because the time to the onset of recrystallization increases considerably at lower temperatures. Although the recrystallization start time is reduced as the amount of deformation is accumulated in this temperature range, the onset of recrystallization can be delayed by more than an order of magnitude in time (with respect to the plain C behavior) by appropriate microalloying. This

is a matter to which we will return below.

The deformation of austenite at low temperatures accelerates ferrite formation and enhances the γ-to-α transformation. It thus has the effect of raising the Ar_3 temperature (18,19). The increase in the transformation temperature appears to be independent of the deformation temperature, but is cumulative for repeated deformations. This temperature also increases with decreasing initial austenite grain size.

The increase in the transformation temperature has two possible effects (10):

(i) it reduces the temperature range within which only austenite is present and consequently the temperature range for controlled rolling if it is desired to avoid deformation within the ferrite region;

(ii) it increases the ferrite grain size that may result from the increased growth rate of the ferrite at higher temperatures.

The effective transformation temperature can be decreased by increasing the cooling rate. Nevertheless, this trend is limited in practice by the improvement in the hardenability that normally accompanies the addition of elements such as Cu, Mn, Mo and Ni.

It is also possible to control roll steels within

the austenite-plus-ferrite, two phase region. This practice
can lead to further improvements in strength and toughness
(13,20). By rolling in this region, the ferrite grains are
preferentially deformed and elongated. Reductions in the
range 10 to 20% increase the dislocation density in the
ferrite without leading to substantial subgrain formation (21).
In this way, the strength can be increased without requiring
a sacrifice in toughness. Further deformation decreases the
toughness due to polygonization of the deformed ferrite. The
yield and tensile strengths continue to increase as the finish
rolling temperature is decreased, and as the amount of defor-
mation applied in the $\alpha+\gamma$ range is increased. This phenomenon
is not of industrial utility, however, because of the toughness
penalty which has already been referred to above, and because
it introduces the possibility of 'splitting'.

The development of a {100} texture when the amount of
deformation is greater than 10% causes the occurrence of
separations during the testing of edge-notched specimens. Due
to this factor, the Charpy shelf energy is reduced even though
the transition temperature is lowered (14). The increase in
strength of the steels rolled in the two phase region also
permits the lowering of the carbon equivalent at a given
strength, which improves the weldability of thick plates.
Deformation in this region furthermore eliminates the decrease

in yield stress due to the Bauschinger effect associated
with the UO process.

2.2 - DESIGN OF ROLLING SCHEDULES FOR CONTROLLED ROLLING

In its broadest sense, the controlled rolling process
consists of reheating, rolling and cooling, and the desired
properties are attained through improvement of the microstruc-
ture by controlling the recrystallization and transformation
behavior of the deformed austenite. It also involves the
effective use of alloying elements. The translation of the
above fundamental considerations into industrial practice
depends for its success on the extent to which the metallur-
gical phenomena associated with the different stages of the
process can be manipulated within the scope of the available
rolling mill equipment and the overall production programs.

2.2.1 - Metallurgical Aspects

Intensive research has been concentrated over the
past decade on the metallurgical aspects of controlled rol-
ling. This includes factors such as slab reheating tempera-
ture, austenite recrystallization rate and cooling rate.
These factors will now be discussed in turn.

- Slab reheating temperature - The selection of the slab
reheating temperature must be based on two competing considera-
tions:

(i)   the formation of large and non-uniform initial austenite grains must be prevented;

(ii)   the complete solution of all the relevant microalloy carbonitrides present in the steel must be ensured.

In addition, now that energy costs have risen so greatly, lower reheating temperatures can involve considerable savings in fuel, even if this entails the incomplete solution of the microalloying elements.

Large austenite grains (about 300 μm in dia.) are produced by the conventional reheating temperature of 1250°C. Thus lower reheating temperatures have the advantage of reducing the initial austenite grain size (15,22). Smaller initial austenite grains decrease the amount of deformation required for the onset of both static and dynamic recrystallization, and this makes easier the refinement of the grain structure during the first stage of rolling.

However, such low reheating temperatures must still be above the solution temperature of the appropriate microalloy carbonitride. This is because the presence of undissolved carbonitrides after soaking reduces both the retardation effect of austenite recrystallization after rolling and the strengthening effect by precipitation in the ferrite (23). By the application of a low reheating temperature, the holding time between passes required for the temperature

to drop to the necessary finishing level is reduced. This can permit the mill output to be increased. The reduction in the energy costs involved in heating to lower temperatures (which has already been mentioned) is somewhat offset by the requirement of higher loads. Thus the total energy requirements can be increased or decreased when the reheating temperature is reduced.

- Recrystallization of the austenite - During the controlled rolling of microalloyed steels, there are three possible austenite grain structures which are dictated by the actual temperature, reduction per pass, strain rate, interpass time and steel composition (24,25):

(i) the fully recrystallized, equiaxed structure. This structure is developed in the temperature range which corresponds to the roughing passes. At high temperatures (above 1050°C), strain hardening is followed by rapid recrystallization (less than 1s), and grain growth during the interpass time may give rise to large austenite grains. At intermediate temperatures (from 1050 to 1000°C) and under suitable conditions, grain refinement occurs by complete static recrystallization, and the interpass time is too short for the new grains to coarsen.

(ii) the unrecrystallized elongated structure - This structure

is produced by rolling at relatively low temperatures (below 950°C and above the Ar_3 temperature). This is the practice which corresponds to finishing when deformation during or after the γ-to-α transformation is avoided. In this case, recrystallization is completely suppressed by controlling the temperature, the reduction per pass, the interpass time, and most importantly, by appropriate microalloying. (The retardation of austenite recrystallization by the addition of microalloying elements will be discussed in more detail in section 2.4.) The combination of a high dislocation density and a high austenite grain boundary area per unit volume results in the rapid nucleation of ferrite and subsequent restricted growth by impingement. This situation leads to a fine-grained equiaxed ferrite with a final grain size related both to the amount of work carried out at these low temperatures and to the rate of cooling through the transformation range.

(iii) the partially recrystallized structure - This structure can result from the application of relatively small reductions at low temperatures. In this condition, fine recrystallized grains coexist with large grains that are deformed but unrecrystallized. Such

a situation can arise whenever the recrystallization times are comparable to the times between passes. When partial recrystallization occurs at some stage of the rolling schedule, leading to an uneven austenite grain size after rolling, the steel will transform to a mixed _ferrite_ grain structure having poor impact properties (11,26). Another condition leading to the development of a mixed austenite grain structure is the occurrence of rapid static recrystallization followed by non-uniform grain growth. Unless the subsequent deformation of this coarse-grained austenite is extremely severe, a mixed austenite structure is produced due to inhomogeneous deformation (27). It is imperative in the design of controlled rolling schedules to avoid the formation of partially recrystallized austenite because this struc- ture, once developed, cannot readily be eliminated by further rolling and, on transformation, a duplex ferrite with inferior properties results.

The microstructural changes taking place in deformed austenite can be followed by measuring the amount of mechanical softening occurring during the interpass time. This is shown schematically in Fig. 2.1 by a fractional softening vs. inter- pass time curve. Such a mechanical method was used in the present work to determine the fractional softening after hot

compression. It will be described in detail in Chapter 3.
The factors influencing the fractional softening are rolling
temperature, reduction, strain rate, austenite grain size,
holding time between intervals of rolling, and the types and
amounts of alloying elements present. The softening due to
recovery is gradual and is affected by the temperature and
time available between the intervals of rolling. The transi-
tion from recovery to recrystallization is affected by the
temperature, reduction, strain rate, austenite grain size and
concentration of alloying elements, and once recrystallization
starts, the progress of softening is very rapid (13). When
recrystallization is complete, the fractional softening is
approximately equal to 100%. It is only equal to 100% exactly
in the absence of precipitation, and when the initial and re-
crystallized grain sizes are the same. If, for example, the
new grains are finer than the original grains, then the frac-
tional softening can be less than 100%, even for full recry-
stallization (28).

At high rolling temperatures, which correspond to the
roughing passes, the complete recrystallization of austenite
during the interpass time is desirable. This condition is
satisfied by rolling after an interpass time longer than t_2
(Figure 2.1). In opposition to the roughing stage, during
the finishing passes, it is necessary to avoid recrystallization
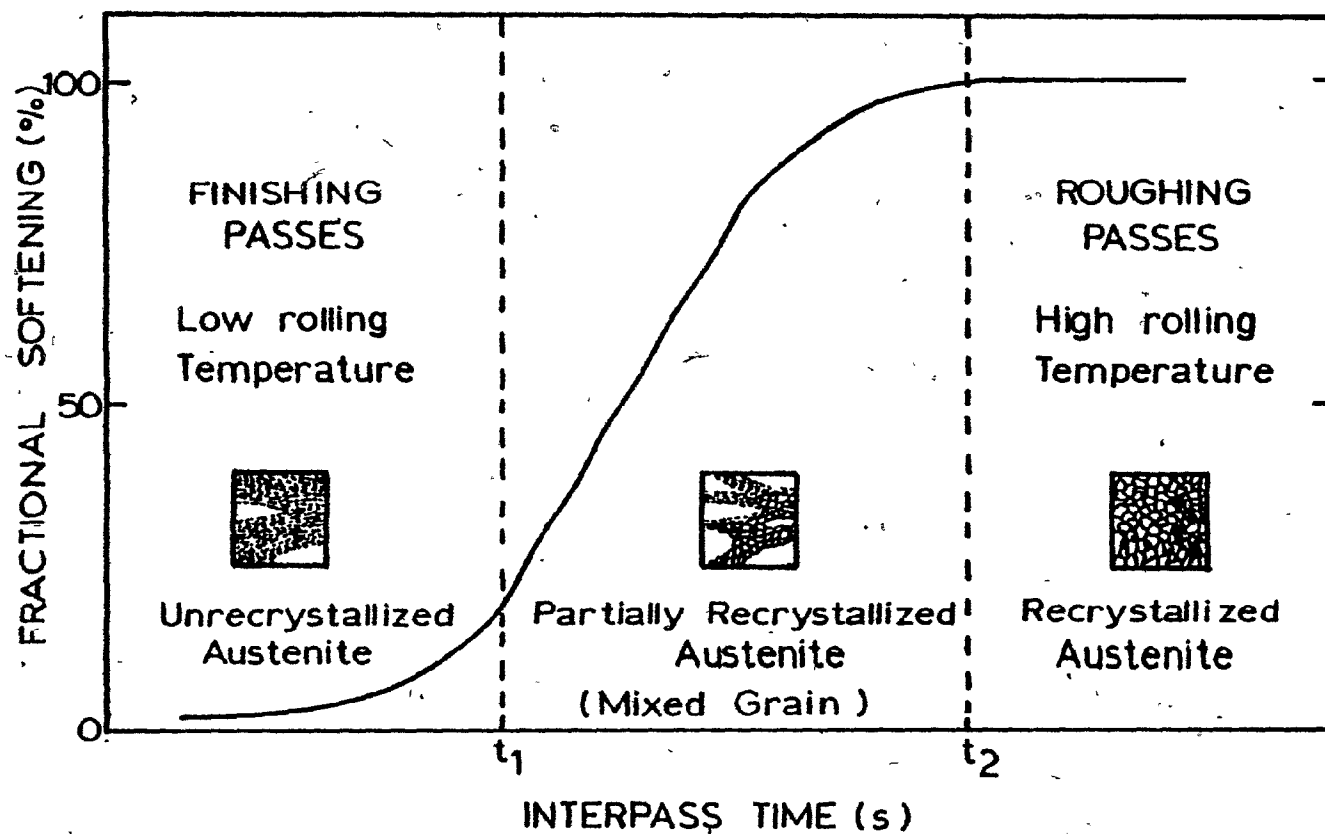
Figure 2.1 – Schematic representation of the correlation between the microstructural changes taking place in deformed austenite and the amount of softening brought about by these processes during the interpass time.

completely. Rolling must be performed in the recovery region with an interpass time shorter than t_1 (Figure 2.1). Deformation under conditions corresponding to the interval between t_1 and t_2 must be avoided because in this condition a partially recrystallized structure is developed.*

- <u>Cooling rate</u> — Controlled cooling after rolling can be used to produce fine ferrite grains and hence to improve both strength and toughness. Rapid cooling rates lower the transformation temperature, prevent austenite recrystallization prior to transformation, and reduce the extent of carbonitride precipitation in the austenite (1). The resulting enhanced precipitation in the <u>ferrite</u> leads to an excellent combination of strength and toughness. This is achieved in part because of the refinement of the ferrite grains, but also in part because the precipitation strengthening produced by the fine particles in the ferrite does not entail a significant sacrifice of toughness.

In the case of hot strip rolling, an increase in the cooling rate on the run-out table followed by coiling at a lower temperature (below 600°C) is a very effective way to increase strength (29,30). Similarly, in the rolling of thick plates, the application of rapid cooling to about 600°C followed by slow cooling below 600°C is recommended to improve the mechanical properties. Nevertheless, when

---

*Note that the time t_2 involved in plate rolling roughing passes is less than the time t_1 for the finishing passes. The softening curve (Fig. 2.1) shifts to longer times as the temperature is decreased.

the cooling rate is too high, the toughness may be reduced because of bainite formation. The optimum cooling rate must therefore be defined in connection with the hardenability of the steel.

2.2.2 - Engineering Aspects

A knowledge of the metallurgical aspects involved in controlled rolling is not enough for the design of optimum processing schedules. The increasing demands for stronger and tougher steels coupled with higher rates of production have made necessary the use of more stringent rolling procedures. Thus, particular attention is currently being paid to the engineering aspects of the controlled rolling process. These are related to mill constraints such as the mill force and torque limits, and economic constraints such as cost and productivity.

As the rolling temperature is decreased, a noticeable increase in mill load is observed because of the increase in deformation resistance. As shown in Fig. 2.2, the hot strength of austenite, K, is affected by processing parameters such as rolling temperature, reduction and strain rate, as well as by metallurgical parameters, such as chemical composition and the extent of microstructural change during rolling. The strength of austenite increases with increase in strain and strain rate, and with decrease in temperature. In the case
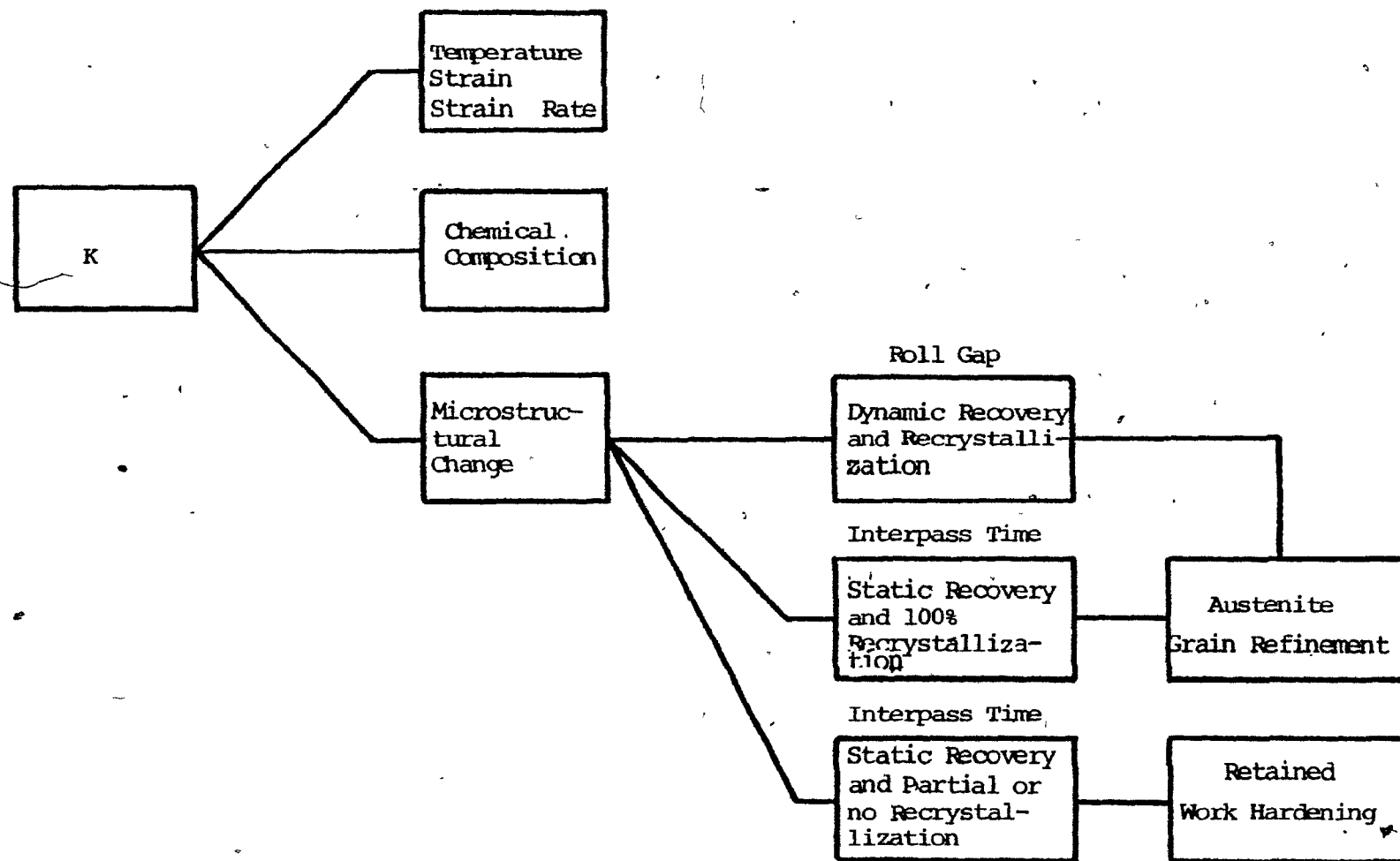
Figure 2.2 – Schematic representation of the metallurgical and processing parameters which affect the hot deformation strength of austenite, K.

of microalloyed steels, the addition of alloying elements strengthens austenite by both solid solution and precipitation hardening (31).

In the past, several formulae were proposed for the hot deformation strength of steels (32,33). In the use of these relations, the effects of microstructural change were generally simplified and the assumption was tacitly made that complete restoration took place by static softening during the interpass time. However, in the microalloyed steels, the hot strength increases with the accumulation of strain hardening during multi-pass rolling in the unrecrystallized austenite region. This "residual strain" reflects the lack of restoration in the microstructure and is dependent on the absence of static recrystallization during the interpass time.

The hot strength of austenite is an important variable for the prediction of roll separating force and torque (34-36). The accurate estimation of these two parameters is essential for the selection of the optimum pass schedule and the design of the mechanical and electrical capabilities of the mill process equipment. Recently, mathematical models have been developed for the deformation resistance in which all the microstructural changes taking place in the austenite during controlled rolling are considered. Such models can improve

the efficiency of rolling mills managed by computer control (37,38).

One of the economic constraints that has to be considered in the application of controlled rolling for the production of HSLA steels is the increase in the process time. This is due partly to the necessity of holding the material between intervals of rolling until the temperature falls to the required level. In addition, more passes are generally required during the finish rolling stage under these conditions. Longer process times cause a reduction in the rolling rate and introduce a serious loss in production, which may however be minimized by the use of lower slab reheating temperatures and by suitably modifying the mill layout(10,39). Another important economic aspect of controlled rolling is the lower yield or higher rejection rate associated with the more stringent process control requirements (40).

2.3 - THE SOFTENING PROCESSES INVOLVED IN CONTROLLED ROLLING

The importance of understanding the role of the static and dynamic restoration processes occurring during the controlled rolling of microalloyed steels is already clear from the discussion in the previous section. These softening mechanisms have a significant effect on the hot strength of

austenite, and their interaction is of vital importance in determining the final structure, and hence the final properties of a hot rolled steel. The restoration processes can act during <u>deformation</u>, i.e. inside the roll gap, or during the <u>interpass time</u>, which is the time between intervals of hot working. Softening takes place inside the roll gap by the mechanisms of dynamic recovery and dynamic recrystallization. The restoration processes occurring during the interpass time are comprised of static recovery, metadynamic recrystallization and static recrystallization (41). The softening mechanism which predominates depends on the interaction between processing parameters such as the temperature, strain and strain rate, and material parameters such as the grain size, stacking fault energy and precipitate character (42). The characteristics of these softening mechanisms will now be examined in turn.

2.3.1 - The Restoration Processes Occurring inside the Roll Gap

2.3.1.1 - Dynamic Recovery

During the initial stages of hot deformation, the flow stress rises, the dislocation density increases and some rearrangement and annihilation also take place. An equiaxed substructure begins to form, the scale of which increases with increasing temperature and decreasing strain rate (43,44). In metals and alloys of high stacking fault energy, such as Al

and the bcc metals, the rate of work hardening gradually decreases with strain until a steady state regime of deformation is established. Beyond this strain, the flow stress remains constant and, even at large deformations, the subgrains maintain a constant size and shape, while the grains undergo extensive elongation. This condition of essentially constant dislocation density represents a balance between the rates of strain hardening and dynamic recovery, with the subgrains continually breaking up and reforming at an equilibrium spacing.

In metals and alloys of moderate or low stacking fault energy, which is the case for steels in the austenite range, subgrains develop with very tangled boundaries and they are smaller than those formed in the metals described previously. In this situation, dynamic recovery alone is not able to reduce the dislocation density to stable levels during deformation (45). Thus, the rate of dislocation accumulation is relatively high and sufficient strain energy can be stored within the subgrains to provide the driving force for dynamic recrystallization.

2.3.1.2 - Dynamic Recrystallization

A critical dislocation density must be exceeded for the onset of dynamic recrystallization (46). The occurrence of this restoration process is marked by a drop in the flow stress, and metallographic observations indicate that dynamic

recrystallization is initiated at a strain considered to be about five-sixths of the strain to the peak in flow stress (47). However, for all practical purposes, this difference can be neglected and the strain at the maximum stress, referred to as the peak strain, can be regarded as the critical strain for the initiation of recrystallization.

Dynamic recrystallization is nucleated by the local bulging of austenite grain boundaries (31,48). The grains formed by dynamic recrystallization display a dislocation substructure, in contrast to the dislocation free nature of the grains observed after static recrystallization (49). The recrystallized grain size is not influenced by the initial grain size and is primarily controlled by the combination of temperature and strain rate. Deformation conditions corresponding to higher values of the Zener-Hollomon parameter, Z, give rise to finer recrystallized grains (48,50).

The peak strain for a given composition increases with increasing strain rate and initial grain size (16), and decreasing temperature (49). As a result, the conditions which favor dynamic recrystallization are rolling at high temperatures, large reductions, and a low strain rate. These factors indicate that dynamic recrystallization is unlikely to occur in microalloyed steels under the hot deformation conditions associated with commercial controlled rolling schedules (19, 25,48).

2.3.2 - The Restoration Processes Occurring during the Inter-
pass Time

2.3.2.1 - Static Recovery

The static recovery process does not involve an incu-
bation time and consists of the annihilation of dislocations
of opposite signs, as well as, of the rearrangement of disloca-
tions within the subgrains. During the process, the sub-
boundaries become sharper and the dislocation density within
the subgrains is reduced, with little change in the shape or
size of these. The main factors affecting the recovery rate
are the temperature, strain, strain rate and the addition of
alloying elements. The rate of recovery increases as the
temperature, strain and strain rate are increased (51). The
effect of alloying additions on the rate of static recovery
will be analysed in detail in the section that follows. The
static recovery process is particularly important during con-
trolled rolling in the unrecrystallized austenite region be-
cause, in this situation, it is the predominant softening
mechanism.

2.3.2.2 - Metadynamic Recrystallization

This type of recrystallization can only occur during
the interpass time if dynamic recrystallization has been ini-
tiated prior to the interruption of deformation (41). Meta-
dynamic recrystallization refers to the continued growth of

dynamic recrystallization nuclei after deformation has ceased. The significant feature of this process is that, unlike static recrystallization, no incubation time is required, as the nuclei are already present when straining is interrupted (52). Although metadynamic recrystallization proceeds very rapidly upon the termination of deformation, nucleation for static recrystallization can still take place in regions which do not contain dynamic nuclei.

The deformation conditions favoring metadynamic recrystallization are the same ones described for dynamic recrystallization, which makes unlikely the occurrence of this softening mechanism during the controlled rolling of micro-alloyed steels.

2.3.2.3 - Static Recrystallization

This restoration process is the most important of the softening mechanisms involved in controlled rolling. By controlling the progress of static recrystallization during the interpass time, the desirable austenite microstructure can be obtained at each stage of the rolling process. In this way, a final product with improved mechanical properties can be obtained. A critical amount of deformation is also required for the onset of static recrystallization. However, the critical strains associated with this softening mechanism are considerably less than those necessary to initiate

dynamic recrystallization (52).

Static recrystallization results in the strained grains being replaced by new strain-free grains, with a large number of dislocations being absorbed by the grain boundaries which are migrating through the metal (53). The recrystallized grain size decreases with a decrease in the initial grain size and an increase in the reduction. Finer recrystallized grains are also produced by deformation at higher strain rates and lower temperatures; such combinations correspond to higher values of Z, the temperature corrected strain rate. The combination of this parameter and the amount of deformation controls the driving force for recrystallization.

Both the incubation time and the rate of static recrystallization are influenced by the strain, strain rate, temperature and initial grain size. Finer initial grains and higher strain rates decrease the incubation time and increase the rate of recrystallization. For dynamically recovered structures, which are generally present in microalloyed steels produced by controlled rolling, the same result is obtained by increasing the strain (54). The effect of temperature is a result of its influence on the driving force and on the kinetics of static recrystallization through the Arrhenius term. For a constant driving force, an increase in the temperature

decreases the incubation time and increases the rate of recrystallization (51). The addition of alloying elements also affects the incubation time as well as the rate of static recrystallization. The manner in which this occurs will now be considered more closely.

2.4 - INFLUENCE OF MICROALLOYING ADDITIONS IN CONTROLLED ROLLING

Microalloying elements such as Mo, Nb, Ti and V play very important roles in the improvement of the strength and toughness of steels by the controlled rolling process. These roles are related to the retardation of recovery and recrystallization in deformed austenite, to the suppression of grain growth, to precipitation strengthening, and to a component of solute strengthening. The effects of these elements are manifested along two lines: they have influence as precipitates and as solutes.

2.4.1 - Effect of the Microalloying Elements as Precipitates

The precipitation of the microalloying elements, in the form of carbides, nitrides and carbonitrides, can take place in austenite and/or in ferrite during both the deformation and the cooling of microalloyed steels. As the time interval during which a steel remains in the roll bite or deformation zone is very short during rolling (e.g. 10 to 100 ms), precipitation during deformation is less important

from a practical point of view than precipitation during hold-
ing or cooling. The precipitates present in austenite have
different effects according to their size and spacing (55).
When the particles are large (100 - 300 nm in dia.), with a
spacing greater than the size of recrystallization nuclei,
there may be little influence on the recrystallization kine-
tics, but a major influence on subsequent grain growth. When
they are fine (5 - 20 nm in dia.), with a spacing less than
the size of recrystallization nuclei, recrystallization may
be severely retarded.

During slab reheating and soaking, the complete dis-
solution of all the microalloying precipitates is desirable.
However, in the case of low temperature reheating, the amount
of these particles that can be taken into solution is reduced
and undissolved precipitates may remain prior to rolling.
These undissolved precipitates may inhibit grain growth of
the initial austenite grains (1,7,56,57), and may also accelerate
recrystallization (58,59), particularly if they are large enough
to generate strain gradients, and hence recrystallization
nuclei, at their interfaces. The precipitation of very fine
and uniformly dispersed particles generally takes place in
deformed austenite (during the interpass time) at low tempera-
tures. The deformation of austenite introduces large quantities
of lattice defects which, together with the pre-existing grain

boundaries, provide the most favorable nucleation sites for precipitation (60). This 'strain-induced precipitation' is affected by the rolling temperature, the amount of deformation, the strain rate and the degree of supersaturation (61,62). Strain-induced precipitates can retard both the onset and the progress of recrystallization. This effect has been attributed to the retardation of both the <u>nucleation</u> and the <u>growth</u> processes by the following mechanisms:

- The stabilization of the substructure by the dispersed particles prevents the nucleation of new grains (51); and

- The pinning action of the precipitates on grain boundaries and sub-boundaries inhibits their migration (60,63-65).

In addition to precipitation in austenite during hot working, precipitation may also take place during the austenite-to-ferrite transformation (66,67). Such interphase precipitation is enhanced by high solute solubility and high transformation temperatures. The characteristic feature of these precipitates is their linear arrangement, the spacings of which correlate with the cooling rate through the transformation. As the cooling rate increases, the rows become more closely spaced and the precipitates more effective as dispersion strengtheners (60). Further precipitation in the transformed ferrite matrix is desirable to impart additional strengthening via precipitation hardening, although a loss in toughness is also produced.

The precipitates formed in ferrite are much finer than the others (68) and, apart from their strengthening effect, they also act as barriers to the migration of ferrite boundaries during cooling, leading to further grain refining in this way (60). In this case, the deterioration in toughness, caused by the precipitation strengthening, may be lessened.

The amount of each microalloying element available for precipitation in ferrite is determined by the amount of prior precipitation in austenite. The precipitates which have already contributed to ferrite grain refinement through the suppression of austenite recrystallization, are no longer effective for the precipitation hardening of the ferrite matrix (22,69). Consequently, hot rolling schedules which emphasize grain refinement tend to minimize precipitation hardening (70). The ideal controlled rolling schedule would be the one in which the relative amounts of precipitation in the austenite and ferrite could be controlled in order to take advantage of all the beneficial effects of these two modes of precipitation.

Among the precipitate-forming elements added in micro-alloyed steels, niobium (Nb) has been found to be the most effective in controlled rolling. The precipitation of Nb(C,N) can take place in both austenite and ferrite, in all the modes described above. Thus, Nb can be very effective for the

refinement of austenite grains upon reheating, for the retardation of austenite recrystallization, and for the strengthening of ferrite. The addition of titanium (Ti) up to 0.02% prevents the grain coarsening of austenite during reheating up to 1200-1300°C. This effect is due to the precipitation of very stable TiN during solidification (55). At higher concentrations, e.g. 0.1 to 0.2%, the precipitation of TiC takes place at lower temperatures in the austenite and causes some retardation of recrystallization (71). Precipitation hardening can also be obtained by the precipitation of TiC in ferrite. Because of its low solution temperature, vanadium (V) cannot prevent austenite grain growth during reheating. Moreover, the influence of the strain-induced precipitation of VN on austenite recrystallization kinetics is weaker than that of Nb(C,N) and TiC, and occurs only at temperatures below about 900°C. Nevertheless V contributes in a substantial way to ferrite strengthening through the precipitation of carbonitrides and is frequently added together with Nb. Molybdenum (Mo) may also contribute to the strengthening by the precipitation of carbides in ferrite. It does not, on the other hand, precipitate in austenite when added alone, but can form co-precipitates in the presence of Nb and V.

2.4.2 - Effect of the Microalloying Elements as Solutes

There has been considerable debate over a period of

years regarding the role of the microalloying elements in the retardation of recovery and recrystallization. Some evidence indicates that it arises from solid solution effects, whilst other evidence indicates that precipitation is essential. The difficulty in distinguishing between the individual effects of solutes and precipitates arises from the following problems:

- Niobium, vanadium and titanium can form carbides or nitrides easily in the presence of very small amounts of C and N;

- The techniques available to detect precipitation in austenite have limitations with regard to the minimum observable size of precipitate; and

- The working variables, such as strain, strain rate, soaking temperature and deformation temperature, have major effects on the recrystallization kinetics.

The delay observed in the recrystallization of microalloyed steels has generally been attributed only to the effect of strain-induced precipitates (26,70,72-74). However, evidence exists supporting the hypothesis of a solute effect. Basically, four groups of experiments can be distinguished according to the approach employed in the attempt to separate the effects of solutes and precipitates:

- The first group includes the work of Le Bon et al. (75), Weiss and Jonas (76-78), and Coladas et al. (57). The approach used by these researchers was related to the interaction of precipitation and recrystallization and was based on the determination of RTT (recrystallization-temperature-time) diagrams for both plain C and micro-alloyed steels with the same base composition. The PTT (precipitation-temperature-time) curves were also determined for the precipitates formed in the latter steels. The results obtained in these investigations showed that, in the microalloyed steels at temperatures above 1000°C, recrystallization starts before the onset of precipitation and is nevertheless delayed in comparison with the plain C steels. It was concluded, therefore, that this retarding effect is due to the microalloying elements in solution. At lower temperatures (e.g. 900°C), precipitation starts before the onset of recrystallization, and the latter mechanism is delayed still further by the additional retarding effect of the fine precipitates.

- The second group corresponds to researches in which the microalloyed steels being investigated are decarburized and/or denitrided. As result of these heat treatments, precipitation is completely suppressed under the testing conditions, and the solute effect of each microalloying

element on the recovery and recrystallization processes
can be determined directly. The studies of Luton et al.
(79) and Ouchi et al. (80) belong to this category.

- The third group concerns investigations which involve
the determination of the recrystallization rate in a
reference plain C steel and in a comparable microalloyed
steel where the experiments are carried out <u>above the
solution temperature</u> (T_{sol}) of the carbonitride. Under
these conditions, precipitation is no longer of importance
and the solute retardation produced by the relevant micro-
alloying addition can again be measured directly. The
investigations of White and Owen (81) and of Akben, Bacroix and
Jonas (82) are good examples of this kind of approach.

- The last group is constituted of the work of Ouchi et al.
(29). These authors have constructed a computerized com-
pression machine which allows the performance of inter-
rupted compression tests involving unloading times as short
as 0.1 s. These tests have permitted the reliable deter-
mination of the solute effect of several elements on the
recovery rate of deformed austenite in the interval prior
to the initiation of precipitation.

The results described in the references reviewed above
show that the microalloying elements <u>in solution</u> retard re-
covery in deformed austenite and consequently delay the onset

of recrystallization. By contrast, they have less influence on the progress of recrystallization, once initiated. The largest effect is produced by Nb, followed in decreasing order by Ti, Mo and V. The retarding effect of these elements in solution has been attributed to the following factors:

- Solutes can obstruct the rearrangement of dislocations, a process associated with recovery in general and with nucleation in particular, delaying the onset of recrystallization in this way (83).

- Solute additions can lower the stacking fault energy, which makes recovery more difficult (51).

- The presence of solute atoms at grain boundaries which are not moving very fast can generate a 'solute drag force' which will impede their motion and, therefore, retard recrystallization (84).

Recently, some authors (76,78,85,86) have suggested that the retardation of recrystallization is due to a suitable combination of both effects of adding microalloying elements: i.e. that they have an influence as precipitates and also as solutes. According to these investigators, precipitation alone is insufficient to prevent austenite recrystallization during steel processing and solute effects are essential to prevent recrystallization until precipitation can become effective.

It is the main purpose of the present work to shed more light on the role played by the microalloying elements on the static recovery and recrystallization processes during the controlled rolling of microalloyed steels.

CHAPTER 3

EXPERIMENTAL MATERIALS AND PROCEDURE

3.1 - EXPERIMENTAL MATERIALS AND HEAT TREATMENT PROCEDURE

Three microalloyed steels were used in the present work, with the purpose of investigating the individual effects of Mo, Nb and V on static recovery and recrystallization after high temperature deformation. These steels were prepared in the Physical Metallurgy Research Laboratories of the Department of Energy, Mines and Resources (Ottawa), and their chemical compositions are listed in Table 3.1, together with the composition of a reference plain C steel.

The specimen preparation and heat treatment procedures were based on those used in previous investigations (87,88). For the compression tests, cylindrical samples were machined from the as-received plates with the compression axis parallel to the rolling direction. A diameter-to-height ratio of 1.5 was selected to promote homogeneous deformation (87-90). The end surfaces of the specimens were grooved following a design based on the work of Luton (91), which allows for the maximum retention of lubricants. The sample dimensions and the details of the groove geometry are indicated in Fig. 3.1.

All the samples were heat treated at 1000° for two

Table 3.1

Chemical Composition of the Steels Investigated, wt.%

Steel	C	Mn	Si	Al	V	Mo	Nb
Plain C	0.06	1.43	0.24	0.025	–	–	–
V	0.05	1.20	0.25	0.030	0.115	–	–
Mo	0.05	1.34	0.20	0.065	–	0.29	–
Nb – Mn	0.06	1.90	0.225	0.030	–	–	0.035

N ≃ 0.006, P ≃ 0.006, S ≃ 0.012

Specimen Dimensions (mm)		
size	Length (L)	Diameter (D)
1	11.4	7.6

Groove Dimensions (mm)				
size	A	B	C	E
1	0.18	0.15	0.36	0.10

Tolerance	0.02
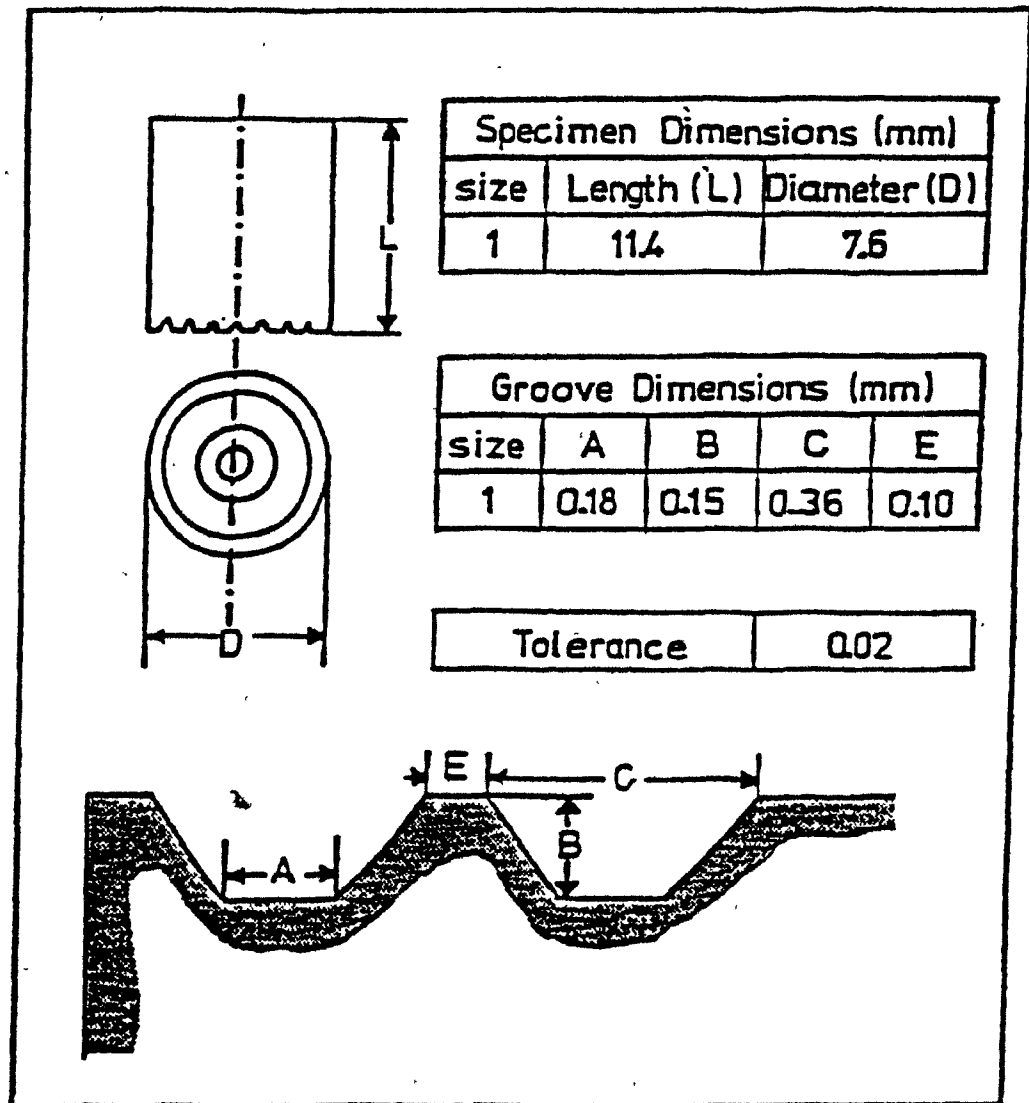
Figure 3.1 - Compression test sample geometry and groove design.

hours under vacuum, and then air cooled. This normalization heat treatment was carried out in order to eliminate the rolling texture present in the as-received material; such textures frequently lead to the production of elliptical cross-sections in deformed samples. An austenitization heat treatment was carried out immediately prior to the testing of each sample with the following aims:

- .To ensure the complete dissolution of all the microalloyed carbonitrides present; and

- To produce approximately the same austenite grain size in all the steels. .

The equilibrium solution temperatures of VN, V_4C_3, NbC and Nb(C,N) were calculated from the relations given by Cordea (reference 2)

$$\log (V) \times (N) = -\frac{7733}{T} + 2.99, \qquad (1)$$

$$\log (V)^{4/3} \times (C) = -\frac{10800}{T} + 7.06, \qquad (2)$$

and

$$\log (Nb) \times (C) = -\frac{7510}{T} + 2.96 \qquad (3)$$

In these equations, (C) (N) (Nb) and (V) are the concentrations in weight percent of C, N, Nb and V respectively, and T is the absolute temperature. The equilibrium solution temperature of Nb(C,N) was calculated from equation (3) by taking the carbon equivalent for (N) as 12/14 (N). In order

to ensure complete solution, the actual austenitization temperatures for the Nb and V steels were raised above the estimated solution temperatures. The times for which the samples were held at these temperatures as well as the austenitization temperatures and holding times for the other steels were chosen to give the same initial grain size (87,88). The equilibrium solution temperature, the austenization temperature, the holding time and the initial grain size for each one of the four steels are listed in Table 3.2.

3.2 - EXPERIMENTAL EQUIPMENT

The hot compression tests were carried out on a 100 kN MTS closed loop electrohydraulic testing machine. A CENTORR model M60 front loading high temperature vacuum furnace was used to provide the temperature requirements for the experiments. In order to perform constant true strain rate compression tests, the MTS testing machine was linked, by means of an MTS 433 interface, to a PDP - 11/04 minicomputer. The load and the displacement measurements stored by the computer during the compression of the sample were displayed visually on a Tektronix 4010 graphics terminal immediately after each test. Flow curves were then plotted using the same terminal and copies were provided by a Tektronix 4613 hardcopy device. Following that, the test data were transferred to a floppy

Table 3.2

Calculated Solution Temperature, Austenitization Temperature, Holding
Time and Initial Austenite Grain Size for the Steels Tested

Steel	Precipitate	Calculated Solution Temperature (°C)	Austenitization Temperature (°C)	Holding Time (s)	Initial Austenite Grain Size (μm)
Plain C	-	-	1030	900	110
V	VN	984	1045	1800	100
	V_4C_3	850			
Mo	-	-	1070	1800	110
Nb - Mn	NbC	1041	1100	1800	120
	Nb(C,N)	1050			

disk for permanent storage, so that they could be recalled
at will at a later date. An external view of the test
assembly, which includes the MTS testing machine, the furnace,
the PDP 11/04 computer, the Tektronix terminal and the con-
trol consoles for the vacuum system and temperature regula-
tion, can be seen in Fig. 3.2. A more detailed description
of the equipment is given in Reference (92).

The compression tooling was comprised of an upper and
lower anvil (Udimet 500) tightly screwed to the respective
stainless steel extension rods. The top extension rod was
fixed to the ram of the MTS machine, whereas the lower one
was attached to the load cell (Fig. 3.2). SiN inserts were
placed at the ends of the anvils and were held in position
by superalloy nuts. These smoothly ground inserts provided
a minimally deforming low friction compression surface for
the samples. An interior view of the furnace chamber, show-
ing the compression tools, test specimen and details of the
heating system, can be seen in Fig. 3.3. Tungsten tools
were also used in 20 compression tests, because no SiN in-
serts were available for the experiments during part of
the period of the investigation.

3.3 - EXPERIMENTAL METHOD

The method of interrupted compression testing de-
veloped by Petkovic (89) was used in the present study to

1) MTS load frame, 2) Centorr furnace, 3) Temperature and vacuum control console, 4) PDP 11/04 computer, and 5) Tektronix terminal

Figure 3.2 – An external view of the high temperature compression testing equipment.
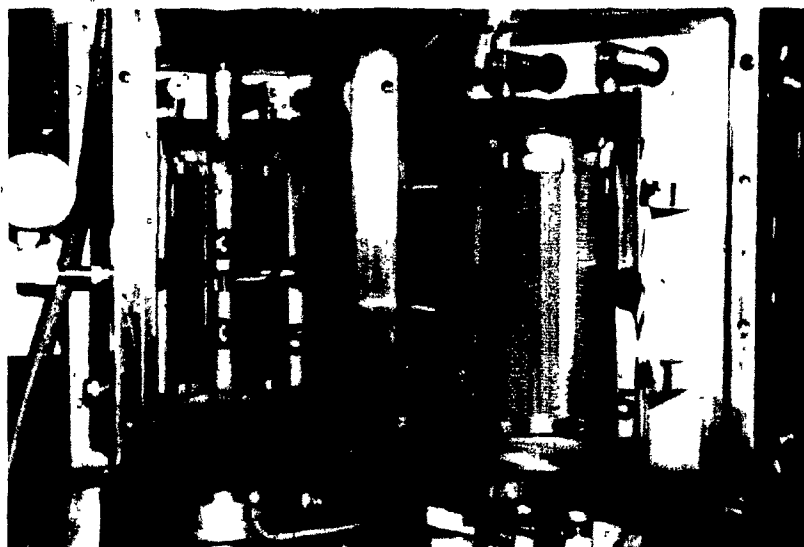
1) Specimen, 2) Thermocouple, 3) Tungsten Tooling, 4) Tungsten mesh heating elements, 5) Tungsten and molybdenum shields and 6) vacuum chamber.

Figure 3.3 – An interior view of the CENTORR high temperature furnace and compression train.

examine the softening behaviour of austenite during inter-
vals of hot working. This technique is based on the principle
that the yield stress at high temperatures is a sensitive mea-
sure of the structural state of the material. A typical true
stress-true strain curve obtained in these experiments is
shown in Fig. 3.4. Samples are loaded, at a constant tempera-
ture and true strain rate, to a fixed strain (point A - Fig. 3.4)
and then unloaded. After a given time interval, the samples
are reloaded at the same strain rate as before. The magnitude
of the yield stress on reloading is governed by the degree of
structural change that has occurred during the holding inter-
val and can therefore be taken as a measure of the progress
of static softening (93).

3.3.1 - Short-Time Interrupted Compression Tests

In order to determine the effects of Mo, Nb and V addi-
tions on the static recovery rate of deformed austenite, a
program was developed to perform interrupted compression tests
at constant true strain rate and at unloading times shorter
than 1 s. As already mentioned, this kind of test has previously been carried out in Japan by the research group of
Ouchi and co-workers (29), with the difference that, in their
experiments the crosshead speed is kept constant. The program
was written in MTS Basic and is listed in Appendix A. A
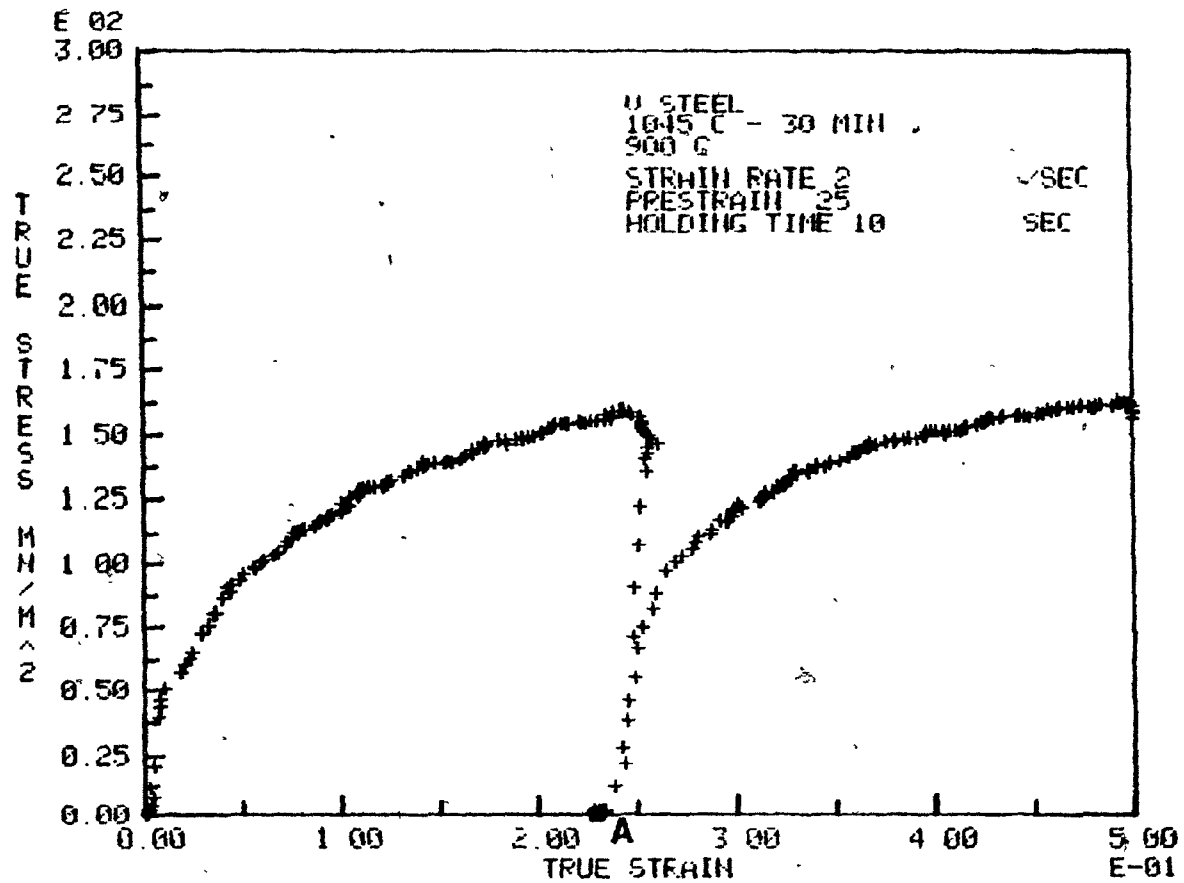
Figure 3.4 - Typical flow curve for an interrupted com-
pression test.

series of preliminary experiments was carried out using
lead and a plain C steel with the purpose of improving the
program and determining the shortest unloading time possible
with the equipment described above. In this way, the mini-
mum holding time between intervals of deformation was found
to be 0.05 s. Shorter times are not possible because of
the mechanical inertia inherent in the MTS loading system.
Fig. 3.5 shows a load vs. time curve for the plain C steel
tested at 900°C and at a constant strain rate of 2 s^{-1}. In
this case, a true strain of 0.25 was applied in the first
compression. The sample was then unloaded and held at zero
load during 58 ms. After that, a second true strain of
0.25 was applied at the same strain rate. It also can be
seen that a time of 15 ms was necessary for the transition
from loading to complete unloading.

3.3.2 - Selection of the Test Conditions

The temperatures chosen for the experiments were 1000
and 900°C. The first one (1000°C) corresponds to the stage
of the controlled rolling process where the refinement of
the austenite grain size is still possible by complete re-
crystallization during the interpass time. At 900°C, by
contrast, recrystallization between the intervals of hot
working should be avoided entirely. The time required for
cooling from the austenitization to the test temperature
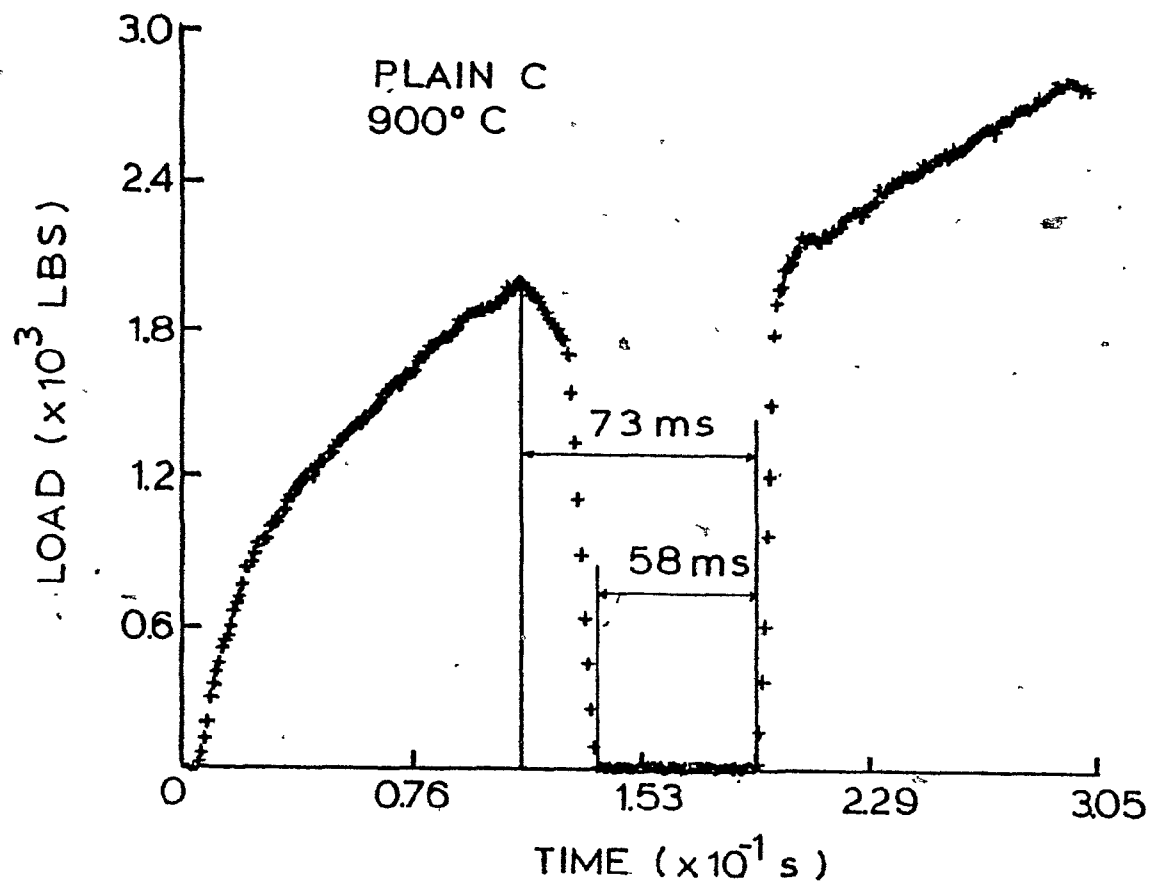
Figure 3.5 - Short-time interrupted compression test for a
plain C steel at 900°C with a load-free time
of 58 ms.

and further stabilization was about 3-4 minutes for the experiments at 1000°C and 5-8 minutes for the experiments at 900°C. These times were somewhat higher than the ones obtained in other studies (87,88), mainly because the practice of cooling by opening the furnace or by injecting an inert gas was not possible with the furnace used in this investigation.

The two other experimental conditions, strain rate and strain, were selected to be as close as possible to those prevailing in industrial rolling processes. For this purpose, a strain rate of 2 s^{-1} was selected. Higher strain rates (which would have been closer to mill strain rates) did not provide enough data points to enable accurate determination of the first and second yield stresses. The true strain vs. time curve which corresponds to the experiment described in Fig. 3.5 is shown in Fig. 3.6. The strain rate is given by the slope of the curve, and it can be seen that its value is equal to 2 sec^{-1} and zero during the deformation and the unloading time, respectively.

The interruption strain was determined mainly by the necessity of avoiding dynamic recrystallization during pre-straining, and the metadynamic recrystallization during the holding time that would inevitably follow. Its selection was based on a continuous compression test performed on the plain C steel at 1000°C and a constant strain rate of 2 s^{-1}.
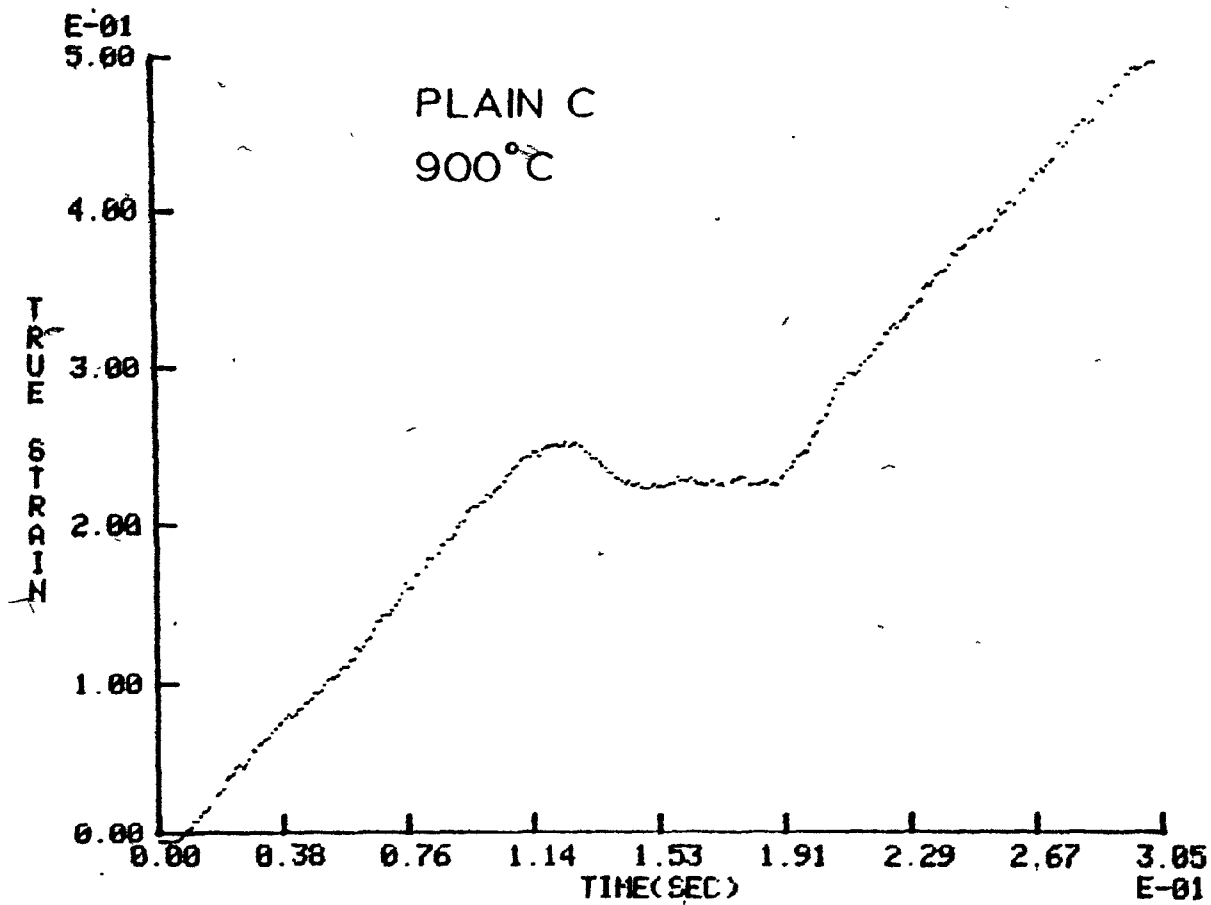
Figure 3.6 - Strain rate behavior during an interrupted compression test.

The true stress-true strain curve of this experiment is given in Fig. 3.7. Based on this curve, a strain of 0.25 was chosen as the maximum amount of deformation to be given in both compressions. It can be seen (Fig. 3.7) that this strain is considerably less than that required for the on-set of dynamic recrystallization, which corresponds to a strain somewhat less than that associated with the peak stress. Because of the conversion from axisymmetric to plane strain, this strain is also equivalent to a reduction of about 20% in rolling.[*] As the critical strain for dynamic recrystallization increases with a decrease in temperature and with the addition of microalloying elements, if a deformation of 0.25 will not provoke dynamic recrystallization in the plain C steel at 1000°C, it is unlikely to do so during the prestraining of the other three steels at 1000 and 900°C.

3.3.3 - Methods for Determining Softening

The degree of softening, X, after an interval of hot working, is given by the expression

$$X = \frac{\sigma_m - \sigma_r}{\sigma_m - \sigma_o} \qquad (4)$$

---

[*]Note that $\varepsilon_{eq} = \varepsilon_{axi} = \ln h_o/h_f$ for axisymmetric compression. Here ε_{eq} and ε_{axi} are the equivalent and axial strains in the compression test, and h_o and h_f are the initial and final sample heights. In rolling, $R = (H-h)/H \times 100\%$, where R is the percent reduction and H and h are the initial and final slab thicknesses. For plane strain deformation, $\varepsilon_{eq} = 1.155 \varepsilon_1$ where $\varepsilon_1 = \ln (H/h) = \ln (1/(1-R))$. Thus, for $\varepsilon_{axi} = \varepsilon_{eq} = 0.25$, $\varepsilon_1 = 0.216$ and $R \approx 19.5\%$.
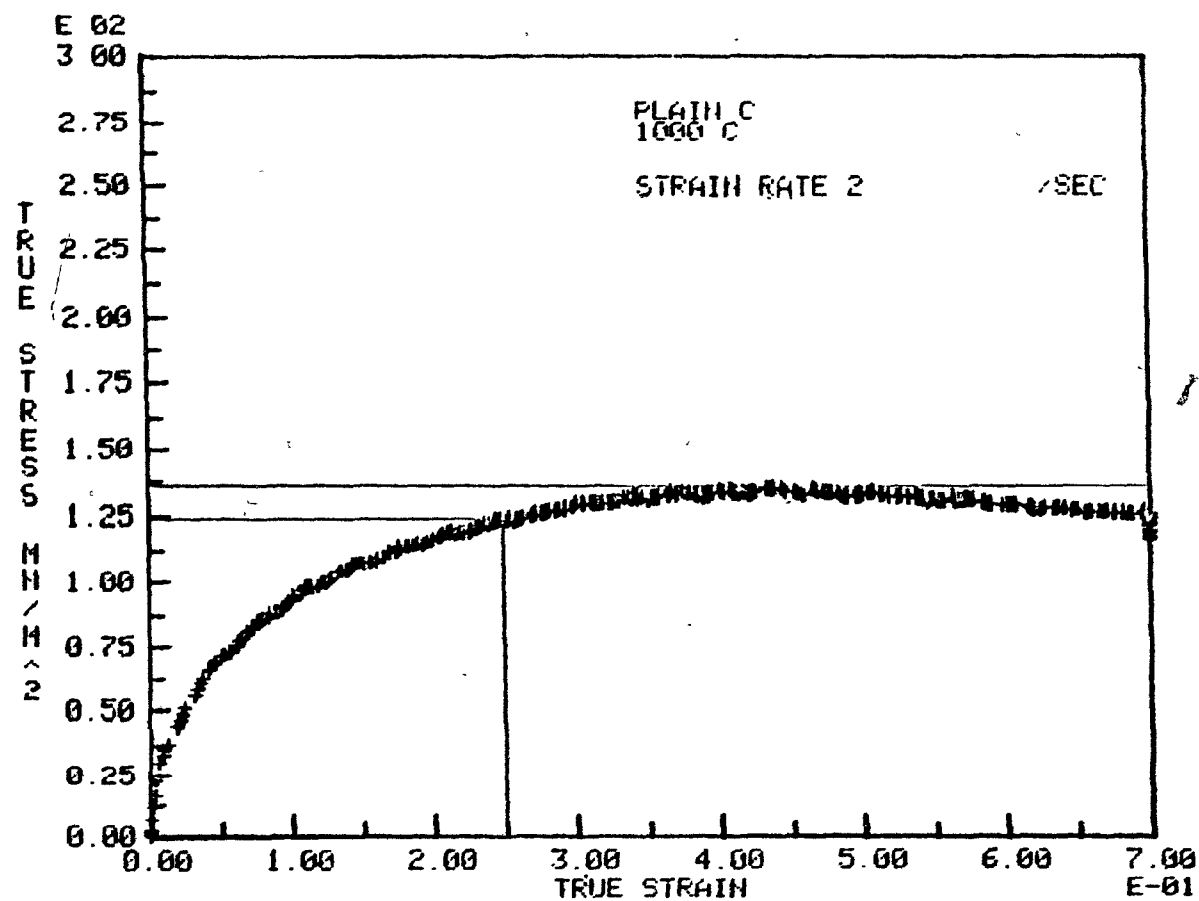
Figure 3.7 - Flow curve for a continuous compression test in a plain C steel at 1000°C and at a constant true strain rate of 2 s^{-1}.

where σ_m is the flow stress immediately before unloading and σ_o and σ_r are the initial flow stresses recorded during prestraining and reloading, respectively (Fig. 3.8).

In this research, two methods were used to determine the initial flow stress on reloading, σ_r: (i) the conventional offset method and (ii) the back extrapolation method. In the offset method, σ_r was defined as the flow stress corresponding to a plastic strain of 0.2% (Fig. 3.8). In the back extrapolation method, σ_r was defined as the stress corresponding to the intersection of the reloading line with the line obtained by superimposing the prestraining curve on the reloading curve (Fig. 3.8). The back extrapolation method was developed on the assumption that, after a small 'transient' strain (of the order of 3 to 5%), the reloading stress-strain curve coincides with the continuous curve for a fully annealed material. This is strictly valid only when recovery is the sole softening mechanism taking place during the holding time. However, in the present work, this assumption was extended to the case where recrystallization follows recovery. The validity of this assumption will be evaluated later in the Discussion, when the results obtained with the two methods will be compared and analysed.
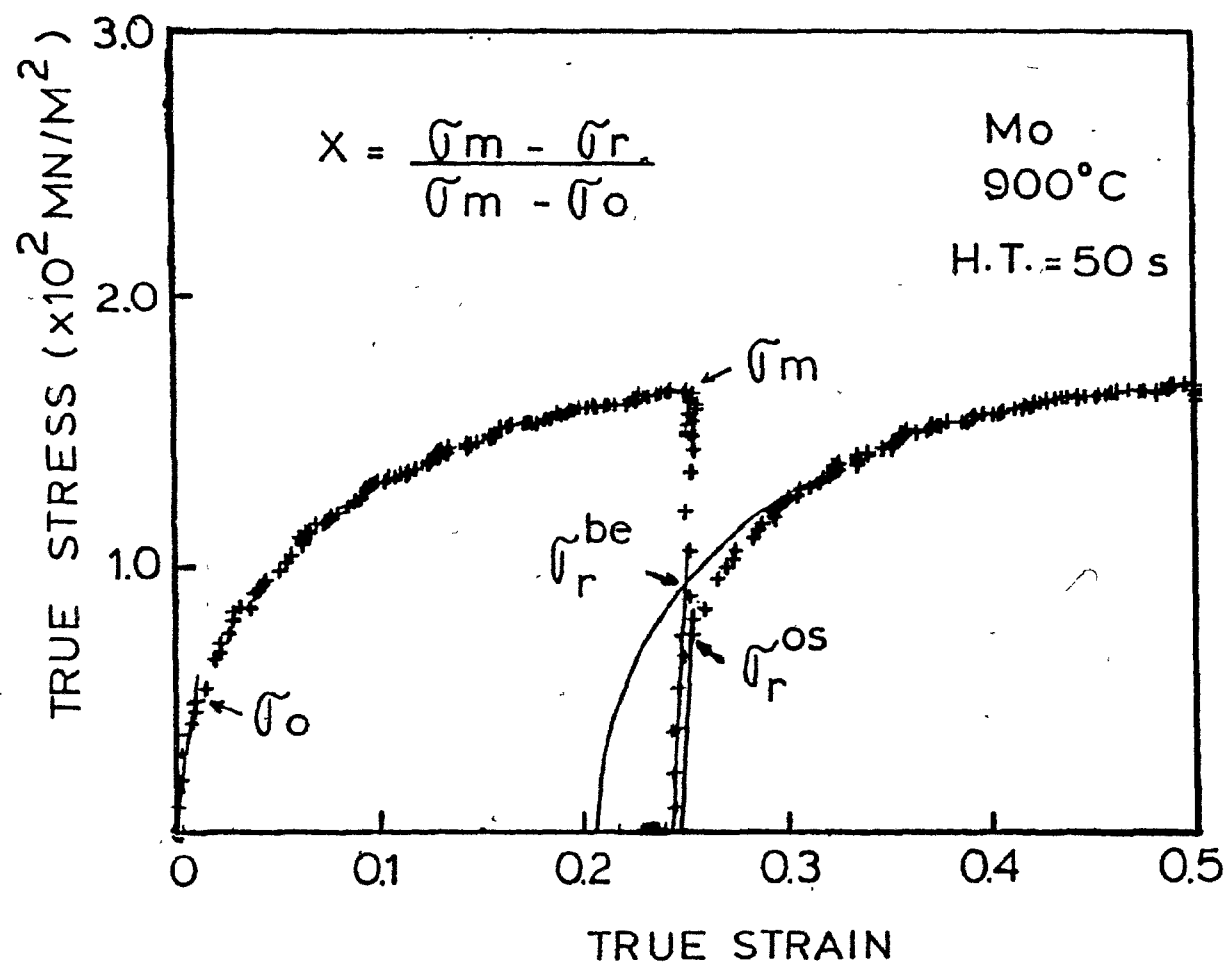
Figure 3.8 – Determination of the reloading flow stress and the degree of softening by the back extrapolation and offset methods.

CHAPTER 4

EXPERIMENTAL RESULTS

The aims of this research were the following:

1) To investigate the effects of Mo, Nb and V in solution
   on static recovery and recrystallization after the high
   temperature deformation of a series of microalloyed
   steels.

2) To study the interaction of strain induced precipitation
   and the static softening processes in these steels.

3) To establish the calibration or conversion factor linking
   the onsets of static and dynamic recrystallization in hot
   worked austenite.

Interrupted hot compression tests were carried out at
900 and 1000°C and at a constant true strain rate of 2 sec^{-1}
on the four steels listed in Table 3.1. In order to accom-
plish objectives 1 and 2 above, the load-free time following
a prestrain of 25% was increased from 50 ms to the time re-
quired for the steel to recrystallize completely. For rea-
sons that will be discussed later, both graphite and glass
were used as lubricants. The third objective will be con-
sidered in the Discussion chapter, where the rates of static
softening determined in this work will be compared with the
dynamic ones obtained in earlier investigations (87,88).

4.1 - FLOW CURVES OBTAINED IN INTERRUPTED COMPRESSION TESTS

In Figures 4.1 to 4.4 are presented selected sets of true strain - true stress curves as plotted by the computer after interrupted compression tests performed at 1000°C and 900°C on the plain C, vanadium, molybdenum and niobium steels, respectively. In order to keep the diagrams simple, a selection of three experiments was made from each series of 10 to 12 tests carried out on each steel at a given temperature. The type of steel, the austenitization temperature and time, the test temperature and the strain rate employed are printed above each set of flow curves. The load-free times are also indicated at the side of each curve. It can be seen that the true stress - true strain curve for the first compression is the same for all the experiments on a particular diagram and corresponds to a prestrain of 0.25. A rapid and complete unloading is then effected and the samples are held under this condition for increasing intervals of time. After short delays, e.g. 50 to 200 ms, the flow stress on restraining rises rapidly to a level comparable to the stress developed just prior to unloading. As the delay time increases, a profound drop in the initial flow stress on reloading is produced and the stress - strain behavior approaches that of the material during prestraining.

Comparison between flow curves for the same steel

tested at 1000 and 900°C (Figures 4.1(a) - 4.1(b), 4.2(a) - 4.2(b), 4.3(a) - 4.3(b) and 4.4(a) - 4.4(b)) shows that a decrease in temperature increases the flow stress level in the first compression and decreases the amount of softening observed after the same 'holding time'. From the experiments performed on the four steels at the same temperature (Figures 4.1(a) - 4.2(a) - 4.3(a) - 4.4(a) and 4.1(b) - 4.2(b) - 4.3(b) - 4.4(b)), it can be seen that the flow stress level during prestraining increases slightly with the addition of V and Mo and more markedly with the addition of Nb. By contrast, the amount of softening after the same holding time decreases with the addition of these microalloying elements and this decrease is more pronounced in the Mo and Nb steels.

4.2 - PROGRESS OF STATIC RECOVERY AND RECRYSTALLIZATION IN PLAIN C, Mo AND V STEELS

As described above, two methods were employed in the present investigation to evaluate the degree of static softening occurring after an interval of hot working: the 'back extrapolation' and 'offset' methods. In what follows, fractional softening vs. holding time curves obtained by the application of these two methods will be presented for the plain C, Mo and V steels. The experimental results illustrated were determined under three slightly different sets of conditions with respect to (i) the type of tool and (ii) the method of lubrication used.
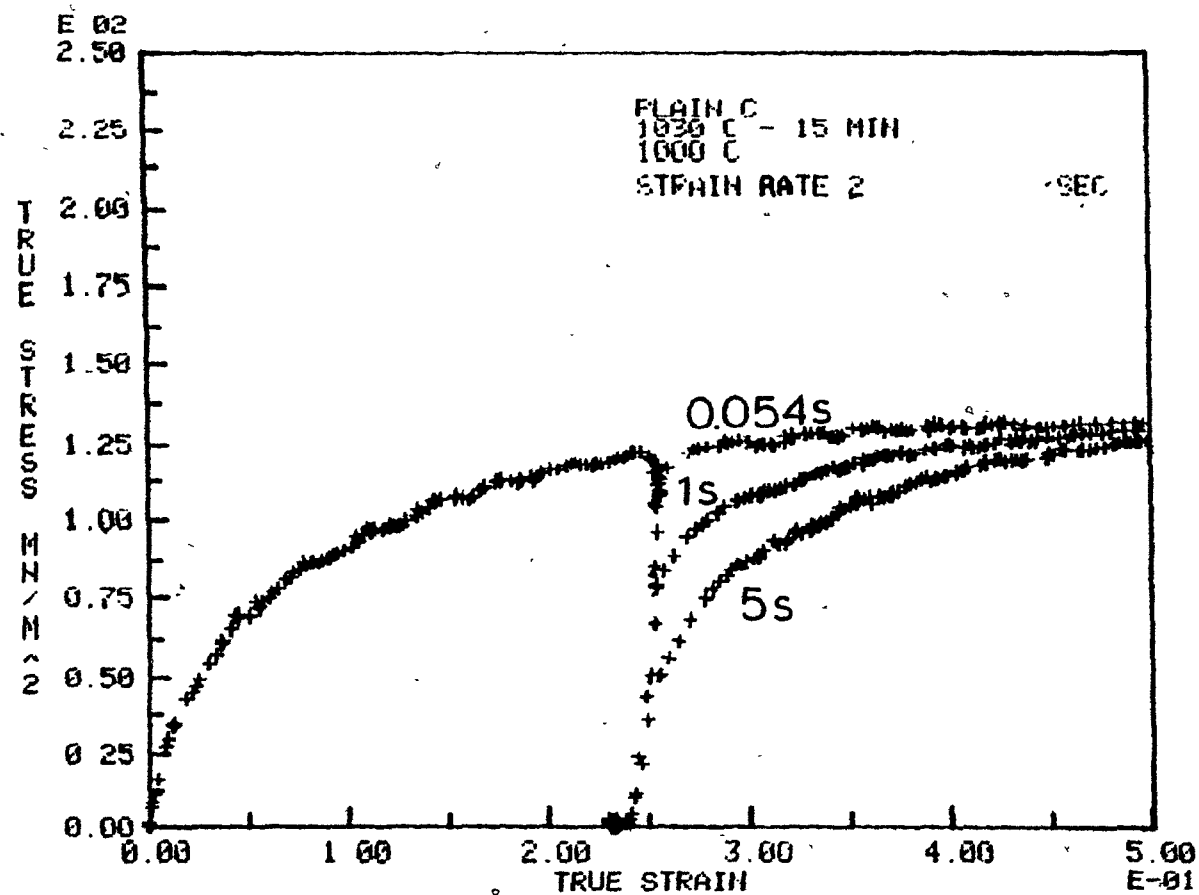
Figure 4.1(a) - Flow curves for the plain C steel at 1000°C after three different holding times.
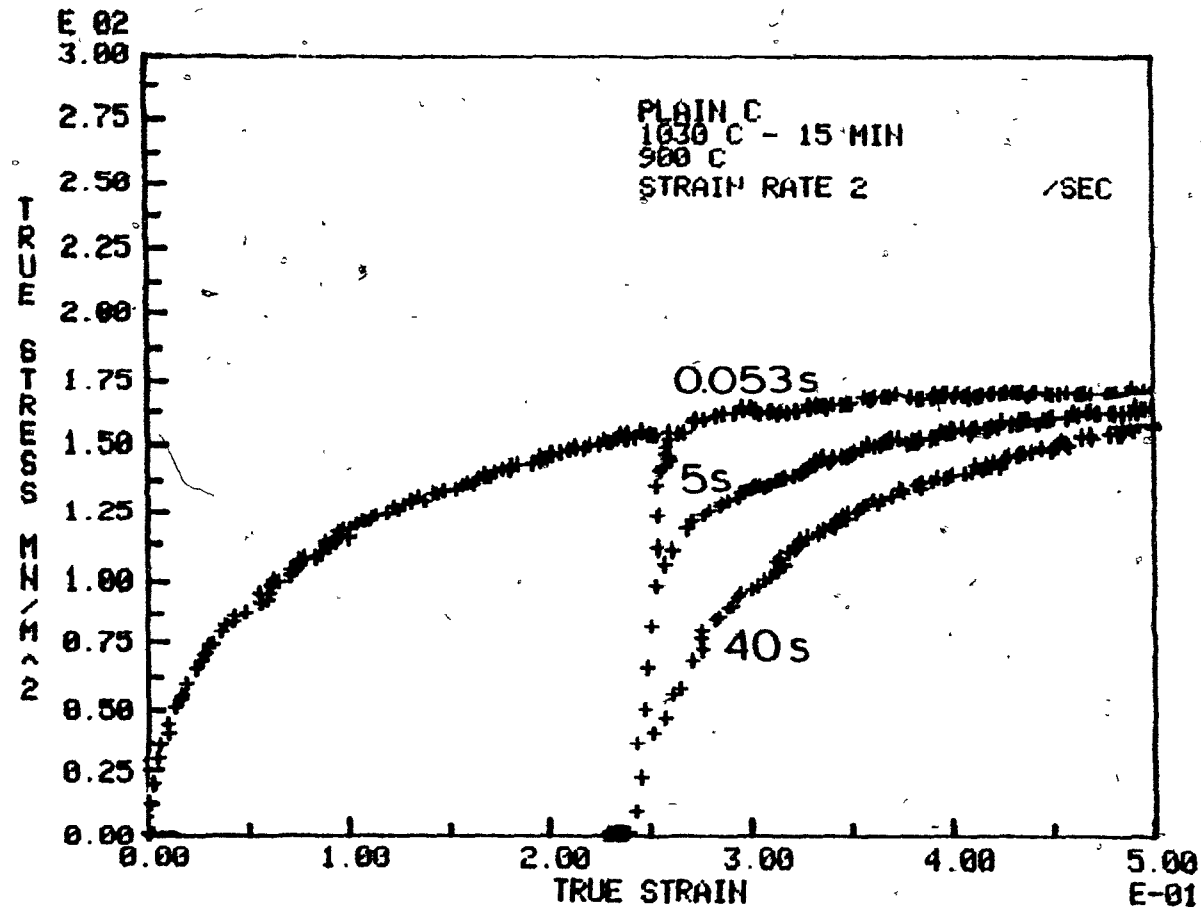
Figure 4.1(b) — Flow curves for the plain C steel at 900°C after three different holding times.
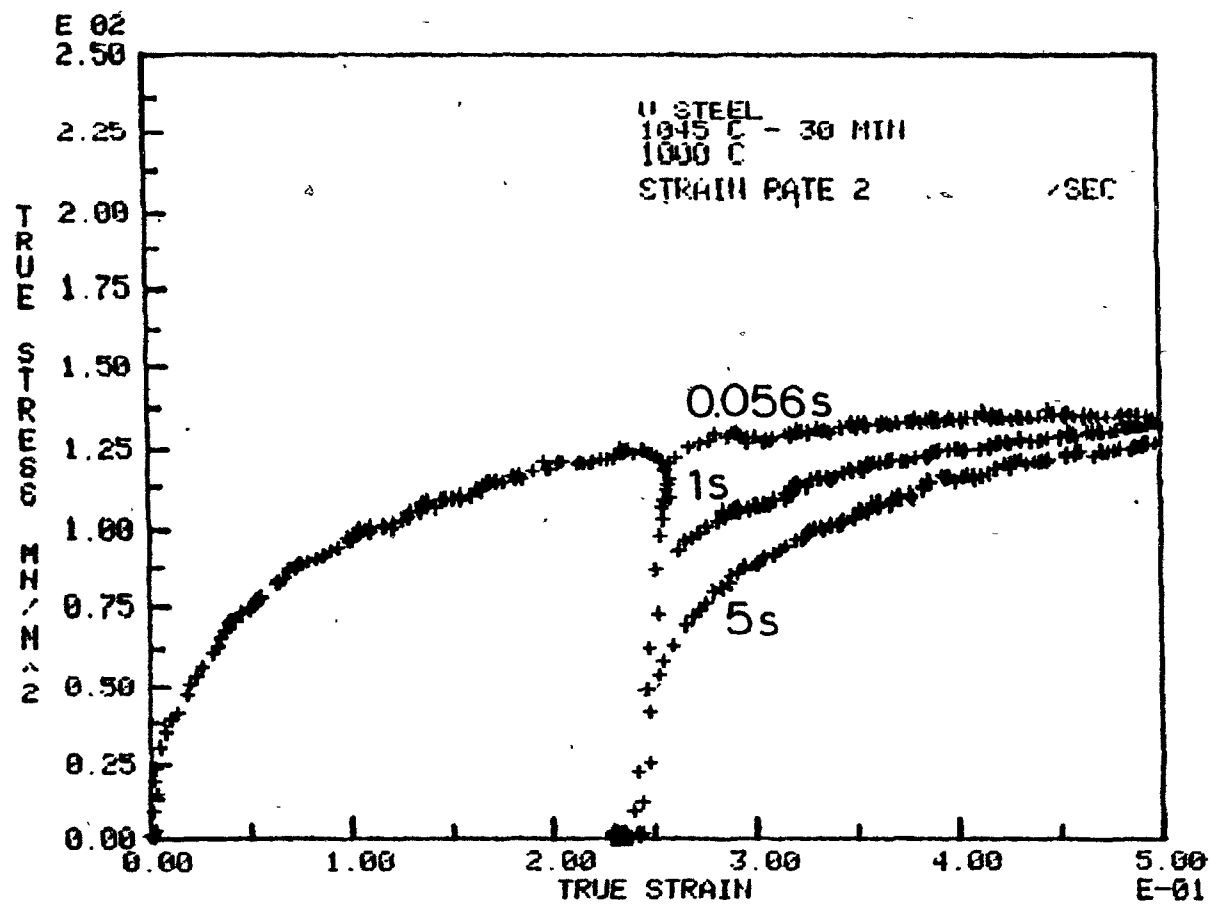
Figure 4.2(a) - Flow curves for the V steel at 1000°C
after three different holding times.
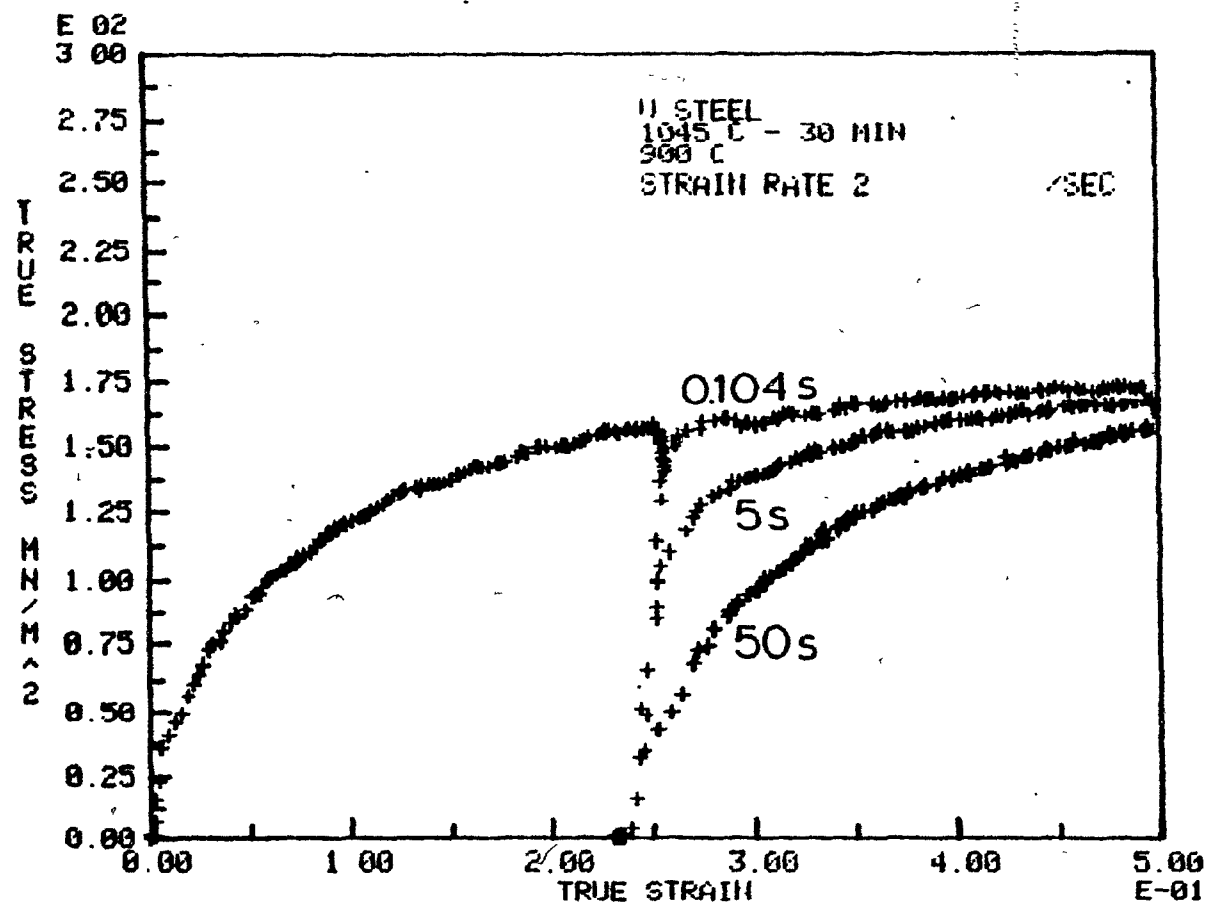
Figure 4.2(b) - Flow curves for the V steel at 900°C
after three different holding times.
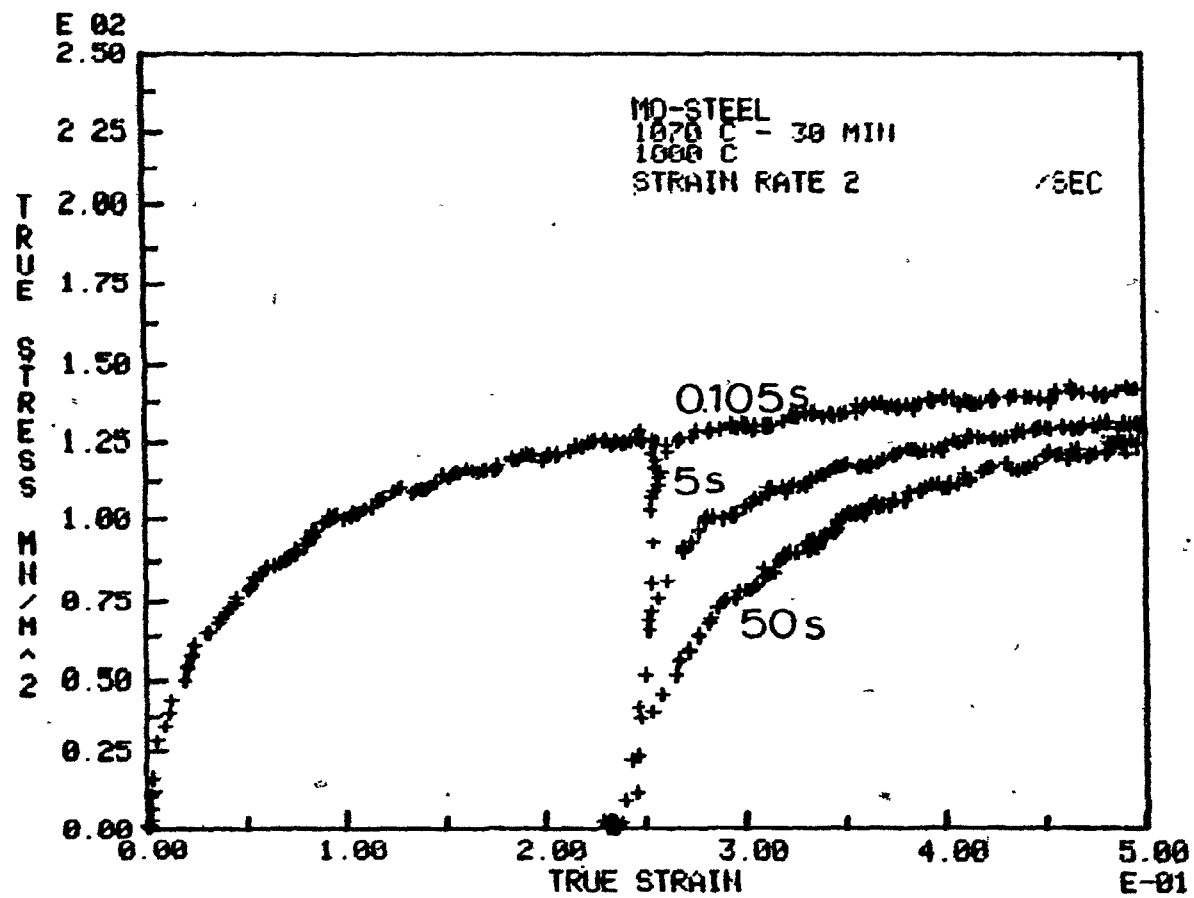
Figure 4.3(a) - Flow curves for the Mo steel at 1000°C
after three different holding times.
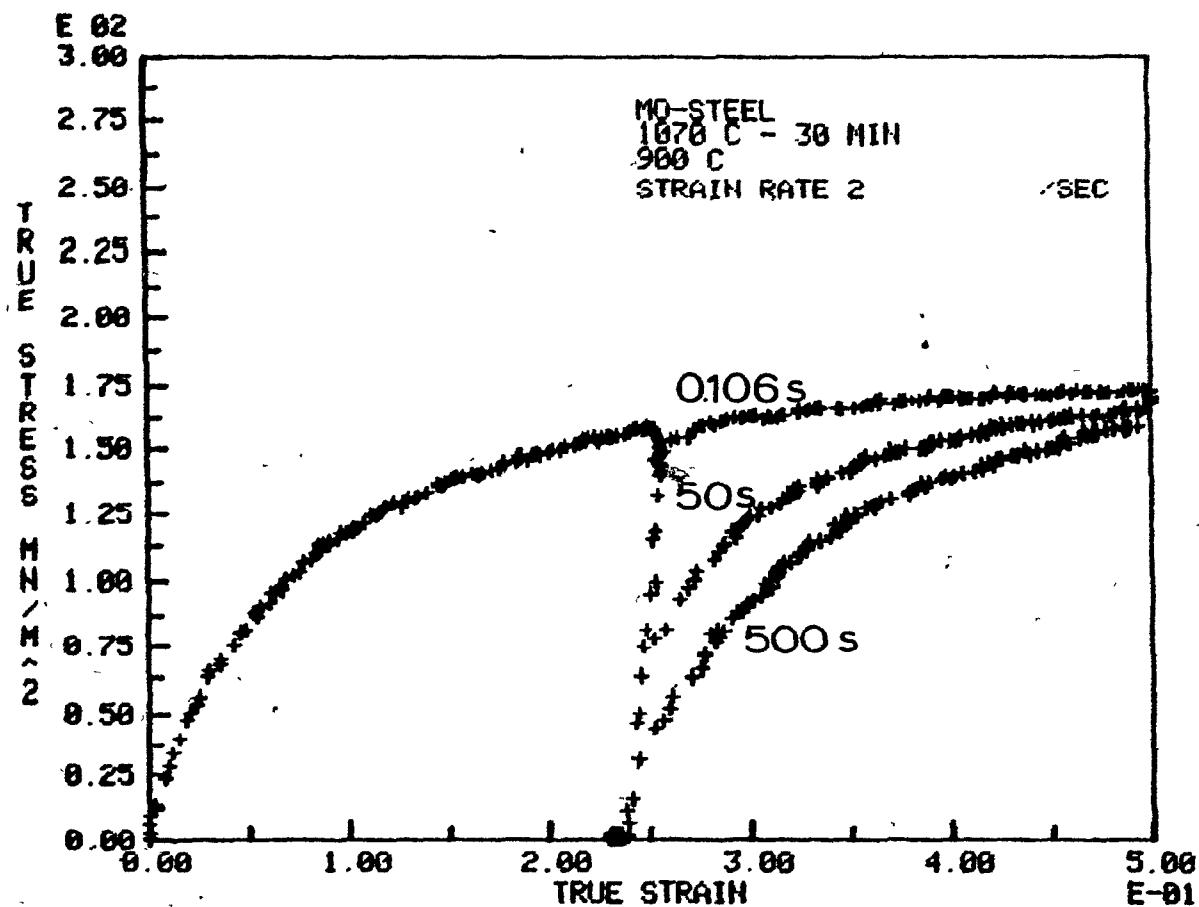
Figure 4.3(b) — Flow curves for the Mo steel at 900°C
after three different holding times.
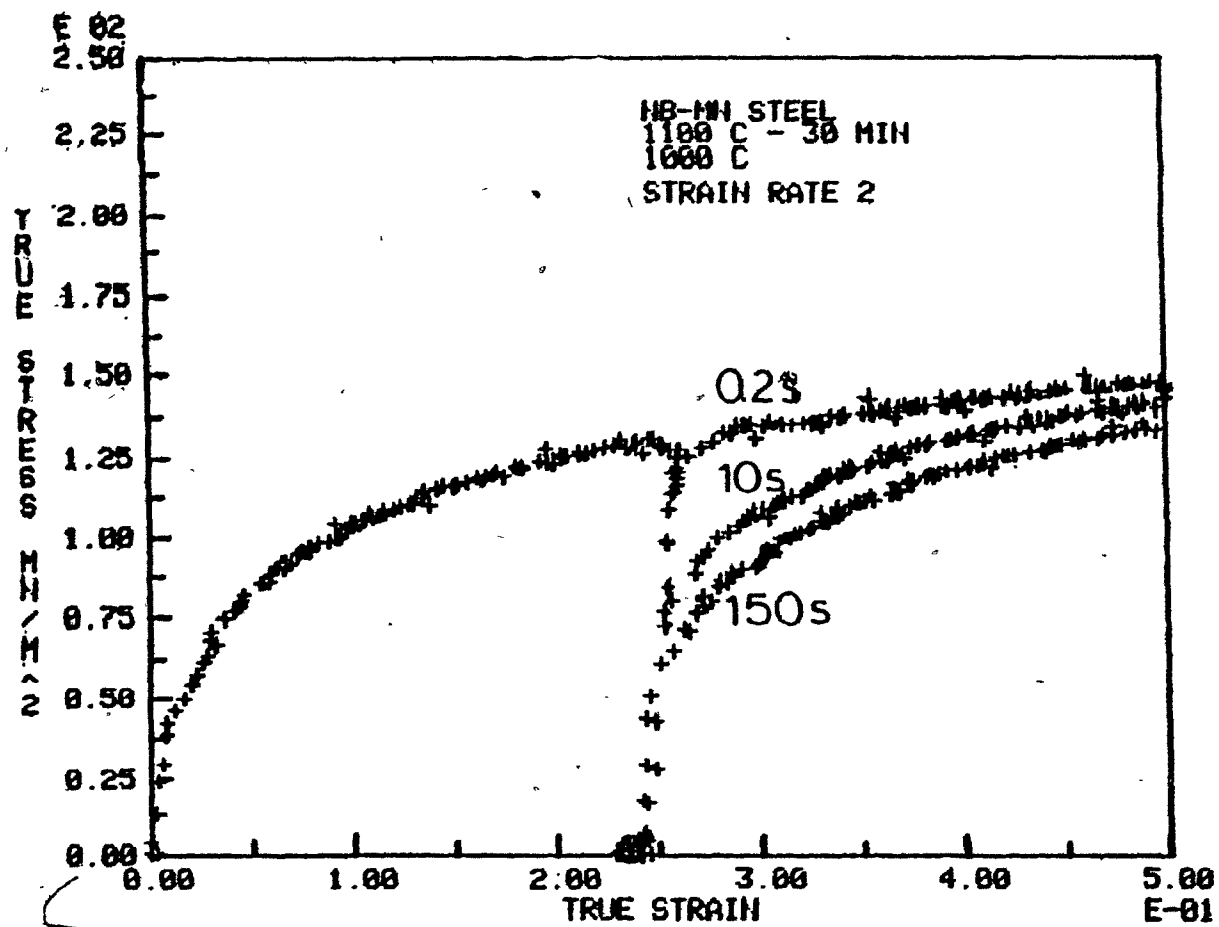
Figure 4.4(a) - Flow curves for the Nb-Mn steel at 1000°C after three different holding times.
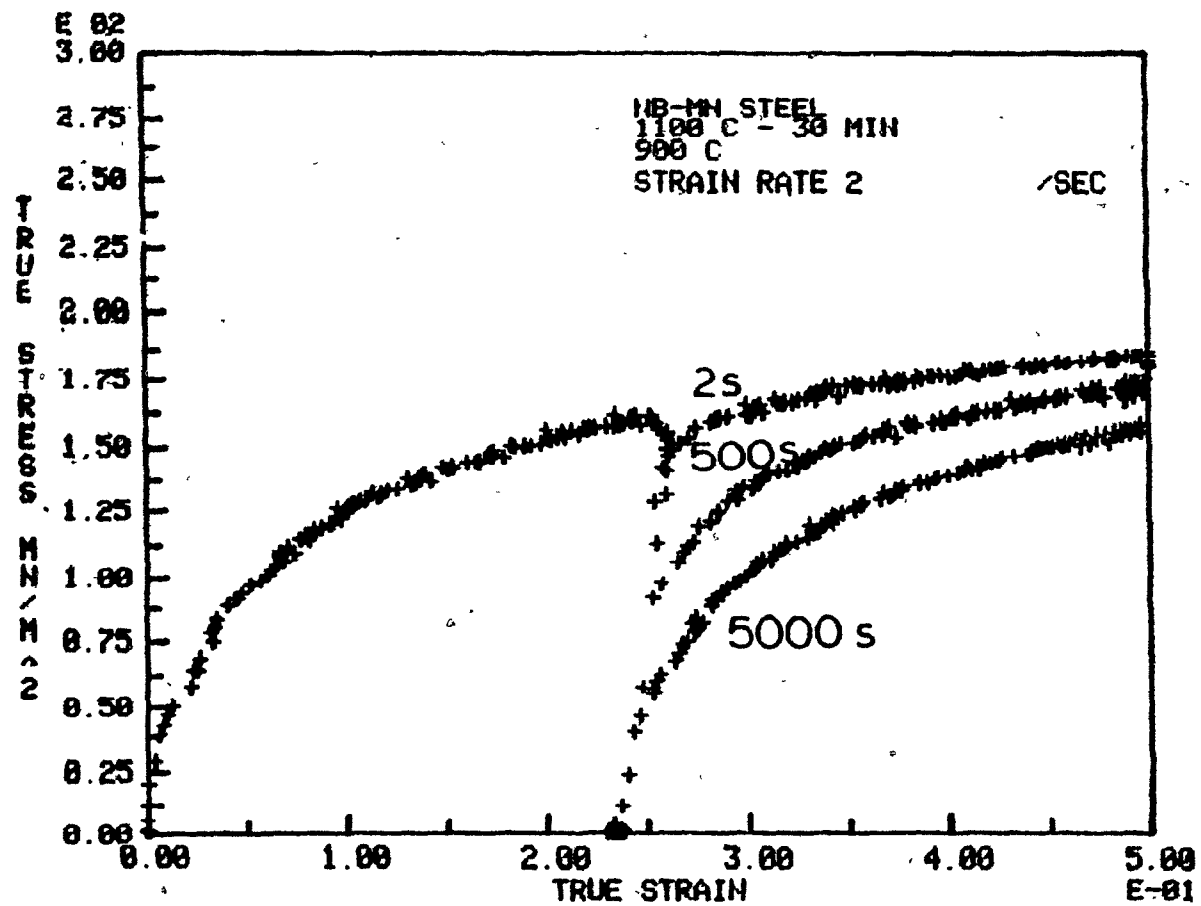
Figure 4.4(b) – Flow curves for the Nb-Mn steel at 900°C after three different holding times.

These sets of conditions are identified by the symbols Gr.,
Gl. and W+Gr. Gr. and Gl. refer to experiments in which SiN
inserts were employed in conjunction with either graphite
(Gr.) or glass (Gl.). The notation W+Gr. indicates the tests
which were performed with tungsten (W) tools and graphite
(Gr.) as lubricant.

4.2.1 - Fractional Softening Determined by the Back Extrapolation Method

4.2.1.1 - Short-Time Static Recovery Results

In Figures 4.5(a) and 4.5(b) the fractional softening
associated with the static recovery process is plotted for
very short holding times. This fractional softening was determined by the back extrapolation method and corresponds to
values within the range 2 to 12%. At 1000°C (Fig. 4.5(a)),
the results presented pertain to experiments in which the
holding time was equal to or shorter than 1 s. At this temperature it can be seen that the progress of static recovery
in the plain C steel is faster than in the V and Mo steels.
The same order is followed at 900°C (Fig. 4.5(b)), with the
difference that at this temperature longer holding times are
required for the same amount of softening. As shown in the
above two figures, the retardation due to the addition of V
and Mo can be detected after unloading times as short as 0.1 s.

Figure 4.5(a) - Short-time static recovery at 1000°C for the plain C, V and Mo steels as determined by the back extrapolation method.

Figure 4.5(b) - Short-time static recovery at 900°C for the plain C, V and Mo steels as determined by the back extrapolation method.

Such retardation is attributable to the presence of the two microalloying elements in solution since, under these experimental conditions, no precipitates can form in either the V or the Mo steel.

4.2.1.2 - Static Recrystallization Results

Figures 4.6(a) and 4.6(b) show the complete fractional softening vs. holding time curves for all the experiments carried out at 1000 and 900°C on the plain C, Mo and V steels. These results were determined by the back extrapolation method and were obtained under the three sets of experimental conditions mentioned previously. Two regions can be distinguished in all the curves presented: the static recovery region, whose features have already been described, and the static recrystallization region. The transition from one mechanism to the other is marked by an acceleration of the softening process and occurs after the passage of the 'incubation time' for recrystallization.

At 1000°C (Fig. 4.6(a)) and at 900°C (Fig. 4.6(b)), the onset of static recrystallization in the V and Mo steels is delayed in comparison with the plain C steel. As can be seen at both temperatures, Mo has a much greater retarding effect than V, which delays only slightly the beginning of this process. Although microstructural examination is essential for

Figure 4.6(a) – Static recovery and recrystallization of the plain C, V and Mo steels determined by the back extrapolation method at 1000°C.

an accurate determination of the onset of static recrystalliza-
tion, such an investigation is difficult when the high tempera-
ture phase (austenite) is unstable, as in the present system.
A reasonable estimate of the onset of recrystallization can
be obtained instead from the intersection of two straight lines,
one each extrapolated from the static recovery and static re-
crystallization regions. Results obtained in this way indicate
that recrystallization starts at softening ratios of about 10%
at 1000°C and about 15% at 900°C. The rate of static recrys-
tallization at each temperature follows the order determined
in the recovery region and recrystallization can be considered
to be complete when the fractional softening is approximately
equal to 100%.

As mentioned earlier, Mo does not precipitate in
austenite when added alone. On the other hand, the solubility
considerations of section 3.1 indicated the possibility of VN
precipitation at 900°C but not at 1000°C. According to the
data obtained in a previous investigation (87) from experi-
ments carried out on the same V steel and under dynamic condi-
tions, the strain induced precipitation of VN starts, at 900°C,
at a time of around 30 s. However, the results presented in
Figure 4.6(b) suggest that recrystallization in the V steel is
nearly complete by the time the strain induced precipitation
of VN is expected to occur. Consequently the retardation of

Figure 4.6(b) – Static recovery and recrystallization of the plain C, V and Mo steels determined by the back extrapolation method at 900°C.

static recrystallization observed in the V. and Mo steels at both temperatures is judged to be largely caused by V and Mo in solution. The change in lubricant (graphite or glass) and in compression tool material (SiN insert or tungsten) does not seem to have any effect on the softening behavior of the three steels investigated.

4.2.2 - Fractional Softening Determined by the Offset Method

4.2.2.1 - Short-Time Static Recovery Results

The results obtained for the static recovery region from the application of the offset method are shown in Figures 4.7(a) and 4.7(b). As expected, no change is observed in the relative position of the curve corresponding to each steel. However, the use of this method leads to values of fractional softening which are considerably higher than the ones determined by the back extrapolation method. At 1000°C (Fig. 4.7(a)), fractional softening of 7 to 8% has already been attained after an unloading time as short as 50 ms. At 900°C (Fig. 4.7(b)), this value is 6 to 7% after a holding time of 0.1 s. At both temperatures, the overall softening produced by static recovery, as measured by the offset method, is double that shown in Figs. 4.6(a) and 4.6(b) for the back extrapolation method.

4.2.2.2 - Static Recrystallization Results

Figures 4.8(a) and 4.8(b) show the complete fractional
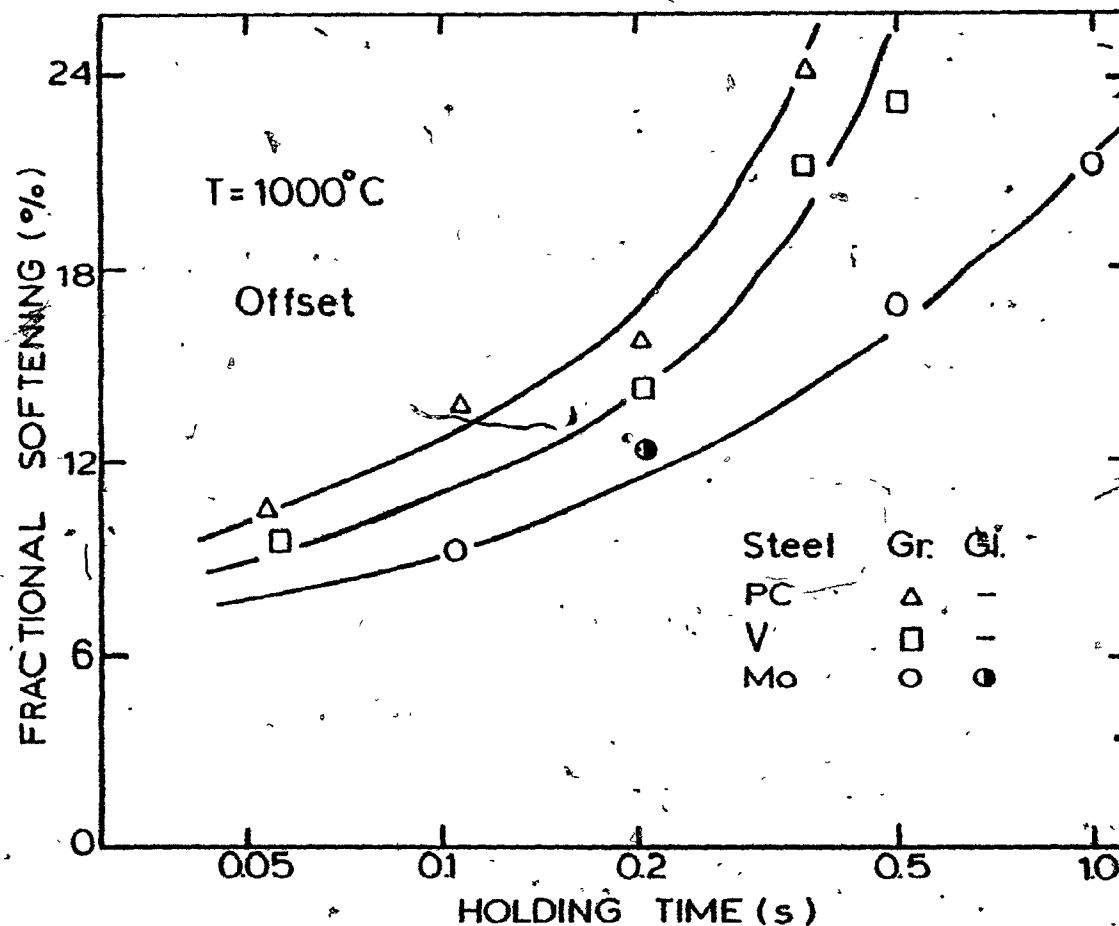
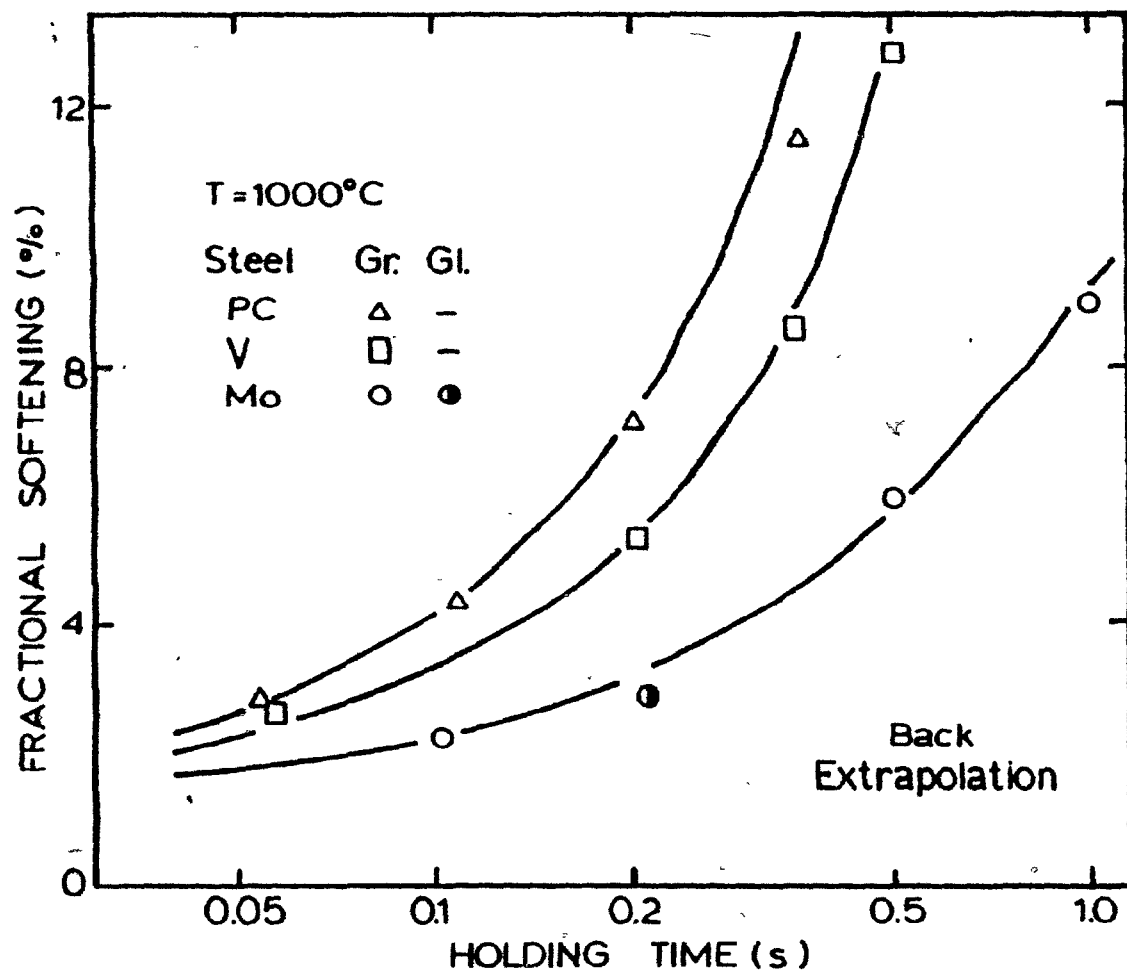Figure 4.7(a) - Short-time static recovery at 1000°C
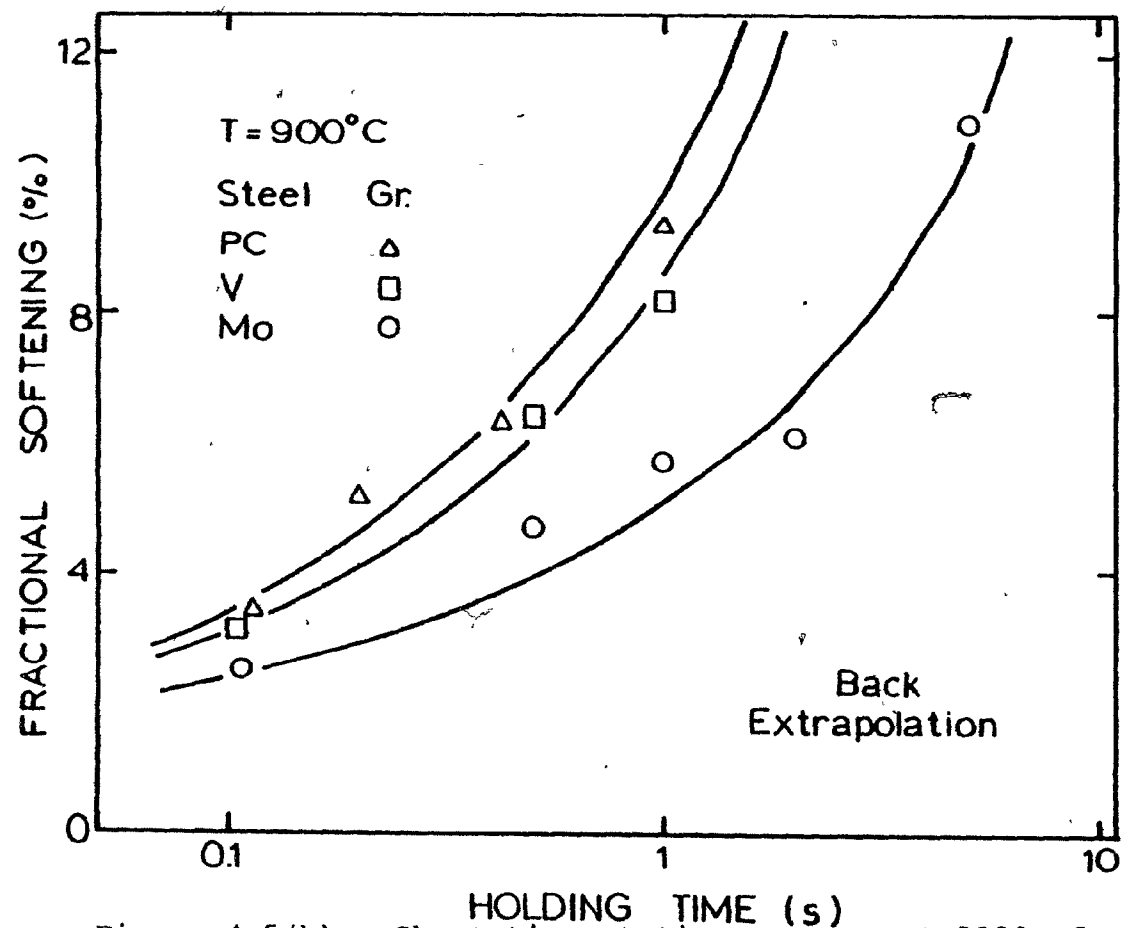for the plain C, V and Mo steels as
determined by the offset method.
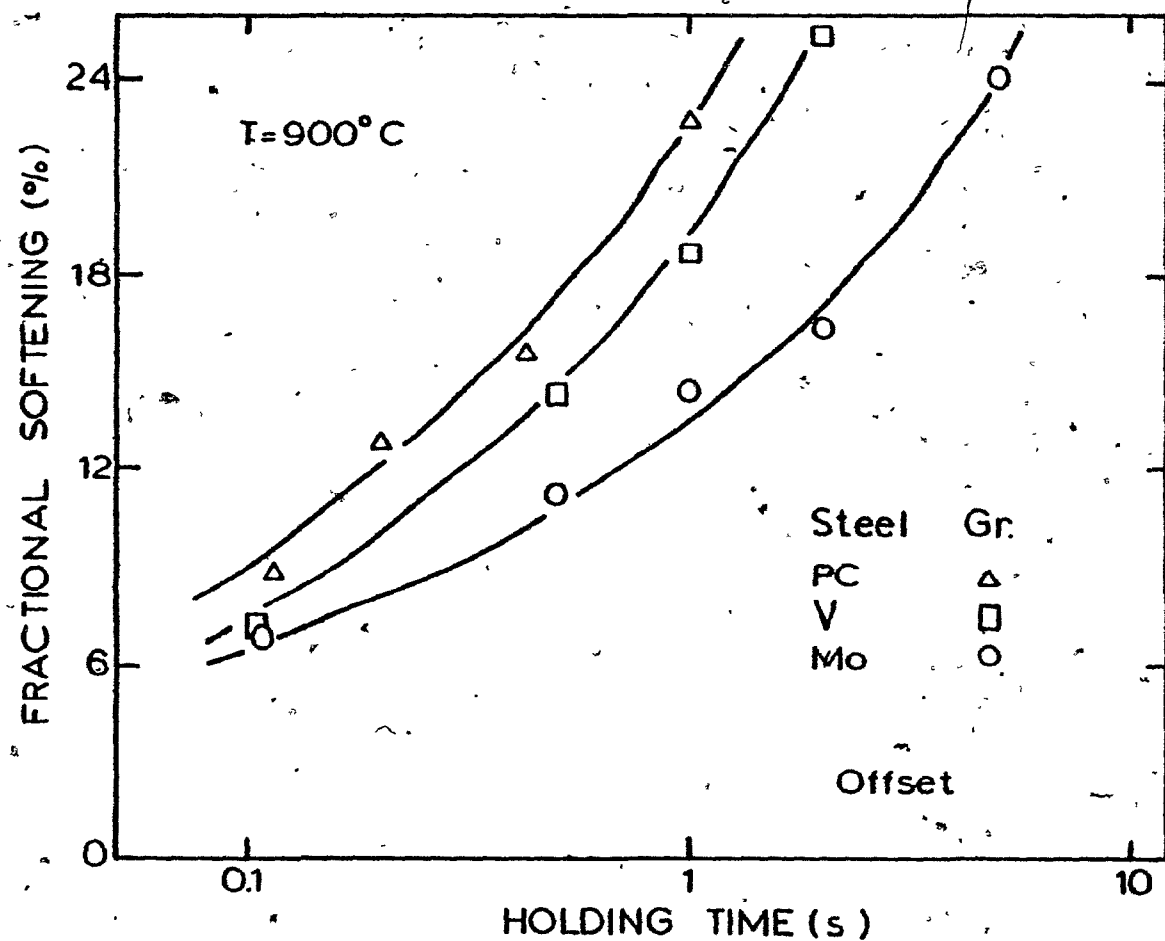
Figure 4.7(b) – Short-time static recovery at 900°C for the plain C, V and Mo steels as determined by the offset method.

softening vs. holding time curves deduced by the offset method. Using this technique, and the intersection method described above, the amount of softening associated with the onset of static recrystallization is seen to be about 20% at 1000°C and about 30% at 900°C. As static recrystallization proceeds, the relative difference in the amount of softening measured by the two methods decreases continuously and tends to zero as the fractional softening approaches 100%.

The difference in the results obtained with the back extrapolation and offset methods is related to the motion of the mobile dislocations during unloading. If the mobile dislocations remained fixed during unloading, there would be no 'short transient' between the 'loading' and 'normal work hardening' portions of the flow curves. Then the offset and back extrapolation methods would lead to the same value of reloading stress. Instead, as the mobile dislocations are no longer in contact (after unloading) with the relevant rate controlling obstacles, an increment of strain must be applied which serves to advance the dislocations to the appropriate obstacles. Once contacted, the flow curve resumes the shape associated with uninterrupted straining. This phenomenon will be discussed in more detail in section 5.3, together with the practical implications of the use of either method for the calculation of roll force during rolling. For reasons that
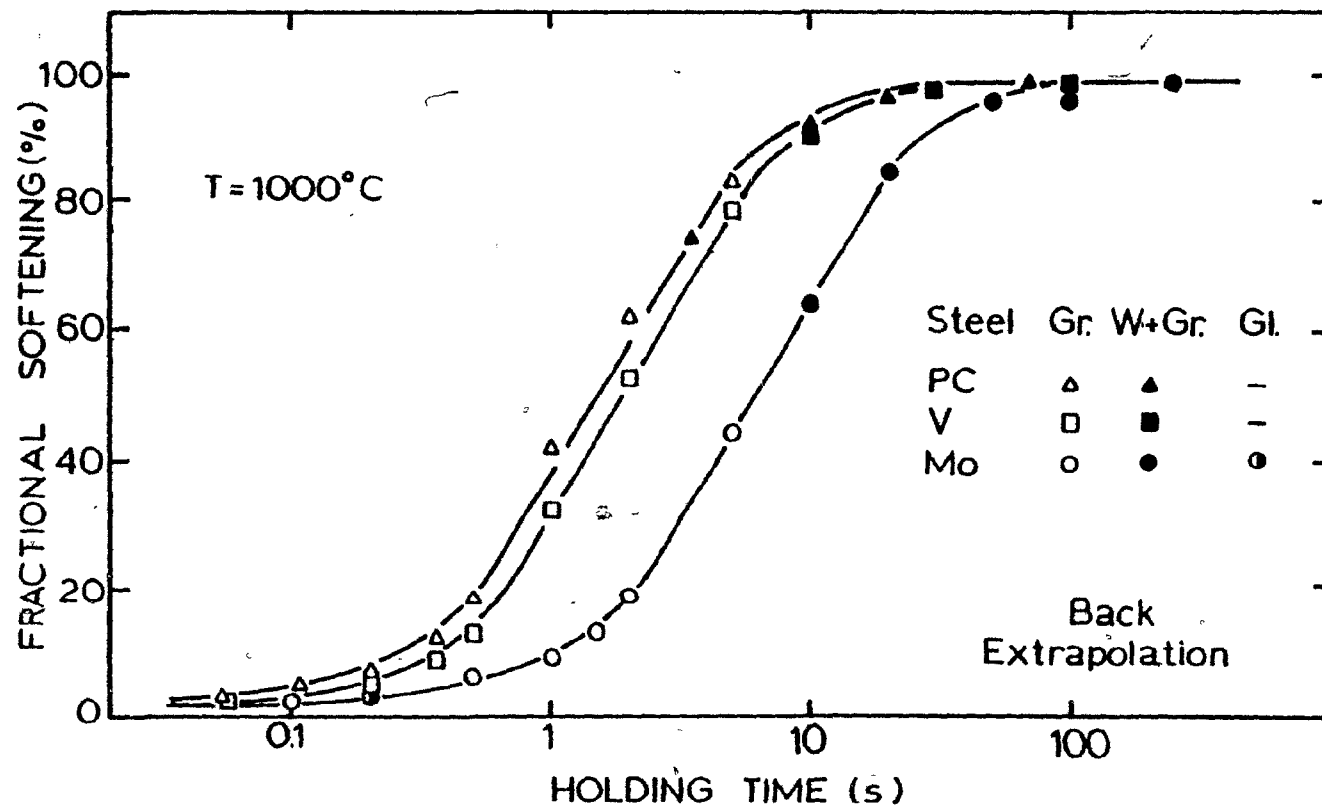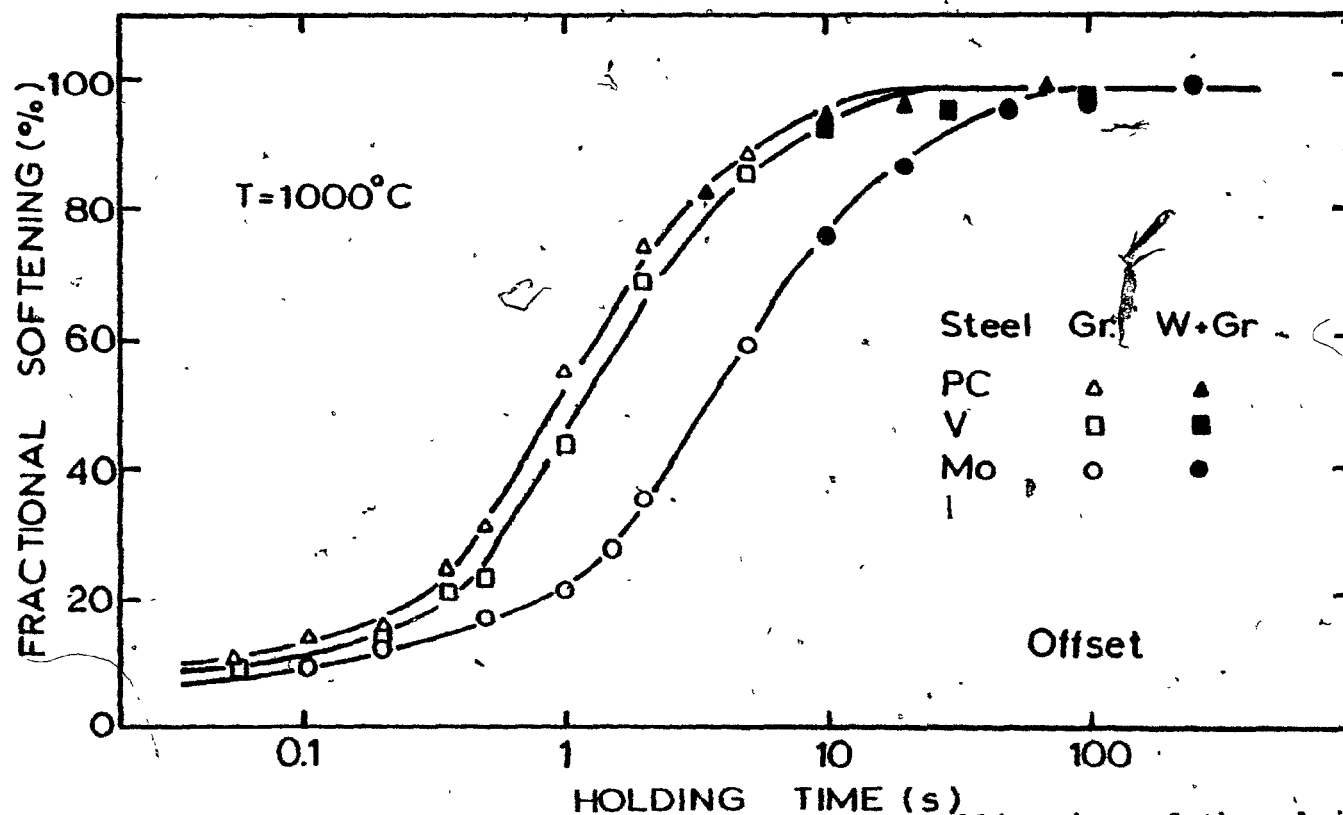
Figure 4.8(a) - Static recovery and recrystallization of the plain C,
V and Mo steels determined by the offset method at
1000°C.

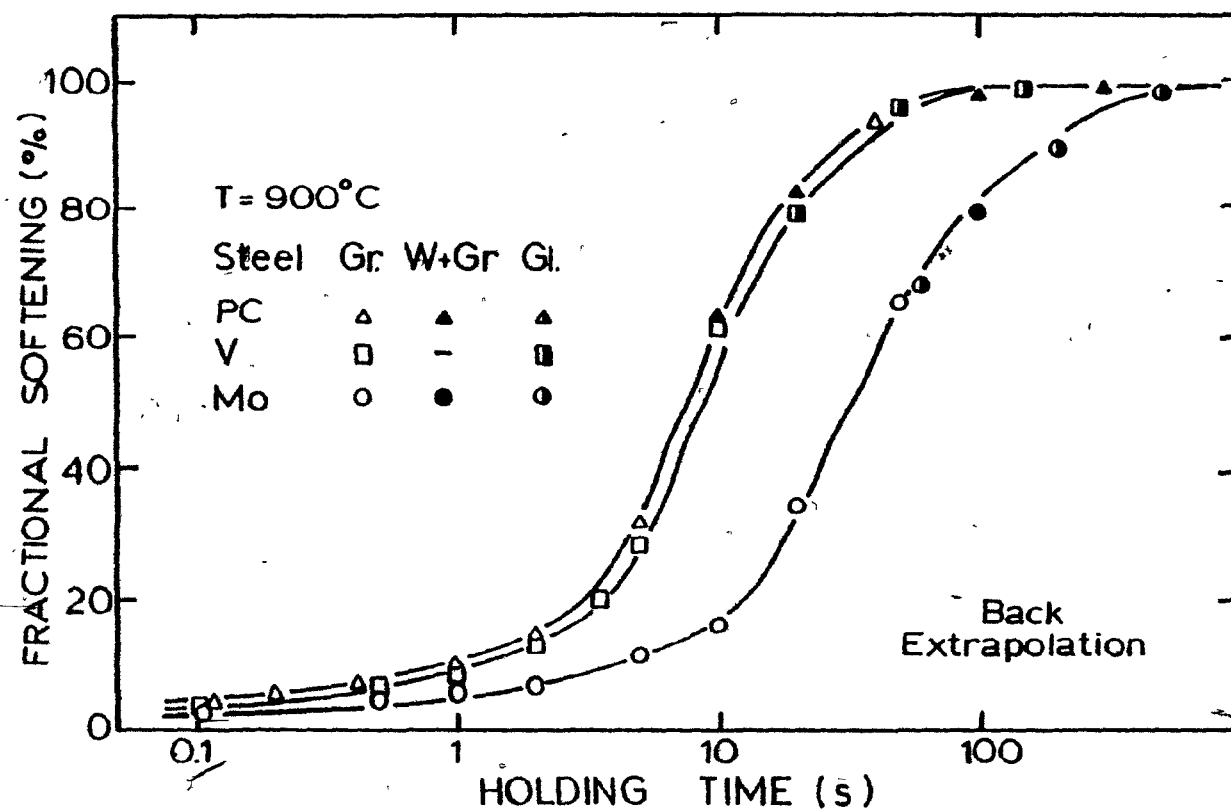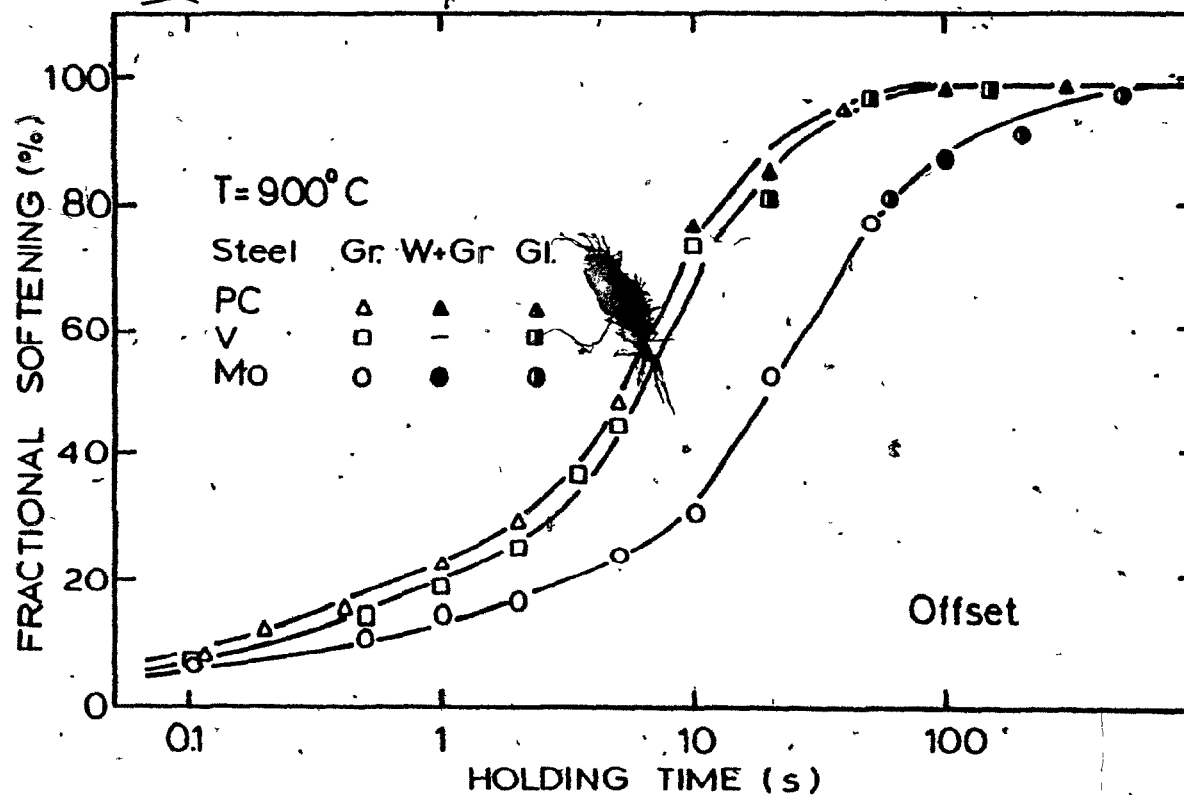Figure 4.8(b) - Static recovery and recrystallization of the
plain C, V and Mo steels determined by the
offset method at 900°C.

will become evident later, the values of softening measured by the back extrapolation method are in better agreement with the actual influence of each static softening process during an industrial rolling operation. Thus, only the results determined by the back extrapolation method will be presented in the sections that follow.

4.3 - TESTS RESULTS FOR NIOBIUM STEEL OBTAINED WITH GRAPHITE LUBRICATION

In this section, the results obtained on the Nb-Mn steel in the experiments performed with graphite as lubricant will be displayed. The softening behavior of this steel at 1000°C is given in Figures 4.9(a) and 4.9(b). For comparison, the fractional softening vs. holding time curves for the plain C, V and Mo steels are also presented. In the static recovery region (Fig. 4.9(a)), it can be seen that the Nb-Mn curve is situated between the V and Mo curves. The order of retardation in this region is thus given, somewhat unexpectedly, by Mo>Nb>V. The same order is evident in the static recrystallization region (Fig. 4.9(b)). As no strain induced precipitation of Nb(C,N) is likely to occur under the above experimental conditions at 1000°C, the retardation must be attributed to the influence of Nb in solution. The results for static recovery at 900°C (Fig. 4.10(a)) are very similar to the ones at 1000°C, with the difference that a deviation can begin to

Figure 4.9(a) - Short-time static recovery of the Nb-Mn
steel at 1000°C after testing with graphite
lubrication.
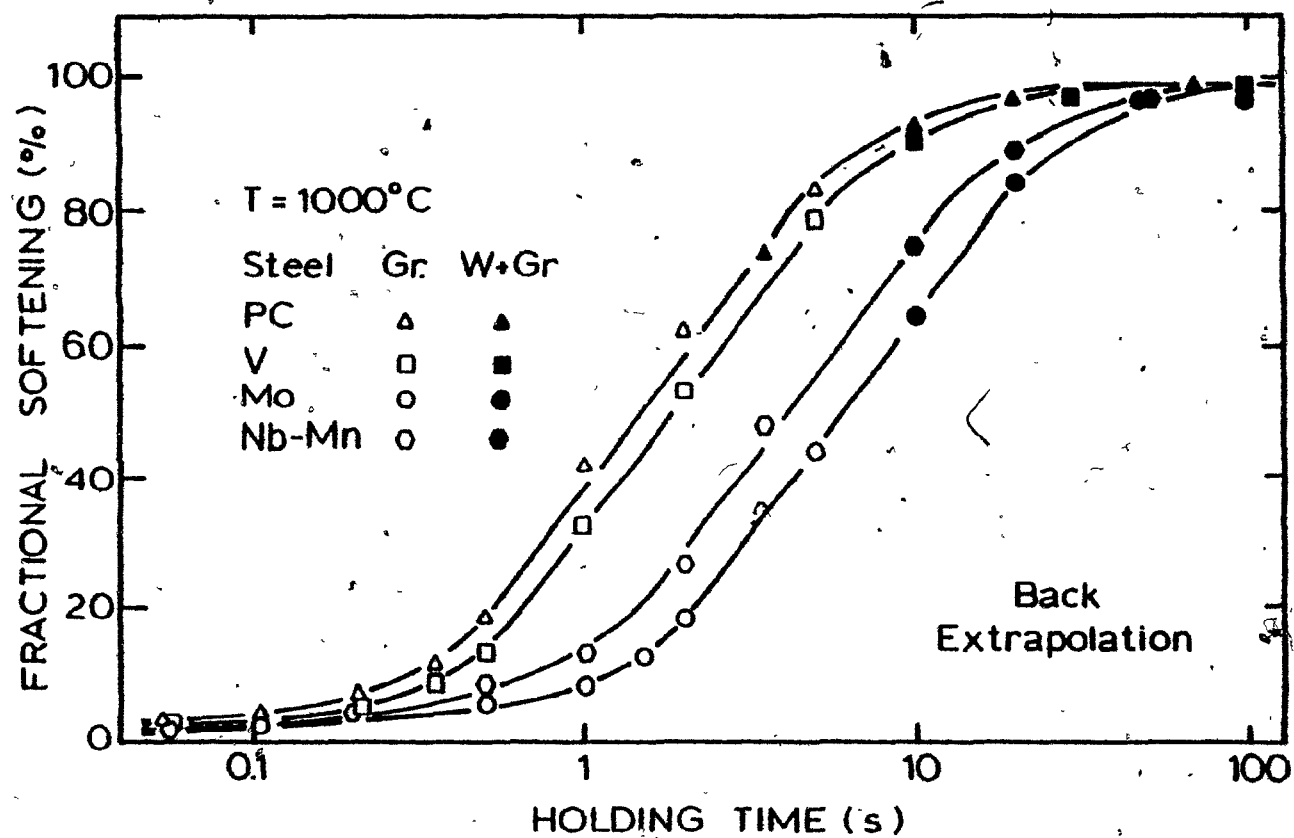
Figure 4.9(b) - Static recovery and recrystallization of the Nb-Mn steel at 1000°C after testing with graphite lubrication.

be noticed in the Nb curve at a holding time of around 2 s. This deviation can be seen to better effect in Fig. 4.10(b). The departure from the expected softening behavior is probably related to the onset of the strain induced precipitation of Nb(C,N), as will be demonstrated more clearly below. The dashed line indicated in Figs. 4.10 (a and b) represents the softening kinetics anticipated in the Nb-Mn steel if no precipitation occurs. Comparison of the underline expected solute Nb curve (represented by the dashed line) and the actual Nb curve shows that the start of the strain induced precipitation of Nb(C,N) delays the onset of static recrystallization considerably in this steel. After a holding time of around 8 s, the Nb curve crosses over the Mo curve and changes the order of retardation in the static recrystallization region to the one normally observed, i.e. to Nb>Mo>V.

Analysis of the experimental data presented above calls attention to two important observations:

- The retardation due to solute Nb is less than that associated with solute Mo (under the present conditions).

- The time for the onset of the strain induced precipitation of Nb(C,N) at 900°C (2 seconds) is less than usual.

It was not initially clear what factors produced this unusual result. The consideration of a number of plausible causes in turn led to the possibility that the use of graphite lubrication
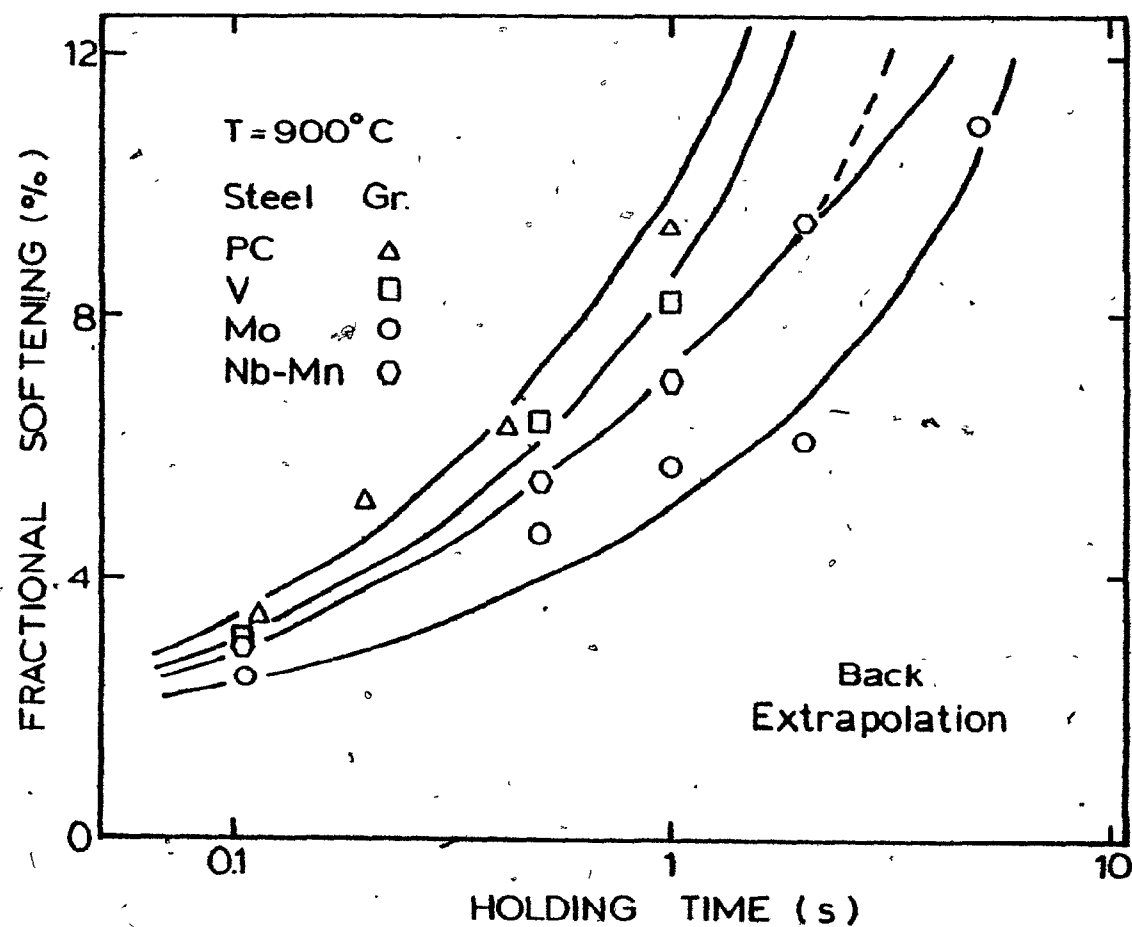
Figure 4.10(a) – Short-time static recovery of the Nb–Mn
steel at 900°C after testing with graphite
lubrication.
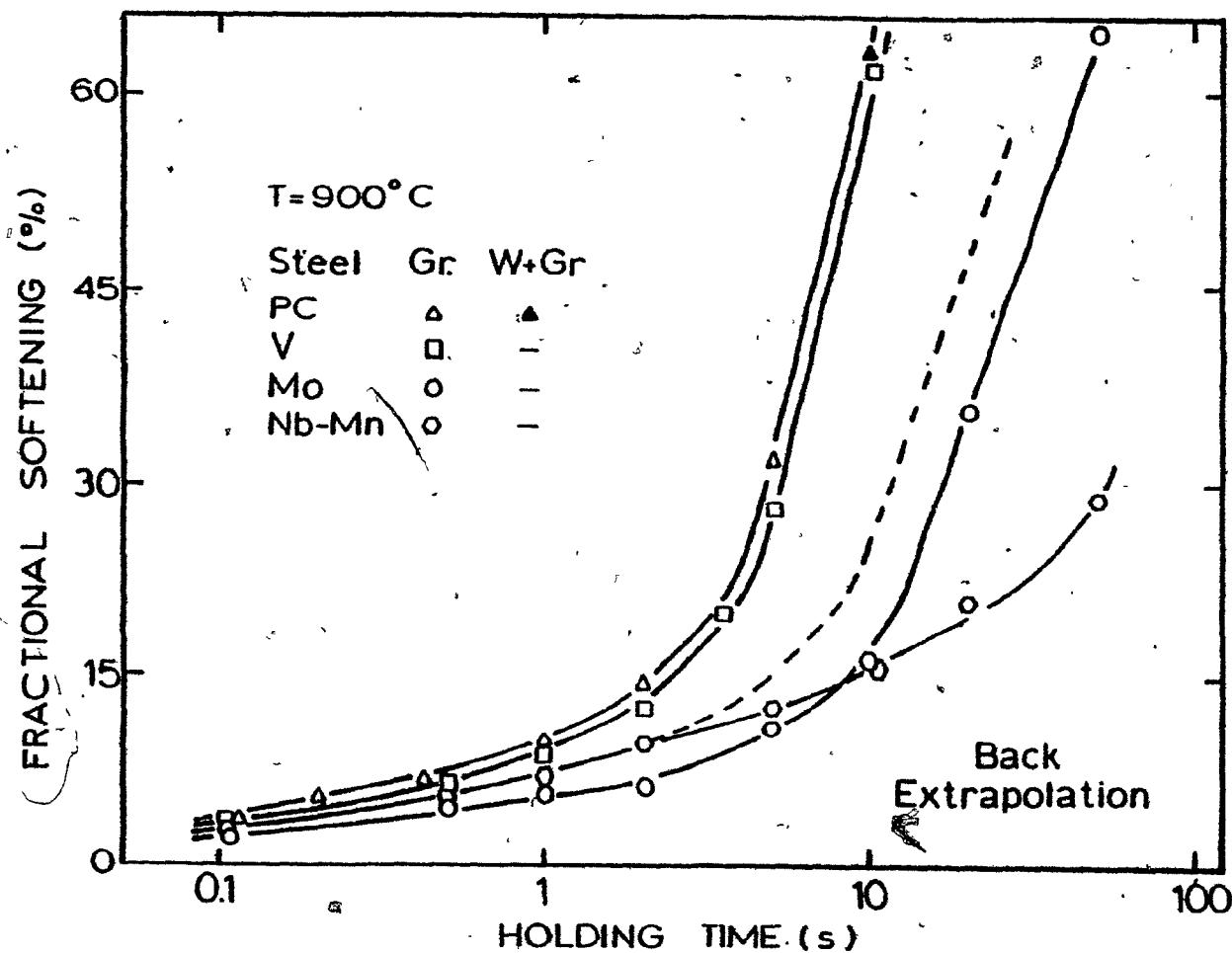
Figure 4.10(b) – Static recovery and recrystallization of the Nb-Mn steel at 900°C after testing with graphite lubrication.

could be affecting the softening characteristics of the Nb
steel. According to this view, the presence of graphite can
cause the diffusion of C into the samples during the austeniti-
zation heat treatment. The resulting increase in the solu-
bility product [Nb].[C] could lead to less Nb being taken into
solution than when austenitization is carried out in the absence
of graphite.

4.4 - TEST RESULTS FOR NIOBIUM STEEL OBTAINED WITH GLASS LUBRI-
CATION

Figures 4.11(a) and 4.11(b) show the fractional softening
vs. holding time curve for the Nb-Mn steel obtained at 1000°C
with the use of glass. In this condition it can be seen that
the change in lubrication affects the softening behavior of the
Nb steel significantly. In particular, it is evident that
solute Nb now has the strongest retarding effect on both the
static recovery process (Fig. 4.11(a)) and on the onset of static
recrystallization (Fig. 4.11(b)). At 900°C, the order of effec-
tiveness in retarding recovery is again Nb>Mo>V (Fig. 4.12(a)),
and the observations are qualitatively similar to those of
Fig. 4.11(a). However, when the scale is extended to 5000 s.,
it is evident that a further phenomenon is involved. As shown
in Fig. 4.12(b), the onset of strain induced precipitation of
Nb(C,N) occurs at a holding time of around 10 s. This leads
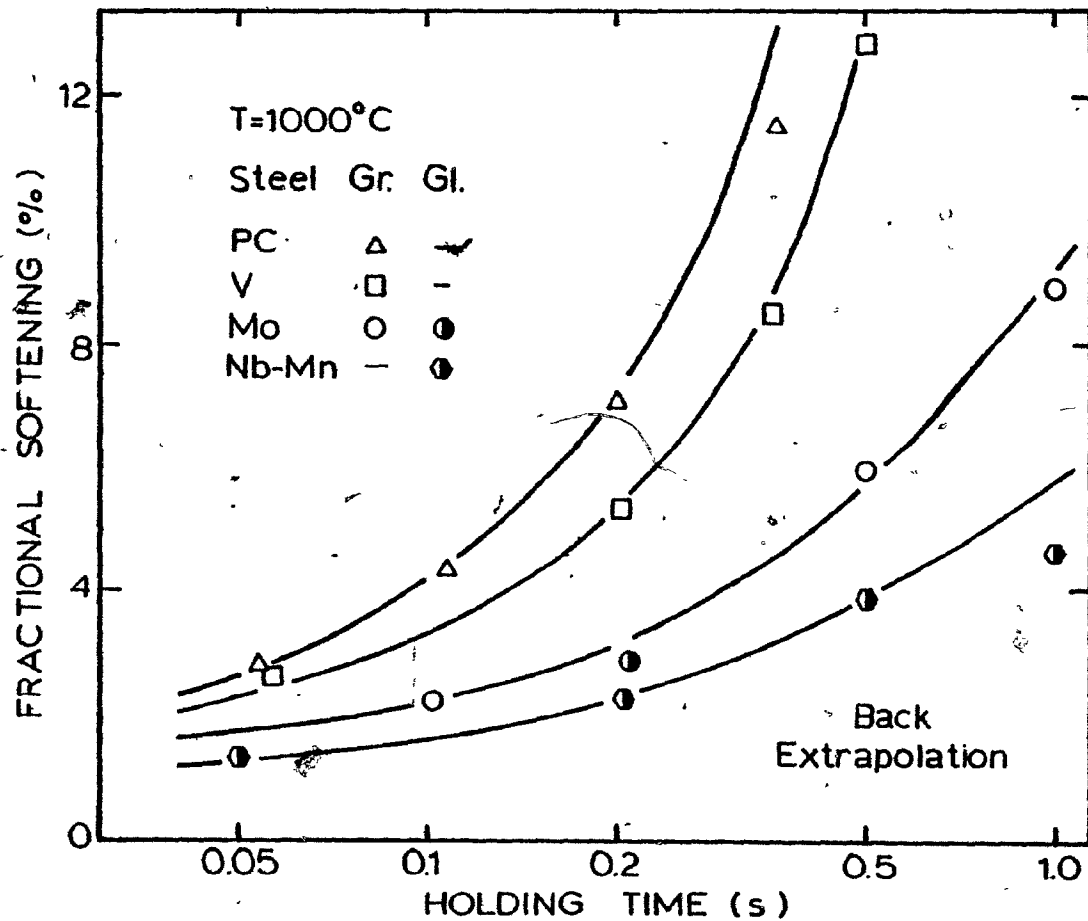
Figure 4.11(a) – Short-time static recovery of the Nb-Mn
steel at 1000°C after testing with glass
lubrication.
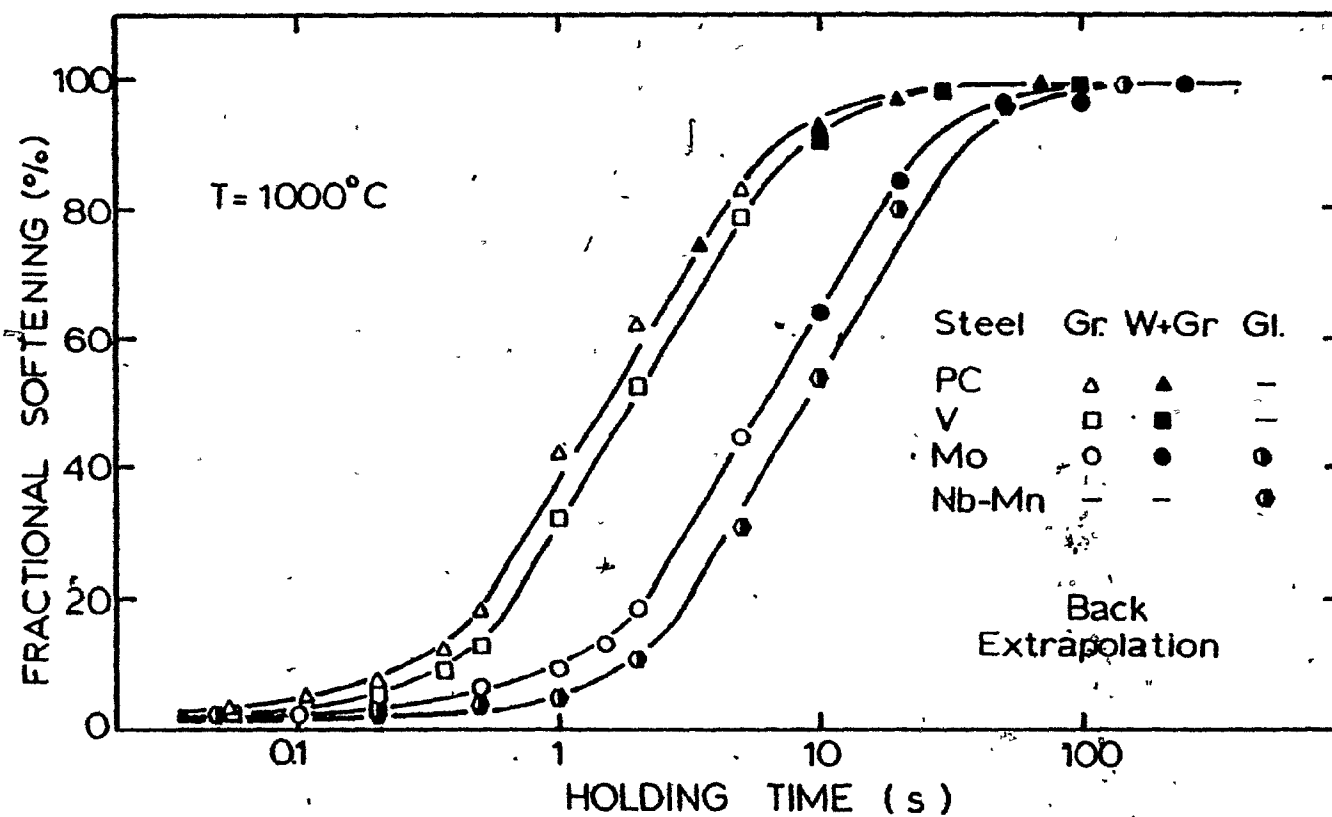
Figure 4.11(b) — Static recovery and recrystallization of the Nb-Mn steel at 1000°C after testing with glass lubrication.

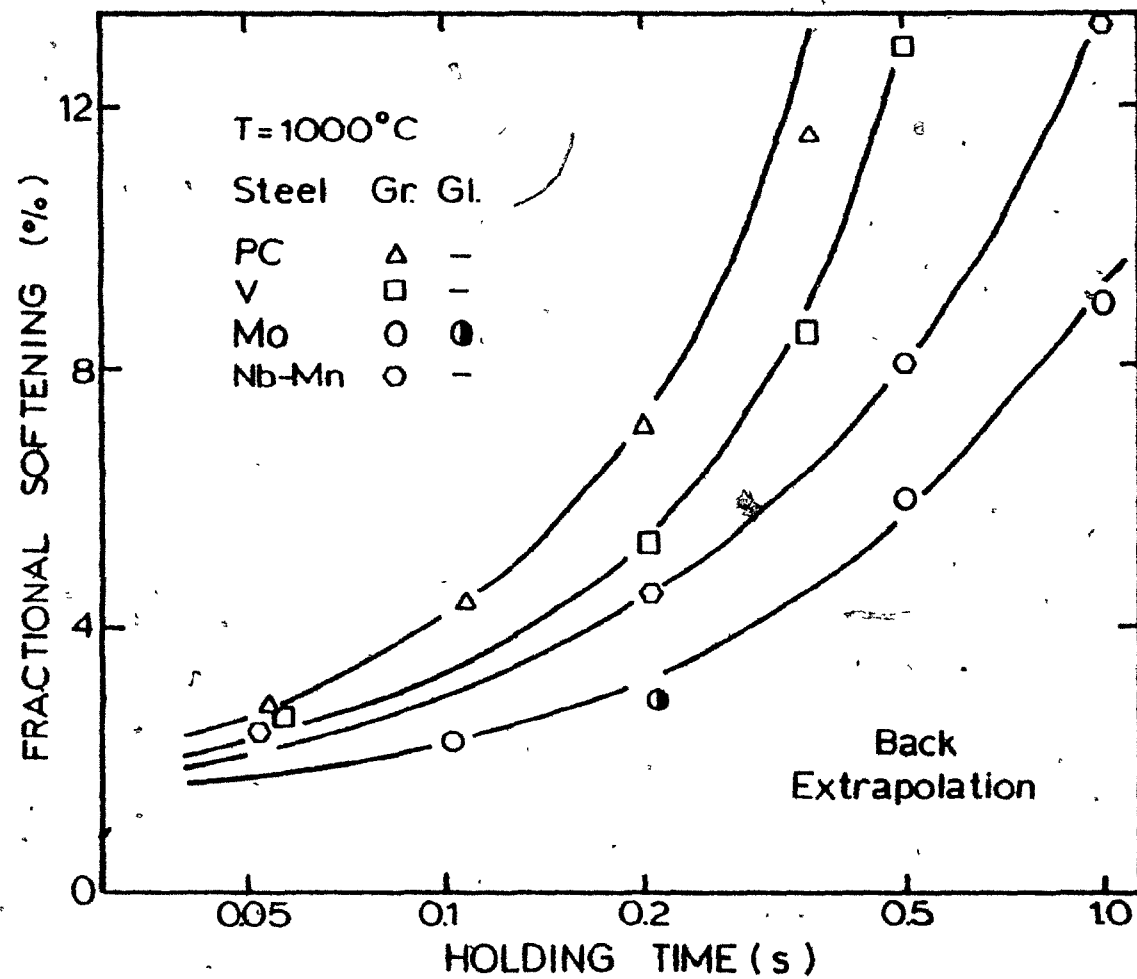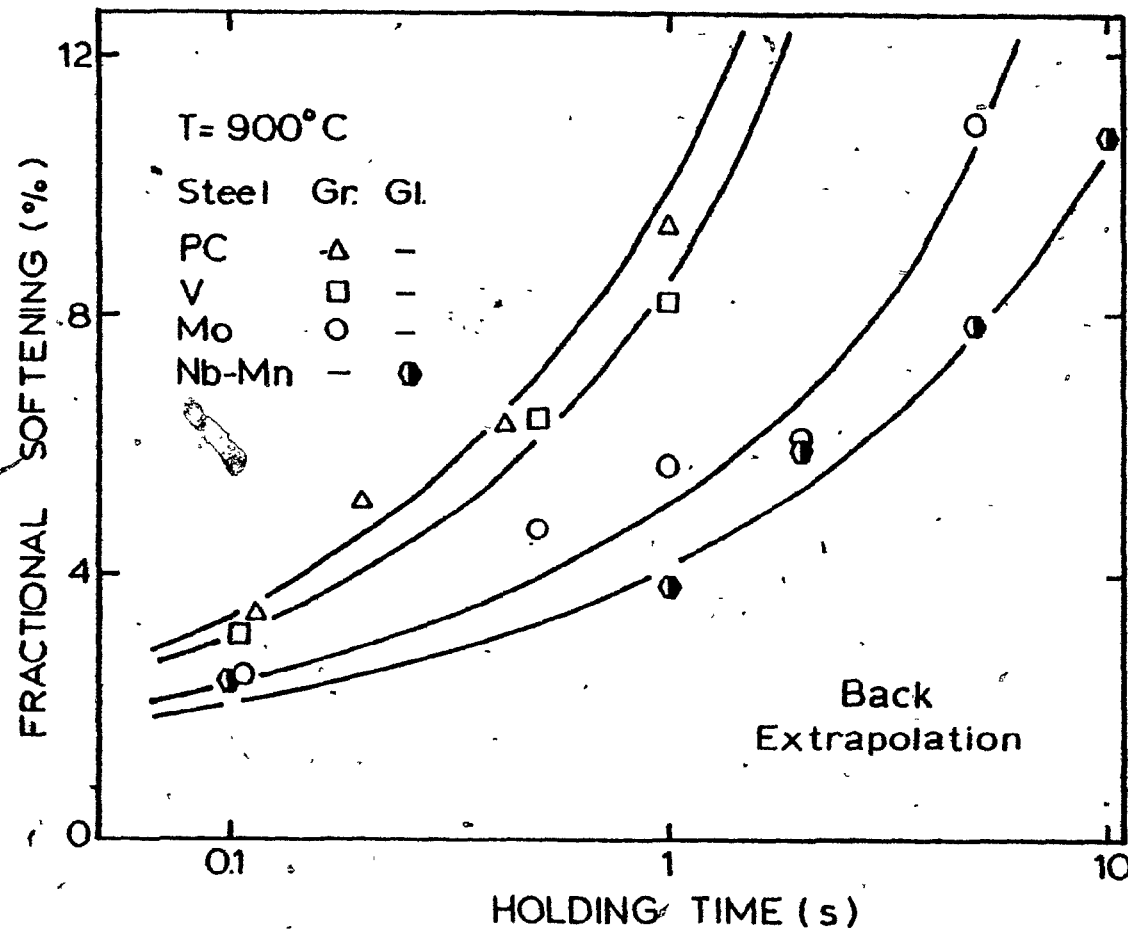Figure 4.12(a) – Short-time static recovery of the Nb-Mn
steel at 900°C after testing with glass
lubrication.
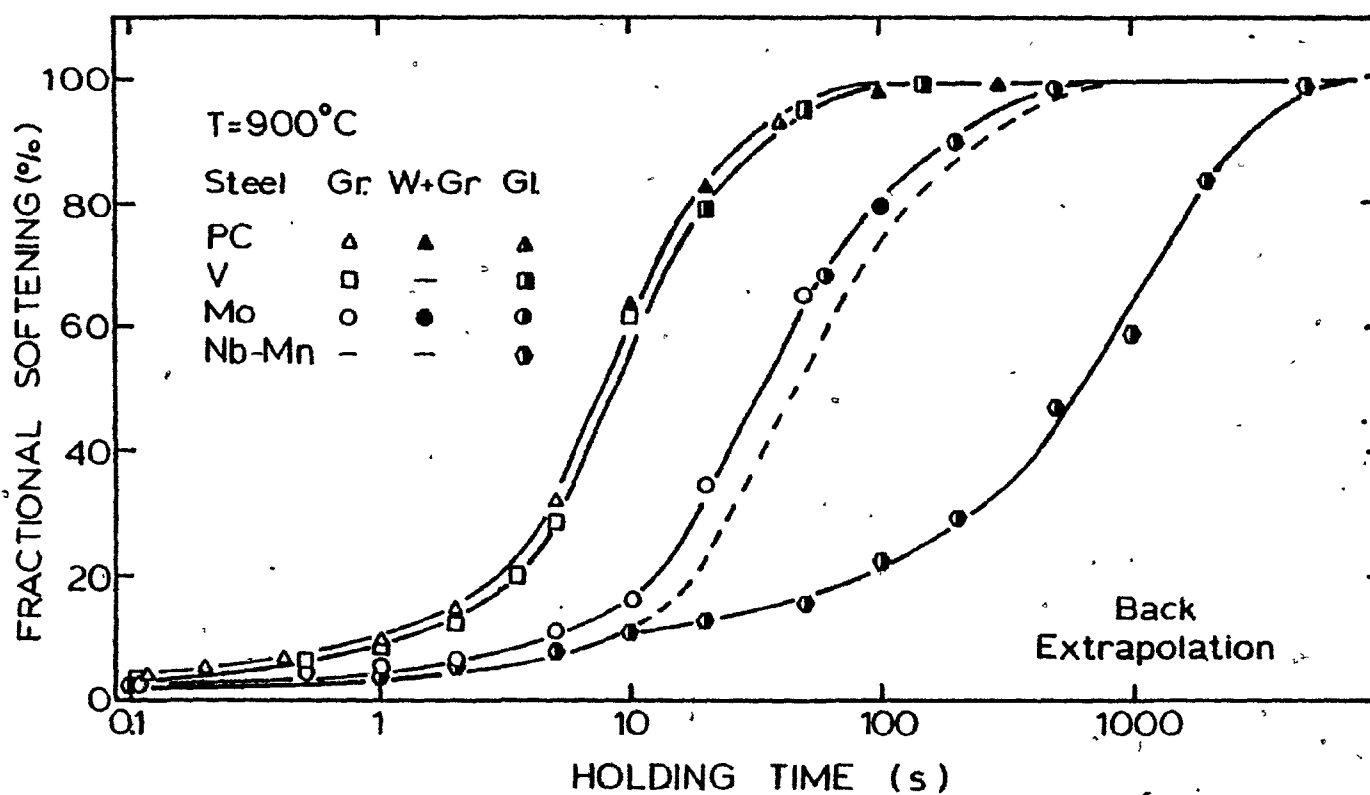
Figure 4.12(b) – Static recovery and recrystallization of the Nb-Mn steel at 900°C after testing with glass lubrication.

to a further delay in the onset of static recrystallization of about an order of magnitude. The dashed line indicates the new position of the estimated Nb curve in the absence of any precipitation. From this line it can be seen that, at 60% softening (which correspond to about 50% recrystallization), the occurrence of precipitation retards recrystallization by more than an order of magnitude in time (with respect to the solute Nb curve). When the dashed line is compared with the softening behavior of the plain C steel, it can be seen that the presence of Nb in solution retards recrystallization by slightly less than an order of magnitude in time.

As already mentioned, when glass instead of graphite lubrication is used, no detectable effect is observed on the softening behavior of the plain C, Mo and V steels. The change in lubricant affects only the Nb-Mn steel and the factors responsible for this difference in behavior will be considered in more detail in Chapter 5.

4.5 - HIGH TEMPERATURE STRENGTHENING PRODUCED BY ADDITIONS OF Mo, Nb AND V.

The strengthening increment per 0.1 at % of alloying addition relative to the reference plain C steel was evaluated from the following equation:

$$\Delta S^a = \frac{\sigma_{ys} - \sigma_{ys}^{PC}}{\sigma_{ys}^{PC}} \times \frac{0.1}{at\% \ s} \qquad (5)$$

In a similar way the strengthening increment per 0.1 wt.% of alloying addition was calculated from

$$\Delta S^W = \frac{\sigma_{ys} - \sigma_{ys}^{PC}}{\sigma_{ys}^{PC}} \times \frac{0.1}{wt\% \ s} \qquad (6)$$

In the above relations, σ_{ys} represents the average yield stress of the steel investigated, σ_{ys}^{PC} is the average yield stress of the reference plain C steel and at% s and wt% s are the atomic and weight proportions of the element under consideration.

The strengthening increments defined in this way were then calculated for each temperature and the average values for each element are displayed in Table 4.1. It is evident from this table that Nb has the greatest strengthening effect, followed in magnitude by Mo and then V. This order is the same on both the atomic and weight bases. The higher stengthening present in the Nb-Mn steel in comparison with the reference plain C steel is actually produced, not only by the addition of Nb, but also by an extra addition of 0.47% Mn. Under the present conditions, it is not possible to separate the contribution attributable to each of these elements. However, data obtained from a previous investigation (87) indicate that the strengthening effect due to Mn is, on an atomic basis, about 1 3/4 orders of magnitude less than the one produced by Nb.

The effect of the additional Mn was therefore neglected and all the observed strengthening was attributed to the presence of the Nb in Table 4.1.

The high temperature yield stresses for the four steels investigated are shown in Table 4.2.

Table 4.1

High Temperature Strengthening Produced

by Mo, Nb and V Addition

Element	ΔS^a (per 0.1 at %)	ΔS^w (per 0.1 wt%)
V (in a V Steel)	7.2	7.9
Mo (in a Mo Steel)	15.2	8.9
Nb (in a Nb-Mn Steel)	212.0	127.0

Table 4.2

High Temperature Yield Stress

of the Steels Investigated

Steel	σ_{ys} at 1000°C[*] (MPa)	σ_{ys} at 900°C[*] (MPa)
Plain C	35.5 ± 1.4	40.6 ± 2.5
V	38.0 ± 2.4	44.0 ± 1.3
Mo	39.0 ± 1.8	56.2 ± 1.7
Nb - Mn	50.0 ± 1.8	58.5 ± 1.6

[*]Limits shown are for a confidence interval of 95%.

CHAPTER 5

DISCUSSION

5.1 - INFLUENCE OF THE USE OF GRAPHITE AS LUBRICANT

The fractional softening vs. holding time curves presented in the previous chapter showed that the static recovery and recrystallization processes in the Nb-Mn steel were significantly accelerated when graphite instead of glass was used as the lubricant. By contrast, no effect could be attributed to the change in the type of lubrication in the results for the three other steels. The analysis of the possible causes of this discrepancy led to the hypothesis that they are related to the diffusion of C from the graphite into the samples during the austenitization heat treatment. The validity of this hypothesis will now be considered.

5.1.1 - Diffusion of C from the Graphite to the Samples

As illustrated in Fig. 5.1, before each experiment, a graphite suspension was painted on the end surfaces of each sample. The suspension was also applied to the lateral areas near the end surfaces. This procedure led to a reduction in the friction during compression. The extent of the C diffusion zones indicated in the figure was estimated in each steel

by Fick's second law solved for the case where the surface concentration remains constant with time. This solution is given by:

$$\frac{C_s - C}{C_s - C_o} = erf \left(\frac{x}{2 \sqrt{Dt}} \right)$$ (7) where

C_s — carbon concentration on the surface

C_o — initial carbon concentration in the sample

C — carbon concentration at given values of x and t

x — distance from the surface (cm)

t — interval of time for diffusion (sec)

D — diffusion coefficient of carbon in austenite (cm^2/sec)

The symbol erf $(x /2 \sqrt{Dt})$ represents the error function with argument $y = x/2 \sqrt{Dt}$. This function is defined by the equation

$$erf (y) = \frac{2}{\sqrt{\pi}} \int_o^y e^{-y^2} dy$$ (8)

The diffusion coefficient of carbon in austenite, D, was calculated from the relation

$$D = D_o \, e^{\frac{-Q_d}{RT}}$$ (9) where

Q_d — activation energy (33800 cal/g-mole)

R — universal gas constant (1.987 cal/(°K)/(g-mole))

T — absolute temperature (°K)

D_o — constant which depends on the structure and vibrational frequency of the atoms (0.21 cm^2/sec)

The values of Q_d and D_o shown above were taken from Reference (94).

The maximum penetration of carbon in each steel was then determined for the condition that C drops down to the vicinity of C_o; i.e. that $C \simeq C_o$. In this case, erf $(x/2\sqrt{Dt}) = 1$ and $x/2\sqrt{Dt} = 3$ (95). For simplicity, only the diffusion of C from the graphite painted on the _end_ surfaces of the samples was considered, and the values obtained in this way are presented in Table 5.1. The diffusion of C during heating to the austenitization temperature was also neglected. The results shown in Table 5.1 indicate that, in 43.4% of the total volume of each Nb- Mn steel sample, the C content is higher than the original concentration of C in this steel. Furthermore, the degree of penetration of C in the Nb-Mn steel is greater than in the others; it is almost double that calculated for the plain C steel, in part because of the higher austenitization temperature, and in part because of the longer holding time.

In order to determine the gradient of the C concentration inside the diffusion zones in the Nb-Mn, Mo and V steels, deformed samples of these steels were ground down to specified distances from the end surfaces and the C concentration in each 'new end surface' was determined by emission vacuum spectrometry. As no barreling was observed in the samples after deformation, the corresponding positions of these surfaces

Table 5.1

Diffusion of C from the Graphite to the Samples

Steel	Austenitization Temperature (°C)	Austenitization Time (s)	Maximum C Penetration (mm)	% of the Total Volume
PC	1030	900	1.3	22.0
V	1045	1800	1.9	33.6
Mo	1070	1800	2.2	37.8
Nb-Mn	1100	1800	2.5	43.4

in the undeformed material were calculated by considering that
the deformation was homogeneous. The results obtained in this
way are displayed in Fig. 5.2. It can be seen that inside the
diffusion zones the C concentration in the Nb-Mn steel is
higher than in the Mo and V steels at the same distance from
the surface. The maximum penetration of C in the three steels
appears to be in agreement with the values calculated theore-
tically (Table 5.1).

5.1.2 - Solubility Products of Nb, Mo and V Carbides in Austenite

The solubility products for NbC and V_4C_3 at the austeni-
tization temperatures of the Nb-Mn and V steels are indicated in
Table 5.2, together with the maximum C concentrations that can
be held in solution in the presence of 0.035% Nb and 0.115% V
at these temperatures. The relations from which these values
were calculated are displayed at the bottom of the Table. The
equation reported by Koyama et al. (96) takes into considera-
tion the effect that Mn has on the solubility product of NbC
in austenite, which increases with the increase in the Mn con-
tent. The Mn levels of the steels on which the equations
given by Narita (97) and Cordea (2) were based are not known,
although the latter are believed to have been determined on
steels with a Mn content in the proximity of 1.2 to 1.4%.

According to the results shown in Table 5.2, the
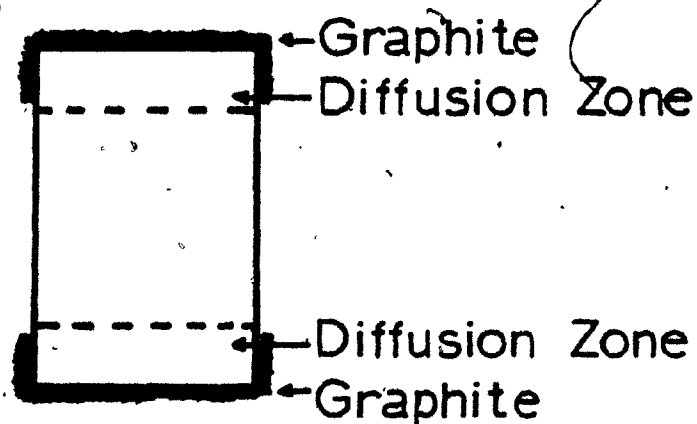
Figure 5.1 - Location of graphite coated regions of the sample and the C diffusion zones after austenitization.
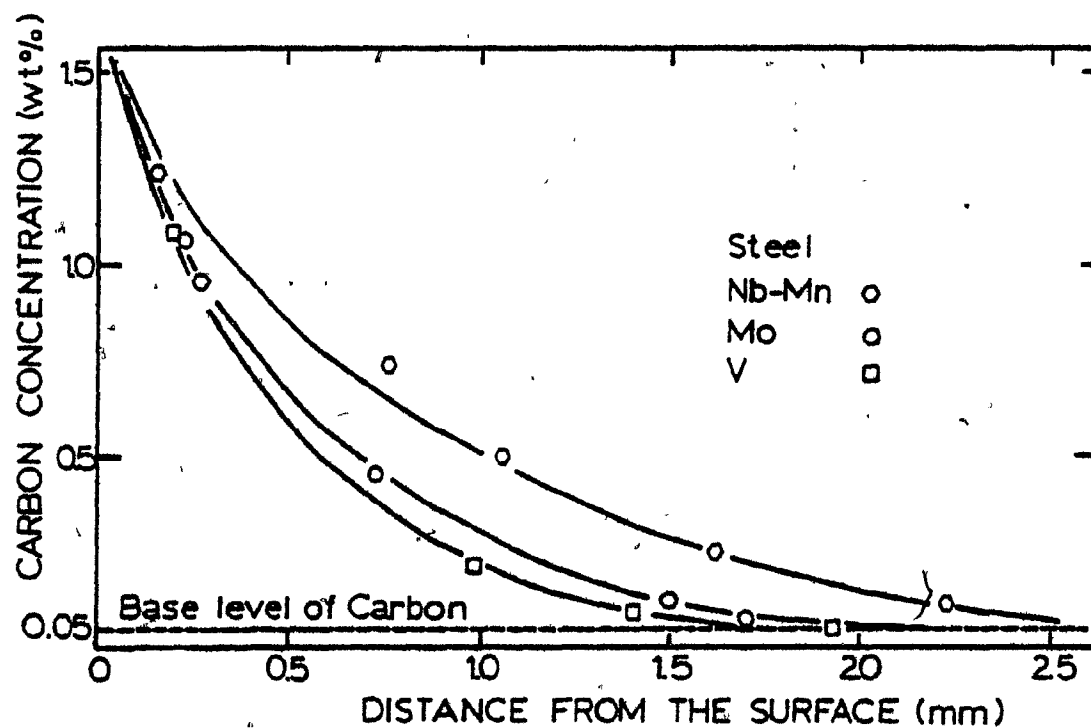
Figure 5.2 - C concentration gradient inside the diffusion zone after austenitization of the Nb-Mn, Mo and V steels.

Table 5.2

Solubility Products for NbC and V_4C_3 in Austenite

Steel	Precipitate	Austenitization Temperature (T_{aus})	Solubility Product at T_{aus} $(x10^{-3})$			Maximum C concentration in Solution* at T_{aus} (wt%)		
			Cordea[1]	Narita[2]	Koyama[3]	Cordea[1]	Narita[2]	Koyama[3]
Nb - Mn	NbC	1100°C	3.10	4.64	4.76	0.09	0.13	0.14
V	V_4C_3	1045°C	73.41	–	–	1.31	–	–

(1) Cordea

$$\log (Nb).(C) = \frac{-7510}{T} + 2.96$$

$$\log (V)^{4/3}.(C) = \frac{-10800}{T} + 7.06$$

(2) Narita

$$\log (Nb).(C) = \frac{-7900}{T} + 3.42$$

(3) Koyama et al.

$$\log (Nb).(C) = \frac{-7970}{T} + 3.31 + \left(\frac{1371}{T} - 0.900\right)(Mn) - \left(\frac{75}{T} - 0.0504\right)(Mn)^2$$

(*) For 0.035% Nb and 0.115 % V.

maximum concentration of C that can be dissolved at 1100°C in the Nb-Mn steel without exceeding the solubility product for NbC at a Nb concentration of 0.035%, is 0.14%. This was determined from the relation given by Koyama et al., which is considered to be the most appropriate due to the high Mn level (1.90%) in this steel. By contrast, a C concentration considerably higher (1.31%) can be dissolved in the V steel(at 1045°C and for 0.115% V) before the solubility product for V_4C_3, is exceeded. Although very few quantitative data are available in the litera-ture for the solubility product of molybdenum carbide, it can be seen from Fig. 5.3 (98) that its value is likely to be higher than the one for vanadium carbide. As a result, a concentration of C higher than 1.31% can be expected to be dissolved at the austenitization temperature of the Mo steel (1070°C) without surpassing the solubility product for molybdenum carbide in the presence of 0.29% Mo. Naturally, one must take into account that these considerations apply only to equilibrium conditions, i.e., to long holding and diffusion times.

The analysis of the results presented above and in Fig. 5.2 leads to the conclusion that, as a result of C diffusion, NbC precipitates formed in the Nb-Mn steel during austenitiza-tion. These precipitates were likely to be present in approxi-mately 32% of the volume of each sample of this steel imme-diately after the austenitization heat treatment. The austeni-tization heat treatments in the Mo and V steels, on the other
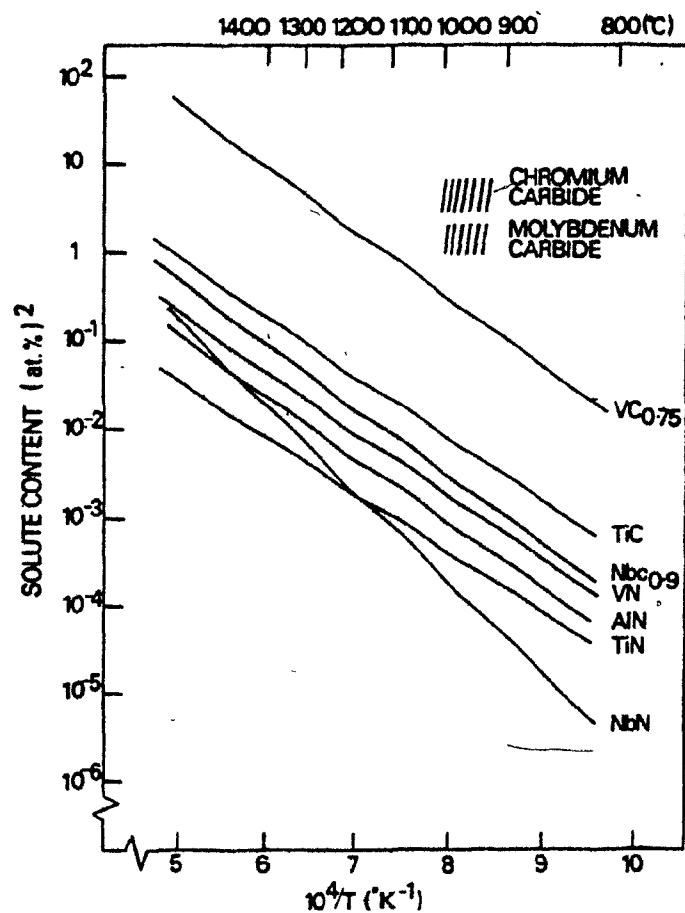
Figure 5.3 - Solubility products (in atomic
per cent) of carbides and nitrides
in austenite as a function of
temperature. (after Aronsson (98))

hand, enabled all the carbides present in at least 99%[*] of the total volume of these samples to be dissolved, despite the diffusion of C inwards from the ends.

5.1.3 - Effect of Graphite on the Softening Behavior of the Nb-Mn Steel

The softening curves for the Nb-Mn steel obtained at 1000 and 900°C with the use of graphite and glass lubricants are compared in Figures 5.4(a) and 5.4(b), respectively. At both temperatures, the static recovery and recrystallization processes were significantly 'accelerated' (with respect to the glass results) when graphite was employed as the lubricant. The faster softening rates observed under these conditions are related to the presence of undissolved precipitates of NbC in the samples. These precipitates probably affect the softening processes in the following direct and indirect ways:

(i) They may inhibit grain growth of the initial austenite grains (1,7,56,57), producing finer initial grains which decrease the incubation time and increase the rate of recrystallization.

(ii) When they are large and widely spaced, they may accelerate recrystallization by generating strain gradients, and hence recrystallization nuclei, at their interfaces (58,59).

---

[*] As a result of C diffusion, some carbide precipitation probably occurred next to the end faces.

(iii) Their most important and indirect effect is that they decrease the amount of Nb in solution. This reduces the solute retarding effect of this element, and also reduces its effectiveness when it forms strain induced precipitates.

Of the various factors described above, the one that appears to be the most influential is the reduction in the amount of Nb in solution after austenitization. This is either because the quantity of initial precipitates that can be dissolved within the diffusion zone is considerably reduced by the local increase in the C concentration. Alternatively, if particle solution is more rapid than C diffusion, the subsequent increase in the C concentration resulting from diffusion can lead to reprecipitation (on grain boundaries?) of dissolved carbonitride, reducing the quantity available for strain induced precipitation, i.e., on dislocations. When glass was used as the lubricant instead, all the initial Nb(C,N) precipitates were dissolved during the austenitization heat treatment and, therefore, the full amount of Nb was in solution before deformation and available for strain induced precipitation.

In the results obtained at 1000°C (Fig. 5.4(a)), the reduction in the overall concentration of Nb in solution
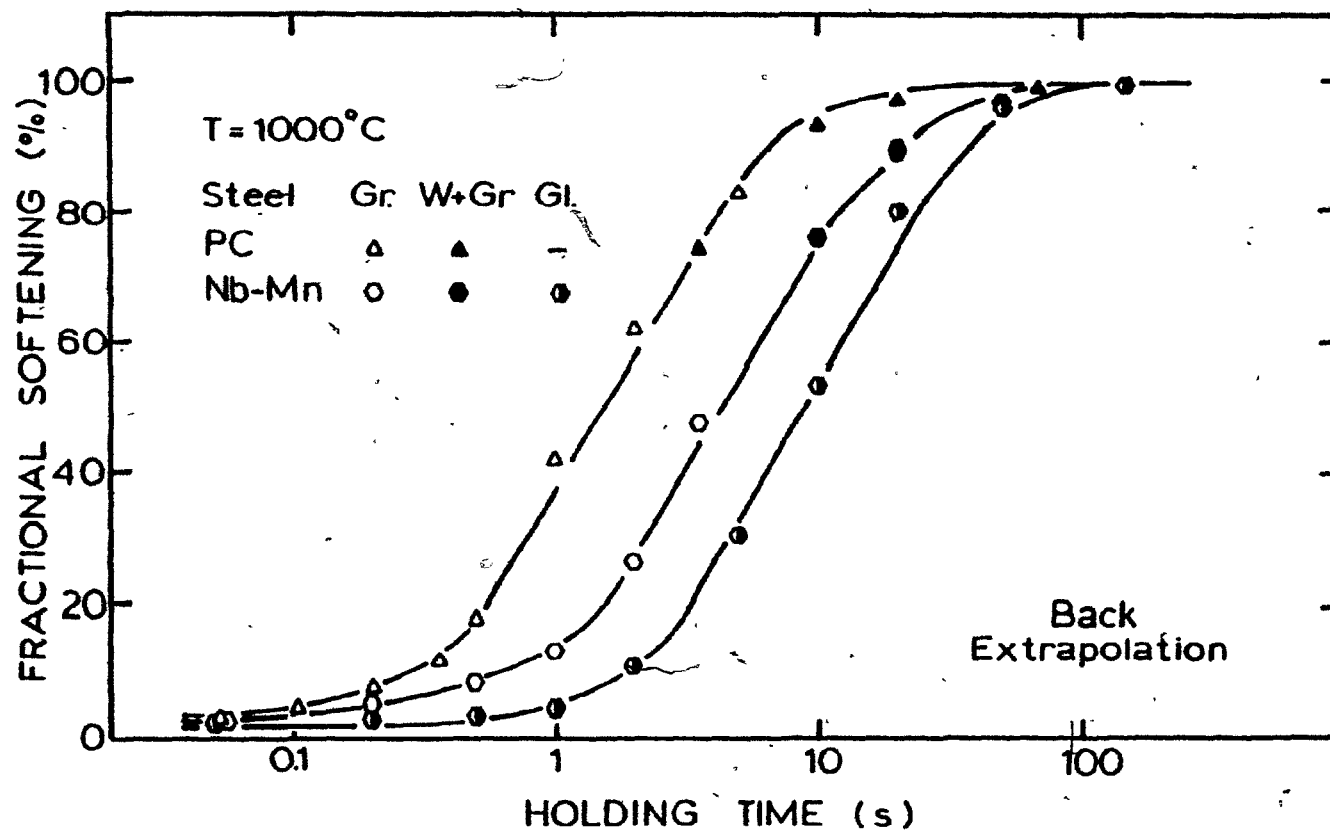
Figure 5.4(a) - Comparison of the softening behaviors of the Nb-Mn
steel at 1000°C associated with the use of (i) graphite
and (ii) glass lubrication.

decreased the <u>solute retardation effect</u> due to this element and thus 'accelerated' (with respect to the glass results) the static recovery and recrystallization processes in the Nb-Mn steel lubricated with graphite. Of course, recrystallization was still <u>retarded</u> in both Nb steels in comparison with the plain C steel (see Fig. 5.4(a)). The relative retardations can be estimated from the times for 60% softening (approximately equal to 50% recrystallization). The time for the steel containing less Nb in solution (the graphite lubricated samples) is 6 s at 1000°C, whereas that for the glass lubricated material is 12 s. Thus, with the aid of the Solute Retardation Parameter introduced below (section 5.3) the average amount of Nb in solution in the first material can be estimated. On the assumption that the value of the parameter for Nb is independent of the level of this element within the current range, the effective concentration of Nb in the graphite lubricated material is 0.021 wt%, i.e., it appears to have been reduced by 2/5. It should be added that previous investigations (87) of the kinetics of the strain induced precipitation of Nb(C,N) in this steel indicate that precipitation is unlikely to occur before 100 s at this temperature. As a result, strain induced precipitation was unlikely to occur prior to the end of static recrystallization, so that the curves of Fig. 5.4(a) are probably influenced by solute effects alone.

At 900°C, on the other hand (Fig. 5.4(b)), an extra
component of retardation begins to be observed. It can be
detected when the softening curves deviate from the be-
havior (indicated by the dashed lines) expected when only
solute effects are involved. These deviations are considered
to be associated with the onset of the strain induced preci-
pitation of Nb(C,N) and occur at around 10 and 2s for the glass
and graphite lubricants respectively.* The earlier onset of
precipitation under the latter conditions can be attributed to
the higher degree of supersaturation under which the Nb and C
were present within the diffusion zones. In these regions, the
strain induced precipitation of NbC appeared to start 8 s before
the precipitation of Nb(C,N) began in the other material. How-
ever, as less Nb was available for precipitation in the Nb steel
lubricated with graphite, the retarding effect of the strain
induced precipitates on the onset and progress of static recry-
stallization was reduced in this steel.

Note that the relative effectiveness of strain induced
precipitation under the two set of conditions can be assessed
from Fig. 5.4(b) in a manner similar to that used for solute
retardation (Fig. 5.4(a)). For this purpose, it is necessary

---

*Due to a lack of time, no electron microscopy was
performed on the present specimens, and so the presence of
precipitates could not be confirmed.
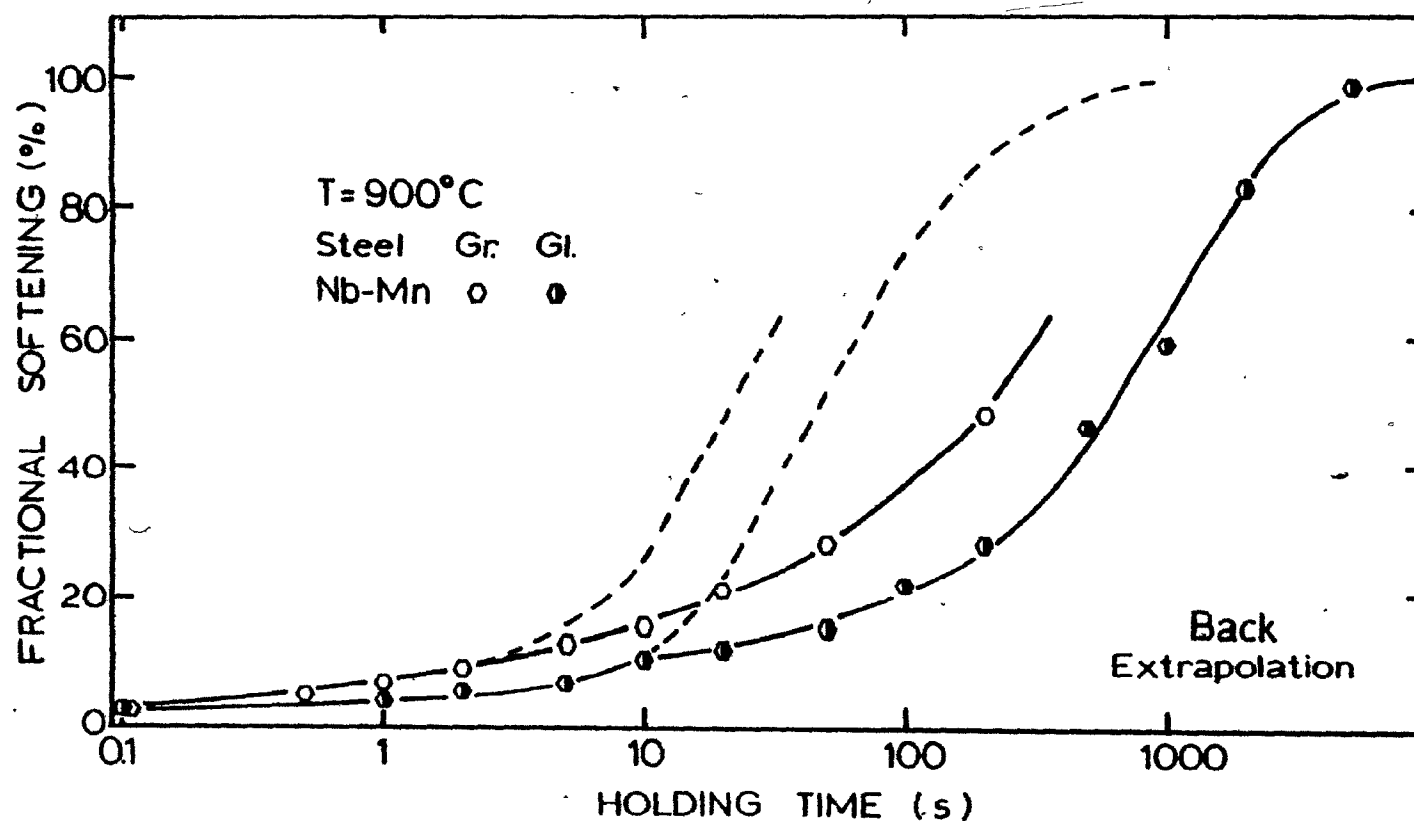
Figure 5.4(b) - Comparison of the softening behaviors of the Nb-Mn steel at 900°C associated with the use of (i) graphite and (ii) glass lubrication.

to determine the times for 50% recrystallization (60% soften-
ing) under straight solute retardation conditions (dashed
curves - 30 and 66 s for graphite and glass lubricated tests,
respectively), as well as under precipitation conditions (full
curves - 300 and 880 s for graphite and glass lubricated
tests, respectively). These data suggest that, in the presence
of graphite, there is only about 75% as much precipitate re-
tardation as under normal testing conditions. This diminished
effectiveness can be linked with the production of a reduced
volume fraction of carbide particles.

The softening behavior of the three other steels was not
affected by the use of graphite. As shown in the previous sub-
section, all the V and Mo were likely to have been dissolved
during the austenitization heat treatment, preserving in this
way their full contribution as solutes to the retardation of
static recovery and recrystallization. Although the diffusion
of C into the samples increases the possibility of the strain
induced precipitation of carbides in the V and Mo steels, the
results presented in Figures 4.6(a) and 4.6(b) suggest that
this precipitation did not take place under the experimental
conditions investigated. As can be seen from these figures,
no deviations, with respect to the plain C steel, are observed
in the softening curves of these steels. It should be added

that there is evidence in the litarature (99) that an increase in C content can _enhance_ softening as a result of the expansion of the austenite lattice and the increase in self-diffusivity. However, the current results (Fig. 4.6(b)) indicate that this effect is negligible under the present conditions.

5.2 - EFFECT OF Mo, Nb and V ON STATIC RECOVERY AND RECRYSTALLIZATION

5.2.1 - Effect of Mo, Nb and V as Solutes

The results obtained in the present work show that static recovery and recrystallization are delayed by the presence of Nb, Mo and V in solution, with the retardation rates increasing in the following ascending order: V<Mo<Nb. These retarding effects are thought to be associated with the strengthening produced by these microalloying elements, which follows the same order described above. A number of theories has been proposed to explain the different strengthening and retarding effects produced by various solute atoms. According to these theories, it is principally the size and electronic differences which are responsible for the phenomena observed. These two possibilities will now be considered in turn.

5.2.1.1 - Size Differences

The effect of adding a given type of solute atom has

generally been evaluated in terms of the size difference between host and solute, a quantity which can be calculated from two different types of data: (i) the atomic size difference between a given solute atom and the gamma iron host; and (ii) the atomic size misfit parameter $(1/a).(da/dc)$ where a is the mean lattice parameter and c is the atomic concentration of the solute. These data are presented in Table 5.3 for the most common solute elements in gamma iron. The atomic sizes were obtained from Reference (100); the values for the size misfit parameter are taken from a survey carried out by Plassiard (101), to whom the author expresses his gratitude for permission to quote prior to publication.

It is apparent from Table 5.3 that Nb, with a size difference of + 15%, is expected to have a stronger effect than either Mo at + 10% or V at + 6%. On this basis, Mn (+ 2%), Cr (+ 1%) and Ni (- 2%) are likely to have only small effects. These observations agree qualitatively with the results obtained in this investigation and also by other researchers (80,102). However, there are two important exceptions in the order of solute effects predicted by the atomic size criterion. The addition of titanium and aluminum, two elements which have almost the same size difference with respect to gamma iron as Nb, produces amounts of solute hardening and solute retardation

Table 5.3

Size Differences with Respect to Iron

Element	$r_x(\overset{\circ}{A})$	$(r_x - r_{Fe})/r_{Fe} \times 100$*	Atomic Size Misfit Parameter** $(1/a).(da/dc)$
Nb	1.468	+15	0.242
Ti	1.462	+15	0.109
Al	1.432	+12	0.056
Mo	1.400	+10	0.133
V	1.346	+6	0.042
Si	1.312	+3	−0.012
Mn	1.304	+3	0.023
Cr	1.282	+1	0.017
Ni	1.246	−2	0.026*

* $r_{Fe} = 1.274 \overset{\circ}{A}$

** For alpha iron

considerably less than that of Nb (71,82,103). In the case
of aluminum, its solute retardation effect is less even than
that attributable to molybdenum on an equal atom fraction
basis. These inconsistencies can be resolved by the use of
the atomic size misfit parameter(101). Examination of Table 5.3
shows that almost all the elements (except Si) listed on this
table increase the lattice parameter. Such dilation of the
lattice is likely to have two opposite effects.

(i)   The solute atoms can interact elastically with the dis-
       locations; this generally increases the strength con-
       siderably.

(ii)   The lattice dilation may produce a measurable decrease
       in the elastic modulus, an effect which should in turn
       lead to softening.

       The latter effect appears to be experimentally detec-
table in the case of interstitials, such as C and N. The
addition of these elements strongly dilates the lattice, which
leads to a large decrease in modulus and, consequently, to
observable softening. The addition of substitutional elements
causes a smaller distortion of the lattice and, in this case,
the strengthening produced by the elastic interactions be-
tween the solute atoms and the dislocations overcomes the
softening expected from the lattice dilation. As a result,
hardening is observed instead of softening. According to this

analysis, the larger the change in the lattice parameter produced by a given element, the more likely is it to produce significant strengthening and retarding effects.

From the values shown in Table 5.3, it is evident that the size misfit parameter seems to give a much better correlation with strengthening than the atomic size criterion.* Nb with a size misfit parameter equal to 0.242 is expected to have stronger effects than Mo, Ti, Al and V, with size misfit parameters equal to 0.133, 0.109, 0.056 and 0.042, respectively. On the other hand, Mn (0.023), Ni (0.026) and Cr (0.017) should have only very small effects. However, the reversed order between Ti and Mo suggests that some electronic effects may be involved, which possibility will be considered in the next section. In addition, there may be a contribution to the misfit parameter from the relative modulus mismatch, as at room temperature, but there are insufficient data available for an assessment to be made of this possibility at this time.

5.2.1.2 - Electronic Differences

According to the basic approach of Abrahamson and co-workers (104), the expected effect of solute additions on the

---

*Although these data are for alpha iron and the absolute values may change at high temperature (for γ - iron), the order of increase in the size misfit parameter determined in this phase is unlikely to be changed in the austenite phase.

recrystallization behavior of Fe depends primarily on the
number of s, p and d electrons in the outer shell of the par-
ticular elements in their ground state. Abrahamson's original
plot is reproduced here as Fig. 5.5. Two assumptions must be
made to compare Abrahamson's model with the results obtained
in the present situation. The first is that his rationaliza-
tion determined experimentally for alpha iron applies to gamma
iron. The second assumption concerns the conversion from iso-
chronal to isothermal conditions, and stipulates that the rate
of recrystallization at a fixed temperature follows the rank-
ing given in Fig. 5.5 for the temperature of recrystallization
at a fixed time, inasmuch as these are kinetically equivalent.

It is apparent from Fig. 5.5 that Nb and Ti have much
more powerful effects on the recrystallization kinetics of
α-Fe than Mo and V. However, significant differences between
the effects of Nb and Ti and between those of Mo and V are not
found on the diagram, although they were observed in the pre-
sent work (for Mo and V), and in the work of Chandra et al.
(71) (for Nb and Ti). This may be because Abrahamson's re-
sults were obtained on α-Fe.

Electronic differences are also related to the concept
of 'associated solutes' introduced by W.C. Leslie (105).
According to this idea, two or more solutes, which display a
strong attraction for each other, can be associated in solution,
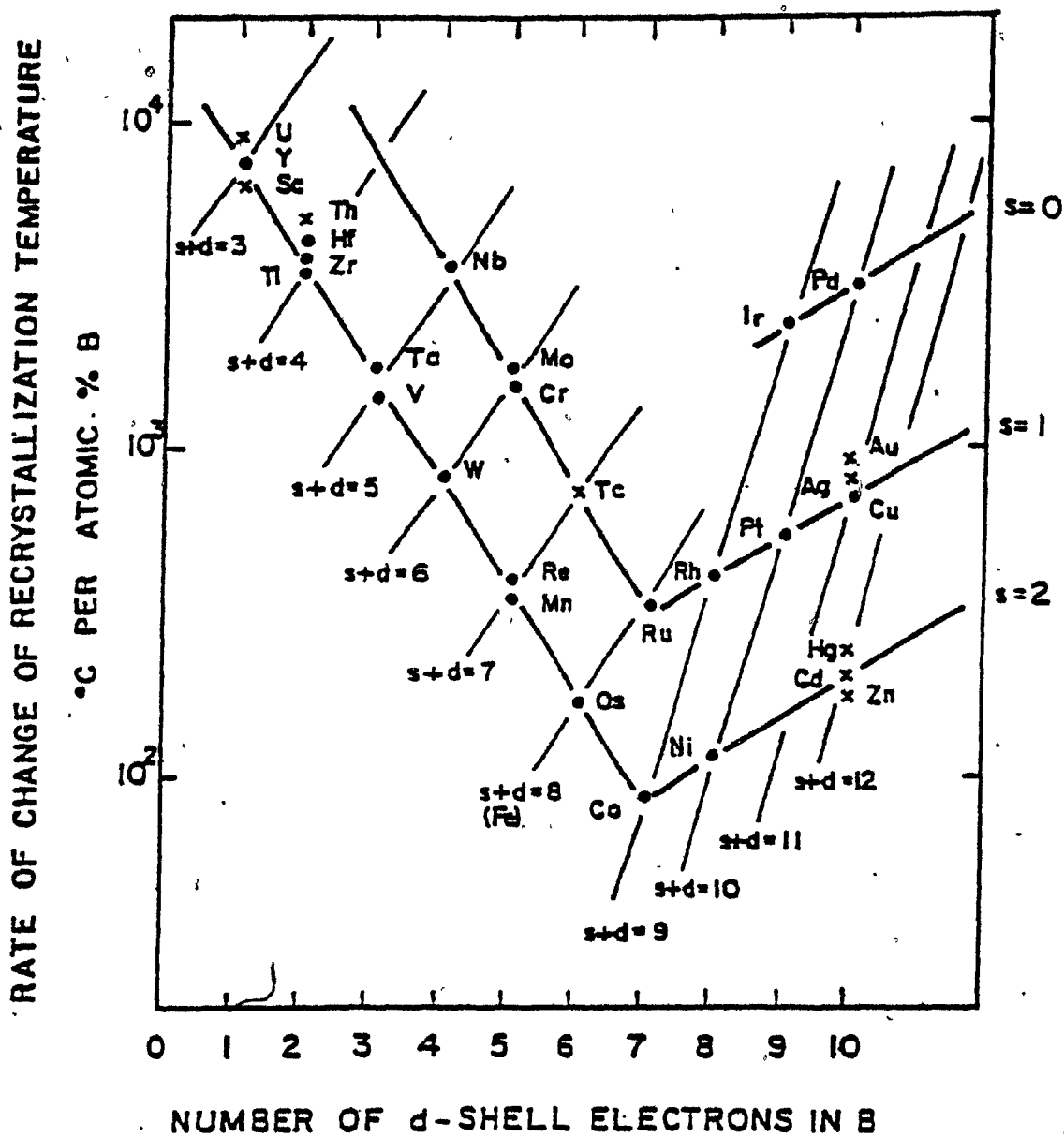
Figure 5.5 - Effect of the addition of transition elements on the recrystallization temperature of deformed α-iron (after Abrahamson (104)).

forming a type of cluster. Such clusters can interact strongly with dislocations, retarding recrystallization or strengthening the material. The relevant solutes may be any combination of interstitial or substitutional elements and the results are most pronounced when these are present in very low concentrations. Observations of this type have already been reported (105) for the case of Ti, C and N in ferrite. The idea that elements such as Nb, Ti, Mo or V might form with C and N some sort of ordered region or cluster without necessarily creating a compound or precipitate is a rather welcome one. It helps to bridge the gap between the 'solute' and 'precipitate' theories of recrystallization retardation.

5.2.2 - Effect of Nb and V as Precipitate Formers

In the present investigation, the effect of precipitation on static recovery and recrystallization was analysed in the Nb and V steels, since molybdenum (when added alone) does not form precipitates in austenite. As already mentioned in Chapter 2, the effect of precipitates is determined by their sizes and by the conditions under which the precipitation takes place. When precipitates remain undissolved before deformation, they are too coarse (1000-3000 $\overset{o}{A}$ in dia.) to interact with dislocations and therefore to inhibit recovery and recrystallization. As described in section 5.1.3, if sufficiently coarse, these precipitates can even lead to an

'acceleration' of the static softening processes. On the other hand, they also decrease the amount of the precipitate forming element available in supersaturation for strain induced precipitation. This kind of effect was observed in the Nb steel when graphite was used as the lubricant.

During strain induced precipitation, very fine particles (30-50 Å in dia.) are deposited on dislocations in the grain interiors and in sub-boundaries. These precipitates can retard both the onset and the progress of static recrystallization by the stabilization of the substructure (which prevents nucleation), and by their pinning of the grain boundaries and sub-boundaries (which inhibits their migration or growth). However, the full retarding effect of the strain induced precipitates is only obtained if precipitation starts before the onset of static recrystallization. In the case of the V steel at 900°C (Fig. 4.6(b)), recrystallization was nearly complete by the time the strain induced precipitation of VN was expected to occur (at a time of around 30 s), so that no effect of precipitation was detected. Nevertheless, in the Nb-Mn steel, the strain induced precipitation of Nb(C,N) took place, at 900°C, after a holding time of around 10 s, i.e. when the material was still completely unrecrystallized. Under these conditions, a further delay of about an order of magnitude in time was observed for the onset of static recrystallization.

The precipitation start time of 10 s determined in this work for the strain induced precipitation of Nb(C,N) at 900°C is somewhat shorter than the one obtained by Akben (87) in the same steel, but under dynamic conditions. In her experiments, a time of about 25 s was found for the onset of this process. As the rate of static precipitation normally increases with an increase in the pre-strain given to the material and tends to approach the dynamic one for large pre-strains, the results described above can be explained by the difference in the techniques employed for their determination. Given a margin of error expressed as a time ratio of 1.6 for each technique, the two methods would be in agreement if the actual P_s time were $10 \times 1.6 = 16 \approx 25/1.6$ sec.

5.3 - COMPARISON BETWEEN THE SOLUTE RETARDATION RESULTS OBTAINED UNDER STATIC AND DYNAMIC CONDITIONS

One of the initial aims of this investigation was to establish the calibration or conversion factor linking the onsets of static and dynamic recrystallization in hot worked austenite. However, lack of time prevented the complete fulfillment of this objective, as further research is probably required for the determination of the kinetics of static recrystallization in a wider range of materials. Nevertheless, a comparison can still be made between the solute retardation results obtained in the present work and the ones reported by

Akben, Bacroix and Jonas (102) under dynamic conditions. For this, the following solute retardation parameter (SRP) was employed (102).

$$SRP = \log (t_x/t_{ref}) \times \frac{0.1}{at\% \ x} \times 100 \ \% \qquad (10)$$

Here, t_x is the time required for the start of static recrystallization in the steel containing the element x, and t_{ref} is the equivalent time for the reference plain C steel. Of course, this equation corresponds only to the retardation produced by solutes. In the case where additional retardation is being produced by precipitates, e.g. in the Nb-Mn steel at 900°C (Fig. 4.1.2(b)), t_x is determined from the 'expected solute curve' (indicated by the dashed line in the same figure). The Solute Retardation Parameter defined in this way can represent the solute retarding effect of element x on the onset of recrystallization under both static and dynamic conditions.

The SRP's[*] calculated for each element from the present data are shown in Table 5.4. Also included are the parameters determined under dynamic conditions (102). It is evident from this table that the order of effectiveness in delaying the

---

[*]The values of SRP were calculated at 1000°C (Fig. 4.11(b)) and at 900°C (Fig. 4.12(b)) for a fractional softening of 10 and 15%, respectively. These amounts of softening correspond to the onset of static recrystallization at these temperatures. The final value of SRP for each element is the average for the two temperatures investigated.

onset of static recrystallization is the same under both sets of conditions: i.e. Nb>Mo>V. Furthermore, the retarding effect of Nb as solute is considerably larger than the ones produced by Mo and V. The much higher values of SRP calculated under static as opposed to dynamic conditions for all the three elements are of particular interest. They suggest that the interaction between solute atoms and dislocations is considerably stronger under conditions of interrupted straining than during deformation. This could be because diffusion makes it easier for solutes to reach stationary, rather than moving, dislocations. As the static SRP is more relevant to industrial rolling schedules, the present results suggest that the SRP's determined by dynamic methods probably underestimate the amount of solute retardation taking place in production. Thus a suitable correction factor should be developed if dynamic SRP's are to be used for the prediction of relative retardations in industrial situations.

It should be added that, while the ratio of SRP (static)/ SRP (dynamic) is about 3 to 4 for Mo and V it is in the range 7 to 8 for Nb. While this finding may be fortuitous, it may also be an indication of the presence of 'associated solutes' in the Fe - Nb - C system.

Table 5.4

Values of the Solute Retardation Parameter

(SRP) for Niobium, Molybdenum and Vanadium

Element	SRP Static Condition $\dot{\varepsilon} = 2 \ s^{-1}$	SRP Dynamic Condition $\dot{\varepsilon} = 5.6 \ x \ 10^{-3} \ s^{-1}$
V	10	3.3 ± 1.2
Mo	37	$10. \pm 5.$
Nb	409	$53. \pm 12.$

5.4 - IMPLICATIONS REGARDING THE DESIGN OF ROLLING SCHEDULES FOR CONTROLLED ROLLING

In this section, the practical implications of the results obtained in this work will be analysed with regard to the design of rolling schedules for the controlled rolling of microalloyed steels. The metallurgical and engineering factors involved will be considered under the following headings: (i) slab reheating temperature; (ii) recrystallization of austenite; and (iii) rolling load.

- Slab Reheating Temperature - The 'accidental' effects produced by the use of graphite with the Nb-Mn steel led to an understanding of the importance of the complete dissolution of all the carbonitrides present in the steel during slab reheating and soaking. Only in this way can the full amount of the precipitate forming element be made available, first as a solute and then as a strain induced precipitate. Both of these will help to prevent static recrystallization during the interpass time at the lower temperatures (finishing passes). If the larger precipitates remain undissolved, the potential retarding effects due to the microalloying element are not fully realized, and the possibility of partial recrystallization during the interpass time increases. This can lead to poor mechanical (particularly fracture) properties in the final product.

- <u>Recrystallization of Austenite</u> - The recrystallization start (R_s) and finish (R_f) times are shown in Table 5.5 for the four steels and two temperatures investigated. The R_s's correspond to the same amount of fractional softening as was employed in the previous section for the SRP calculations (Figures 4.11(b)) and 4.12(b)). The R_f's were determined at a fractional softening of 90%, which was considered to give a reasonable approximation to 100% recrystallization.

In industrial controlled rolling practice, the temperature of 1000°C is generally the lower limit for the roughing passes, where the complete recrystallization of the material during the interpass time is desirable. From the results displayed in Table 5.5, it can be seen that at this temperature, recrystallization is terminated in the plain C and V steels after a holding time of only 7 and 9 s, respectively. These times are about the same as those used in industrial rolling schedules in a reversing mill. In the case of the Mo and Nb steels, longer interpass times (27 and 38 s, respectively) would be necessary to prevent partial recrystallization. This suggests that rolling should be avoided at this temperature in these steels and that the roughing stage should be completed at higher temperatures. However, under industrial conditions, the R_f time at 1000°C for all the above steels will be somewhat

Table 5.5

Recrystallization Start (R_s) and Finish (R_f)

Times for the Steels Investigated

Steel	1000°C		900°C	
	R_s	R_f	R_s	R_f
	(s)	(s)	(s)	(s)
Plain C	0.27	7.0	1.9	30
V	0.38	9.0	2.3	35
Mo	1.0	27.0	9	200
Nb - Mn	9.0	38.0	90[*]	2800

[*] This value corresponds to 20% softening, rather than the 15% employed for the other cases. Because the onset of static recrystallization was delayed by the strain induced precipitation of Nb(C,N), the relative softening attributable to recovery was increased by 5%.

shorter than the ones listed in Table 5.5, so that full re-crystallization during the interpass time may still be possible in the Mo and Nb steels. This is mainly because of the higher strain rates (between 5 and 10 s^{-1}) that are employed indus-trially and because the 'initial' austenite grain size (with respect to a particular pass) produced by the successive cycles of recrystallization in the previous passes will generally be smaller under industrial conditions by comparison with those produced by austenitization in these experiments. These two factors make an important contribution to accelerating the static softening processes in industrial practice.

By contrast, recrystallization must be completely pre-vented at 900°C. At this temperature, recrystallization starts after 1.9, 2.3 and 9 s for the plain C, V and Mo steels, re-spectively. The presence of V in solution has a very small effect on the retardation of the onset of recrystallization and the retarding effect of solute Mo is only moderate. Due to this, partial recrystallization will unavoidably take place in these steels during finishing passes in plate mills, and in the plain C and V steels in finishing passes in strip mills, so that controlled rolling cannot be applied success-fully in these cases. However, in the Nb-Mn steel, recrystalli-zation only starts after 90 s, so that it is possible to pre-vent this softening process from occurring during the entire

finishing stage of rolling. Consequently, the benefits of controlled rolling can be obtained in this steel.

It is important to note, from the results presented in Table 5.5, that in the Nb-Mn steel, the retardation of the onset of recrystallization by the strain induced precipitation of Nb(C,N) is only possible because of the retarding effect of Nb as solute prior to the onset of precipitation. If no solute effect were present, recrystallization in this steel would start at the same time as in the plain C steel (1.9 s), and by the time the strain induced precipitation of Nb(C,N) occurs (10 s), the material would be partially recrystallized and the retarding effect of these precipitates would be largely reduced. The delay in the onset of static recrystallization in the Nb-Mn steel is therefore a combination of solute and precipitate effects.

It should be pointed out that the softening rates expected under industrial conditions are likely to be faster than the ones indicated by the present data. This is because, in addition to the higher strain rates mentioned earlier, when no recrystallization takes place, there is an accumulation of retained work hardening from pass to pass during the finishing stages of controlled rolling. The accumulated and retained work hardening increases the driving force for both recovery and recrystallization, which in turn increases the rate of each of these processes.

The above analysis suggests that, for controlled rolling purposes, better results could be obtained by combining the retarding effects produced by several alloying elements. For example, appropriate amounts of Mo, V and Nb could be combined in such a way that, at lower temperatures than employed here, the solute retardating effect of Mo would prevent recrystallization from starting until the precipitation of VN has begun. In this way, a long delay in the onset of recrystallization could be produced in this 'hypothetical' steel. However, the effects caused by multiple microalloying additions are not simply additive, and the complex interactions that take place between these elements have to be considered carefully when the chemical composition of a microalloyed steel is being selected (102).

- Rolling Load - The rolling load is an important variable, not only in the design of a controlled rolling schedule, but also for the operation of the mill by computer control. In the development of mathematical models for load prediction, it is essential to know the mean deformation strength (K) of the steel during the different stages of the rolling process. Interrupted compression tests have already been used (37) in the development of equations for the calculation of K which take into consideration

the residual strain accumulated between passes. These equations are particularly important for the prediction of loads during rolling in the unrecrystallized austenite region. The residual strain is proportional to the amount of work hardening retained after an accumulation of stages of deformation. As the amount of softening established experimentally depends on the method used to determine the initial flow stress on reloading, and as the estimated softening affects the predicted 'residual strain' quite critically, it is now of interest to consider which method gives the better results.

In the present work two methods were used to determine the fractional softening after a given holding time: (i) the back extrapolation; and (ii) the offset methods. These methods are illustrated in the true stress - true strain curves shown in Fig. 5.6 pertaining to a particular interrupted compression test. Here σ_r^{be} and σ_r^{os} are the flow stresses in the second compression as defined by the back extrapolation and offset methods, respectively, which were described in the Experimental Materials and Procedure Chapter. It is evident from this figure that the amount of softening given by the offset method is larger than the one determined by back extrapolation. This difference is associated with the transient behavior represented by the portion AE of the flow curve for the second
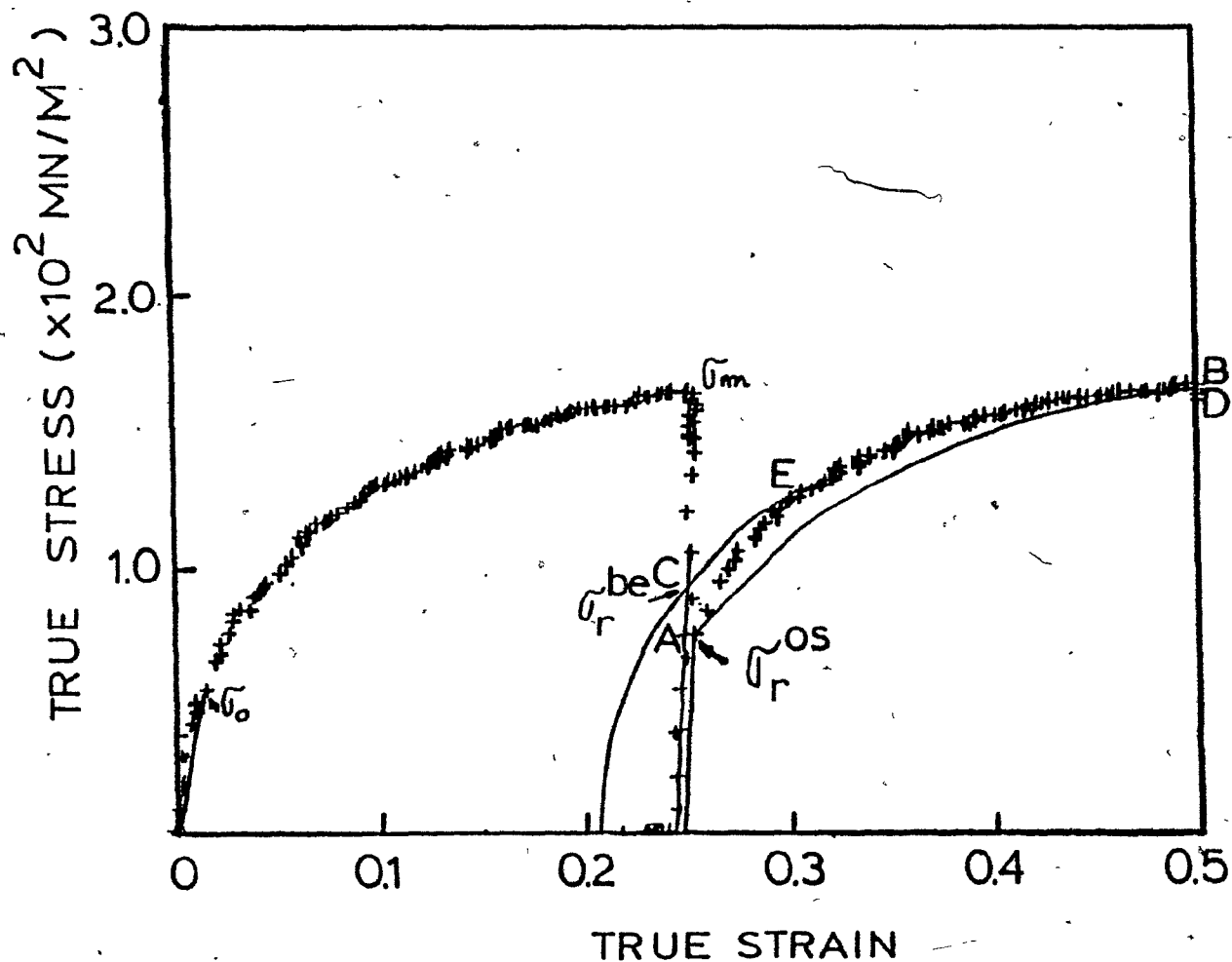
Figure 5.6 – Schematic representation of the reloading flow
curves estimated on the basis of the flow stresses
σ_r^{be} (curve CB – back extrapolation) and σ_r^{os}
(curve AD – offset) by a computer containing
the work hardening relation σ_O to σ_m (and beyond).
The 'short transient' (curve AE) is also indicated.

compression. This 'transient' is caused by the 'retreat' or 'runback' of mobile dislocations from the obstacles to glide during the unloading, as well as some loss of dislocations due to static recovery. On reloading, an increment of strain must be applied in order to regenerate the missing dislocations and to cause them to 're-contact' the obstacles. During this period, the stress is lower than 'normal', a phenomenon which leads to the 'short transient' observed in Fig. 5.6.

The curves CB and AD represent the flow curves expected by a computer containing an algebraic form of the work hardening relation σ_o to σ_m (and beyond), which estimates the reloading flow curve on the basis of the position of the reloading flow stress (i.e., σ_r^{be} or σ_r^{os}) on the work hardening relation. If the second compression is considered as a simulated rolling pass, the _actual_ load will be proportional to the area under the flow curve AB. The load given by the back extrapolation method (area under CB) will be slightly larger than the actual one, whereas the load calculated by the offset method (area under AD) will be considerably smaller. Thus it is evident that the estimation error will be larger for the offset method, and that the fractional softening measured by the back extrapolation method is in better agreement with the actual softening observed after intervals of deformation. Its use is therefore indicated in applications where accurate predictions of softening and of retained work hardening are desired.

The error associated with the offset technique is essentially due to the difficulty of representing the short transient AE (and its dependence on temperature, prestrain, etc.) in the computer in a convenient fashion. Even for the alternative method described above to be employed, however, the kinetics of softening must be expressed in a simple mathematical form which takes into account the current temperature, the accumulated and retained work hardening, the composition of the steel, etc. This remains a formidable challenge, and will require the availability of information such as that produced in this investigation over a wider range of temperatures, steel compositions and prestrains.

CHAPTER 6

CONCLUSIONS

In the present research, the effects of Mo, Nb and V addition on the retardation of static recovery and recrystallization were investigated in a series of microalloyed steels. In order to determine these effects, interrupted compression tests were carried out at 1000 and 900°C, and the fractional softening taking place after intervals of deformation was measured by two methods: the back extrapolation and the off-'set techniques. The influence of Nb and V in solution was distinguished from their influence as precipitates by determining the amount of softening occurring after holding times as short as 0.05 s and, therefore, prior to precipitation. From the analysis of the results obtained in this study, the following conclusions can be drawn:

1. Mo, Nb and V <u>in solution</u> retard the static recovery and recrystallization of deformed austenite to a significant degree. The strongest effect is due to Nb, followed by that of Mo and then V, the last of which delays these static softening processes only slightly. The relative influence of the three elements in solution can be detected

after unloading times as short as 0.1 s, and appears to be associated with their size and electronic differences with respect to γ-iron.

2. At 900°C, the occurrence of the strain induced precipitation of Nb(C,N) after a holding time of around 10 s leads to a further delay of about an order of magnitude in the onset of static recrystallization in the Nb steel. This extra component of retardation is only possible when static recovery is already delayed significantly by solute Nb which prevents the initiation of recrystallization prior to precipitation. If insufficient solute retardation is present, precipitation must take place in a recrystallized structure, and the resulting absence of dislocations means that strain induced precipitation cannot occur. A plain C steel deformed in the same manner recrystallizes in about 1.9 s., and therefore <u>prior to</u> the initiation of strain induced precipitation.

3. At 900°C in the V steel, recrystallization is nearly complete by the time the strain induced precipitation of VN is expected to take place. Thus only matrix precipitation is possible, and the recrystallization retarding effect of strain induced precipitation is absent. At 900°C in the Mo steel, only the solute retardation of recovery and recrystallization is observed. This is in agreement with

the view that the precipitation of Mo in austenite is unlikely under the present conditions.

4. In the Nb-Mn steel, lubrication by graphite instead of glass reverses the order of effectiveness of Nb and Mo at 1000°C. At 900°C, the use of graphite decreases by about 25% the retardation due to the strain induced precipitation of Nb(C,N). This effect appears to be due to the <u>incomplete solution</u> of Nb as a result of the diffusion of carbon into the end regions of the specimens. The presence of un-dissolved precipitates of NbC reduces the concentration of Nb in solution before deformation to about 3/5ths of the total Nb concentration. Consequently, the solute retarda-tion attributable to this element is decreased as is the amount available for strain induced precipitation.

5. The values of the Solute Retardation Parameter (SRP) show that Nb in solution is considerably more effective than is either Mo or V in retarding recrystallization; their relative effectivenesses are in the ratio 41:4:1. This order of effectiveness agrees with that reported by others for dynamic recrystallization. However, the static SRP's are considerably higher than the corresponding dynamic ones. In consequence, when the relative effectiveness of various solutes is assessed by <u>dynamic</u> means, the predic-tions that can be made regarding their influence on

industrial processes are likely to underestimate their true (static) effects.

6. The single addition of Nb, Mo or V produces a strengthening component, measured with respect to a reference plain C steel, of about 212, 15 and 7%, respectively, per 0.1 atomic per cent of addition.

7. At both temperatures investigated, the total amounts of fractional softening due to recovery measured by the offset method are double the ones determined by the back extrapolation technique. The results obtained by the application of the latter method are considered to be more useful for predicting the influence of recovery on mill loads in industrial practice.

REFERENCES

1. F.B. Pickering: "Microalloying 75", Union Carbide Corporation, New York, (1977), p. 9.

2. J.N. Cordea: 6ymposium on Low Alloy High Strength Steels, Nurnberg, BRD, (1970), Metallurg. Companies, p. 61.

3. E.O. Hall: Proc. Phys. Soc., Series B, 64 (1951), p. 747.

4. N.J. Petch: J. Iron and Steel Inst., 174 (1953), p. 25.

5. N.J. Petch: Proc. Swampscott Conference, MIT Press (1955), p. 154.

6. H.J. Wiester and H. Ulmer: Stahl and Eisen, 69, (1959), p. 1120.

7. K.J. Irvine, T. Gladman, J. Orr and F.B. Pickering: J. Iron and Steel Inst., 208 (1970), p. 717.

8. W.E. Duckworth: Iron and Steel Inst. Pub. 104 (1967), p. 61.

9. R.W. Vanderbeck: Weld. J., 37 (1958), p. 114.

10. W.B. Morrison and J.A. Chapman: Phil. Trans. Roy. Soc., Series A, 282 (1975), p. 289.

11. J.K. MacDonald, G.E. Wood and A. A. Towers: Proc. of the International Conference on Steel Rolling, ISIJ, Tokyo (1980), 2, p. 921.

12. J.J. Irani, D. Burton, J.D. Jones and A.B. Rothwell: Iron and Steel Inst. Pub. 104 (1967), p. 110.

13. I. Tamura: Ref. 11, 1, p. 59.

14. T. Tanaka, N. Tabata, T. Hatomura and C. Shiga, Ref. 1, p. 107.

15. T. Tanaka, T. Funakoshi, M. Ueda, J. Tsuboi, T. Yasuda and C. Utahashi: ibid., p. 399.

16. J.P. Sah, G.J. Richardson and C.M. Sellars: Met. Sci., 8 (1974), p. 325.

17. T. Tanaka, N. Tabata, T. Hatomura and C. Shiga: Kawasaki Steel Tech. Report, 6 (1974), p. 522.

18. Y.E. Smith and C.A. Siebert: Met. Trans., 2 (1971), p. 1711.

19. I. Kozasu, C. Ouchi, T. Sampei and T. Okita: Ref. 1, p. 120.

20. P. Bufalini and A. Aprile: Ref. 11, 2, p. 945.

21. M. Nagumo, H. Morikawa, N. Okumura Y. Kawashima, Y. Sogo and O. Mantani: ibid., 2, p. 1075.

22. K.J. Irvine, F.B. Pickering and T. Gladman: JISI, 205 part 2 (1967), p. 161.

23. A.M. Sage: Proc. of the International Conference on Hot Working and Forming Processes, Sheffield (1979), C.M. Sellars and G.J. Davies ed., The Metals Society, England, p. 119.

24. L.J. Cuddy: "Recrystallization and Grain Growth of Multi-Phase and Particle Containing Materials", N. Hansen, A.R. Jones and T. Leffers ed., Risø National Laboratory, Denmark (1980), p. 317.

25. A. Le Bon and L.N. de Saint-Martin: Ref. 1, p. 90.

26. J.D.Jones and A.B. Rothwell: Met. Rev., 72 (1975), p. 78.

27. I. Kozasu, T. Shimizu and K. Tsukada: Trans. Iron and Steel Inst., Japan, 12 (1972), p. 305.

28. M. Lamberigts and T. Gréday: "The Hot Deformation of Austenite", J.B. Ballance ed., AIME, N.Y., (1977), p. 286.

29. C. Ouchi, T. Okita, M. Okado and Y. Noma: Ref. 11, 2, p. 1272.

30. M. Fukuda, T. Hashimoto and K. Kunishige: Ref. 1, p. 136.

31. W.J. McG. Tegart and A. Gittins: Ref. 28, p. 1.

32. K. Misaka and T. Yoshimoto: J. Japan Soc. Tech. Plasticity, 8 (1967), p. 414.

33. S. Shida: J. Japan Soc. Tech. Plasticity, 10 (1969), p. 610.

34. I. Weiss, J.J. Jonas, P.J. Hunt and G.E Ruddle: Ref. 11, p. 1225.

35. A. Gittins, J.R. Everett and W.J. McG. Tegart: Metals Tech., 4 (1977), p. 377.

36. T.G. Oakwood, W.E. Heitmann and E.S. Madrzyk: Ref. 28, p. 204.

37. C. Ouchi, T. Okita, T. Ichihara and Y. Ueno: Trans. Iron and Steel Inst., Japan, 20 (1980), p. 833.

38. Y. Saito, N. Koshizuka, C. Shiga, T. Sekine, T. Yoshizato and T. Enami: Ref. 11, p. 1063.

39. B. Orrling, A. Sjöström and P. Heedman: ibid., p. 909.

40. C. Parrini, N. Pizzimenti and A. Pozzi: Ref. 1, p. 288.

41. R.A.P. Djaic and J.J. Jonas: J. Iron and Steel Inst., 210 (1972), p. 256.

42. J.J. Jonas, C.M. Sellars and W.J. McG. Tegart: Met. Rev., 14 (1969), p. 1.

43. C.M. Sellars and W.J. McG. Tegart: Met. Rev., 17 (1972), p. 1.

44. D.J. Michel, J. Moteff and A.J. Lovell: Acta Met., 21 (1973), p. 1269.

45. J.J. Jonas and M.J. Luton: "Advances in Deformation Processing", J.J. Burke and V. Weiss ed., Plenum Publishing Corporation (1978), p. 215.

46. W. Roberts and B. Ahlblom: Proc. 4th Int. Conf. on the Strength of Metals and Alloys, Nancy, France, 1 (1976), p. 400.

47. C. Rossard: Proc. 3rd Int. Conf. on the Strength of Metals and Alloys, Cambridge, England, 2 (1973), p. 175.

48. C. Ouchi and T. Okita: Tetsu-to-Hagane, 62 (1976), S208.

49. M.J. Luton and C.M. Sellars: Acta Met. 17 (1969), p. 1033.

50. T. Sakai, M.G. Akben and J.J. Jonas: Proc. of the International Symposium on the Thermomechanical Processing of Microalloyed Austenite, Pittsburgh, Pa (1981), AIME (in press).

51. H.J. McQueen and J.J. Jonas: "Treatise on Materials Science and Technology", R.J. Arsenault ed., Academic Press, New York, N.Y., 6 (1975), p. 393.

52. R.A.P. Djaic and J.J. Jonas: Met. Trans., 4 (1973), p. 621.

53. F. Haessner: "Recrystallization of Metallic Materials", F. Haessner ed., Dr. Rieder-Verlag GMBH, Stuttgart (1978), p. 1.

54. C.M. Sellars and J.A. Whiteman: "The Metallurgist and Materials Technologist", 6 (1974), p. 441.

55. C.M. Sellars: Ref. 24, p. 291.

56. T. Gladman and F.B. Pickering: JISI, 205 (1967), p. 653.

57. R. Coladas, J. Masounave and J.P. Bailon: Ref. 28, p. 341.

58. T. Gladman, I.D. McIvor and F.B. Pickering: JISI, 209 (1971), p. 380.

59. E. Hornbogen and U. Köster: Ref. 53, p. 159.

60. M. Korchynsky and H. Stuart: Ref. 2, p. 17.

61. T.M. Hoogendoorn and M.J. Spanraft: Ref. 1, p. 75.

62. R.K. Amin, G. Butterworth and F.B. Pickering: Ref. 23, p. 27.

63. A. Le Bon, J. Rofes-Vernis and C. Rossard: Met. Rev., 70 (1973), p. 571.

64. T. Gladman and D. Dulieu: Met. Sci., 8 (1974), p. 167.

65. S.S. Hansen, J.B. Vander Sande and M. Cohen: Met. Trans., 11A (1980), p. 387.

66. J.M. Gray and R.B. G. Yeo: Trans. ASM, 61 (1968), p. 255.

67. L. Meyer, F. Heisterkamp and W. Mueschenborn: Ref. 1, p. 153.

68. H. Watanabe, Y.E. Smith and R.D. Pehlke: Ref. 28, p. 140.

69. H. Sekine, T. Maruyama,   S. Sekiguchi and T. Ohno: Tetsu-to-Hagané, $\underline{56}$ (1970), p. 569.

70. A.T. Davenport, R.E. Miner and R.A. Kot: Ref. 28, p. 186.

71. T. Chandra, M.G. Akben and J.J. Jonas: ICSMA 6, Melbourne, Australia, August 1982.

72. H. Sekine and T. Maruyama: Trans. ISIJ, $\underline{16}$ (1976), p. 427.

73. A.T. Davenport and D.R. DiMicco: Ref. 11, $\underline{2}$, p. 1237.

74. M. Cohen and S.S. Hansen: "MiCon 80:   Optimization of Processing, Properties and Service Performance Through Microstructural Control", ASTM STP 672 (1979), p. 34.

75. A. Le Bon, J. Rofes-Vernis and C. Rossard: Met. Sci., $\underline{9}$ (1975), p. 36.

76. I. Weiss and J.J. Jonas: Met. Trans., $\underline{10a}$ (1979), p. 831.

77. I. Weiss and J.J. Jonas: Met. Trans., $\underline{11a}$ (1980), p. 403.

78. J.J. Jonas and I. Weiss: Met. Sci., $\underline{13}$ (1979), p. 238.

79. M.J. Luton, R. Dorvel and R.A. Patkovic: Ref. 77, p. 141.

80. S. Yamamoto, C. Ouchi and T. Osuka: Ref. 50, in press.

81. M.J. White and W. Owen: Ref. 77, p. 597.

82. B. Bacroix, M.G. Akben and J.J. Jonas: Ref. 50, in press.

83. W. Roberts: Swedish Institute for Metals, Research Report No. 1M. 1333 (1978).

84. H.P. Stüwe: Ref. 53, p. 11.

85. M.G. Akben, I. Weiss and J.J. Jonas: Acta Met., $\underline{29}$ (1981), p. 111.

86. J.J. Jonas and M.G. Akben: Metals Forum, $\underline{4}$, (1981), p. 92.

87. M.G. Akben: Ph.D. Thesis, McGill University, Montreal (1980).

88. B. Bacroix: M. Eng. Thesis, McGill University, Montreal (1982).

89. R.A. Petkovic: Ph.D. Thesis, McGill University, Montreal (1975).

90. L.V. Briseño: M. Eng. Thesis, McGill University, Montreal (1980).

91. M.J. Luton: Ph.D. Thesis, McGill University, Montreal (1971).

92. R. Choubey: Ph.D. Thesis, McGill University, Montreal (1981).

93. R.A. Petkovic, M.J. Luton and J.J. Jonas: Canadian Metallurgical Quarterly, 14 (1975), p. 137.

94. M.M. Eisenstadt: "Introduction to Mechanical Properties of Materials", 1st ed., The Macmillan Company, New York, N.Y., (1971), p. 325.

95. R.E. Reed-Hill: "Physical Metallurgy Principles", 2nd ed., D. Van Nostrand, New York, N.Y., (1973), p. 398.

96. S. Koyama, T. Ishii and K. Narita: Journal of the Japan Institute of Metals, 35 (1971), p. 1089.

97. K. Narita: Trans. ISIJ, 15 (1975), p. 145.

98. B. Aronsson: Climax Molybdenum Symposium, Zurich, 1969, p. 77.

99. P.J. Wray: Met. Trans., 13A (1982), p. 125.

100. W.B. Pearson: "The Crystal Chemistry and Physics of Metals and Alloys", Wiley - Interscience, New York, N.Y. (1972), p. 151.

101. P. Plassiard: Ph.D. Thesis, McGill University, Montreal (1982).

102. M.G. Akben, B. Bacroix and J.J. Jonas: (1982), submitted to Acta Met.

103. J.P. Michel and J.J. Jonas: Acta Met., 29 (1981), p. 513.

104. E.P. Abrahamson II and B.S. Blakeney: Trans. AIME, 218 (1960), p. 1101.

105. W.C. Leslie: "The Physical Metallurgy of Steel", 1st ed., McGraw Hill Book Co., New York, N.Y., (1981), p. 77.

```
20 CNTR(3)\PRINT "PUT THE STOP/RUN SWITCH ON STOP"
40 INPUT P$\PRINT "PUT LOW PRESSURE"\INPUT P$
60 PRINT "LEAVE ENOUGH SPACE BETWEEN SAMPLE  AND"
80 PRINT "UPPER GRIP. PUT ON RUN"\INPUT P$
100 MSW1(2)\FG1(0)\EDMP\FG1(0)\PRINT "PUT HIGH PR"\INPUT P$
120 CNTR(3)\PRINT "SAMPLE# & MATERIAL?"\INPUT H$,M$
140 PRINT "HEAT TREATMENT & TEST TEMP(C)?"\INPUT H$,T$
160 PRINT "PRESTRAIN?"\INPUT E2
180 PRINT "TOTAL STRAIN?"\INPUT E
200 PRINT "TRUE STRAIN RATE (1/SEC)?"\INPUT E1
220 PRINT "STROKE(MM) & LOAD(LBS) RANGE?"\INPUT R1,R2
240 PRINT "SPECIMEN HEIGHT(MM) AND SPECIMEN DIAMETER(MM)?"\INPUT L0,D0
260 PRINT "HOLDING TIME AT INTERR.(SEC)?"\INPUT T2
280 PRINT "ENTER # OF LEVELS,FREQ.& FREQ. RANGE BEFORE INTERR.?"
290 INPUT N1,R4,A4
300 PRINT "ENTER # OF LEVELS,FREQ. & FREQ.RANGE DURING INTERR.?"
310 INPUT N2,R5,A5
320 PRINT "ENTER # OF LEVELS,FREQ. & FREQ.RANGE AFTER INTERR.?"
330 INPUT N3,R6,A6
360 DIM P(600),S(600),P3(600)
400 DIM X(100),Y(20),Z(100)
410 DIM S3(600),E2(600)
420 MSW1(2)\A0=PI*D0^2/4
440 T1=E2/E1\K=2047/R1\K1=2047/R2
460 T3=(E-E2)/E1\T=T1+T3\N=N1+N3
461 PRINT "DO YOU WANT RECALL DATA?"\INPUT P$
462 IF P$="YES" THEN 466
463 IF P$="NO" THEN 480
466 OPEN "DX1:TEST"&N$ FOR INPUT AS FILE #1\P=20
467 FOR I=1 TO 2\AINP(P,1,0,E6)\NEXT I
468 P=P(1)+2\S1=P(2)
```

```
469 FOR I=3 TO P\AINP(P,1,0,E6)\NEXT I
470 P=P-2
471 FOR J=1 TO P\AINP(S,1,2,E7)\NEXT J
472 FOR I=1 TO P\P(I)=P(I+2)\NEXT I
473 CLOSE #1
474 GO TO 2000
480 X(1)=4095*N1/T1/R4/2
500 Y(1)=4095*N2/T2/R5/2
520 Z(1)=4095*N3/T3/R6/2
540 QUIT
560 PRINT "ENTER Y AND U"\INPUT Y,U
580 PRINT "IS THE X'HEAD IN THE RIGHT POSITION?"\INPUT A2$
600 IF A2$<>"YES" THEN 580
620 DACQ(0,S1,2,0)
640 FOR I=2 TO N1+1
660 X(I)=K*L0*(EXP(-E2*(I-1)/N1)-1)+S1+.5\NEXT I
680 X=N1+1\Q3=X(N1+1)+35
740 FOR I=2 TO N3+1
760 Z(I)=K*L0*(EXP(-E*(I-1)/N-E2)-1)+S1+.5\NEXT I
800 PRINT "START"
820 TIME(Y,E9)\DACQ(3,P,0,U)\DACQ(6,S,2,2)
840 FG1(X,1,7,A4)\STAR
920 BUF1(Z1)\IF Z1>-1 THEN 920
960 FG1(Q3)
1020 Z=N3+1
1040 FG1(Z,1,7,A6)
1120 BUF1(Z3)\IF Z3>-1 THEN 1120
1140 QUIT
1160 PRINT "THE EXP. IS OVER"
1180 PRINT " PRESS THE C/R"\INPUT K$
1200 DACQ(0,S4,2,0)
1220 FOR I=S4 TO S1+200\IF I>1500 GO TO 1260
1240 FG1(I)
1260 NEXT I
1280 PRINT "DO YOU WANT TO SEE A PLOT OF THE EXP.?"\INPUT D$
```

```
1300 IF D$="YES" THEN 2000
1320 IF D$="NO" THEN 1360
1360 PRINT "DO YOU WANT TO SAVE THE DATA?"\INPUT B$
1380 IF B$<>"YES" THEN 1420
1400 GO TO 1440
1420 PRINT "YOU CAN TURN OFF THE HYDRAULICS NOW"\DUMP\MSW1(2)\STOP
1440 FOR I=P+2 TO 3 STEP -1\P(I)=P(I-2)\NEXT I
1460 P(1)=P\P(2)=S1\P=P+2
1480 OPEN "DX1:TEST"&N$ FOR OUTPUT AS FILE #1
1500 FOR I=1 TO P\AOUT(P,1,0,E4)\NEXT I
1520 P=P-2\S=P
1540 FOR J=1 TO P\AOUT(S,1,2,E5)\NEXT J
1560 CLOSE #1\GO TO 1420
2000 FOR I=1 TO P\L1=L0+(S(I)-S1)/K
2020 S3(I)=9.81*ABS(P(I))*L1/2.2046/A0/K1/L0\E2(I)=-LOG(L1/L0)
2040 PRINT I,S3(I),E2(I)
2060 NEXT I
2080 INPUT K$
2100 PRINT "ENTER DT?"\INPUT D1
2120 T4=D1*P/10000
2140 CNTR(3)\CNTR(0)\PHYL(100,900,80,700)
2160 SCAL(0,0,T4,0,E)\AXES(0,0)\CNTR(2)\PLOT(0,0)
2180 LABL("TIME(SEC)","TRUE STRAIN",T4/8,.1,1)
2190 CNTR(1)\COMM("SAMPLE #",.5*T4,.96*E)\PRINT N$
2200 CNTR(0)\A8=0
2220 FOR I=1 TO P\A8=A8+D1/10000
2240 MARK(".",A8,E2(I))\NEXT I
2260 CNTR(2)\INPUT F$\CNTR(3)
2280 CNTR(3)\CNTR(0)\PHYL(100,900,80,700)
2300 SCAL(0,0,T4,0,5000)\AXES(0,0)\CNTR(2)\PLOT(0,0)
2320 LABL("TIME(SEC)","LOAD LBS",T4/8,250,1)
2330 CNTR(1)\COMM("SAMPLE #",.5*T4,4800)\PRINT N$
2340 CNTR(0)\A8=0
2360 FOR I=1 TO P\A8=A8+D1/10000\P3(I)=ABS(P(I))/K1
2380 MARK("+",A8,P3(I))\NEXT I
```

```
2400 CNTR(2)\INPUT F$\CNTR(3)
2600 PRINT "ENTER I1,P1,P2"\INPUT I1,P1,P2
2620 PRINT "INPUT MIN STRAIN AND STRESS"\INPUT B1,B2
2640 PRINT "INPUT MAX STRAIN AND STRESS"\INPUT S5,U
2660 PRINT "ENTER STRAIN & STRESS INCREMENT"\INPUT B3,B4.
2680 CNTR(3)\CNTR(0)\PHYL(100,900,80,700)
2700 SCAL(0,B1,S5,B2,U)\AXES(0,0)\CNTR(2)\PLOT(B1,B2,
2720 LABL("TRUE STRAIN","TRUE STRESS MN/M^2",B3,B4,1)
2740 LABL(" "," ",B3/2,B4/2,3)\CNTR(0)\PLOT(B1,U)
2760 PLOT(S5,U)\PLOT(S5,B2)\PLOT(B1,B2)\CNTR(1)
2780 IF I1=1 THEN 3000
2800 IF I1=2 THEN 3300
2820 IF I1=3 THEN 3500
3000 COMM("SAMPLE#",.5*S5,.96*U)\PRINT N$
3020 COMM(M$,.5*S5,.93*U)\COMM(H$,.5*S5,.9*U)
3040 COMM(T$,.5*S5,.87*U)\COMM("STRAIN RATE",.5*S5,.83*U)
3060 PRINT E1\COMM("/SEC",.9*S5,.83*U)
3080 COMM("PRESTRAIN",.5*S5,.8*U)\PRINT E2
3100 COMM("HOLDING TIME",.5*S5,.77*U)\PRINT T2
3120 COMM("SEC",.9*S5,.77*U)\CNTR(2)
3140 PLOT(B1,B2)\CNTR(0)
3160 FOR I=1 TO P\MARK("+",E2(I),S3(I))\NEXT I
3180 CNTR(2)\INPUT F$\CNTR(3)
3200 GO TO 2600
3300 COMM("INITIAL YIELD REGION",.5*S5,.96*U)
3320 COMM("SAMPLE #",.5*S5,.93*U)\PRINT N$
3340 CNTR(2)\PLOT(B1,B2)\CNTR(0)
3360 FOR I=1 TO P\MARK("+",E2(I),S3(I))\IF E2(I)>.05 THEN 3380
3365 NEXT I
3380 CNTR(2)\INPUT F$\CNTR(3)
3400 GO TO 2600
3500 COMM("INITIAL YIELD REGION",.5*(S5+B1),.96*U)
3520 COMM("SAMPLE #",.5*(S5+B1),.93*U)\PRINT N$
3540 CNTR(2)\PLOT(B1,B2)\CNTR(0)
3560 FOR I=P1 TO P2\MARK("+",E2(I),S3(I))\NEXT I
```

```
3580 CNTR(2)\INPUT F$\CNTR(3)
3600 PRINT "INPUT P1,P2,DT"\INPUT P1,P2,D1
3620 T6=P1*D1/10000\T7=P2*D1/10000
3640 PRINT "MIN AND MAX STRESS"\INPUT B2,U
3660 PRINT "ENTER STRESS INCREMENT"\INPUT B4
3680 B3=(T7-T6)/8
3700 CNTR(3)\CNTR(0)\PHYL(100,900,80,700)
3720 SCAL(0,T6,T7,B2,U)\AXES(0,0,\CNTR(2)\PLOT(T6,B2)
3740 LABL("TIME(SEC)","TRUE STRESS MN/M^2",B3,B4,1)
3760 CNTR(0)\PLOT(T6,U)\PLOT(T7,U)\PLOT(T7,B2)\PLOT(T6,B2)
3780 CNTR(1)
3800 COMM("SAMPLE #", .5*(T6+T7),.96*U)\PRINT N$
3820 CNTR(2)\PLOT(T6,B2)\CNTR(0)\A8=T6
3840 FOR I=P1 TO P2\A8=A8+D1/10000
3860 MARK("+",A8,S3(I))\NEXT I
3880 CNTR(2)\INPUT F$\CNTR(3)
3900 GO TO 1360

READY
```